EXPERIMENTS ON THE INTERACTIONS BETWEEN A RIGID PLATE AND VORTICES

By

Shaun Milke

RECOMMENDED:

Dr. Yujiang Xiang

Dr. Jifeng Peng
Advisory Committee Co-Chair

Dr. Rorik Peterson
Advisory Committee Co-Chair

Dr. Rorik Peterson
Chair, Department of Mechanical Engineering

APPROVED:

Dr. Doug Goering
Dean, College of Engineering and Mines

Dr. John Eichelberger
Dean of the Graduate School

11 August 2015
Date

EXPERIMENTS ON THE INTERACTIONS BETWEEN A RIGID PLATE AND VORTICES

A

THESIS

Presented to the Faculty

of the University of Alaska Fairbanks

in Partial Fulfillment of the Requirements

for the Degree of

MASTER OF SCIENCE

By

Shaun Milke

Fairbanks, Alaska

August 2015

Abstract

This study provides a quantitative analysis, and subsequent comparison, of flow field behavior under varied experimental parameters for vortex production by, and vortex ring interaction with, a rigid plate. The relationship between the experimental parameters: flapping amplitude and average rotational speed, and flow field characteristics: vorticity, circulation, total kinetic energy, and vortex trajectory, were examined for the cantilevered plate. The relationships between the parameter of plate inclination and the flow field characteristics of vorticity, circulation, and vortex trajectory, were examined for the inclined plate. All experiments involved a particle image velocimetry (PIV) analysis followed by processing of the data to produce quantified flow field data. The cantilevered plate experiments revealed that a flapping cantilevered plate produces two primary vortices: a tip vortex and a plate hugging vortex, and in some cases a stopping vortex above the tip. It was determined that the maximum magnitudes attained, the accumulation rate, and the dissipation rate of both circulation and kinetic energy are speed dependent. However, rate of accumulation and dissipation of either quantity does not vary with total flapping amplitude. It was concluded that flapping amplitude does not influence the shape of vortex trajectory or the trajectory angle relative to the horizontal, though the total distance traveled along the vortex trajectory is dependent on flapping amplitude. In the case of the inclined plate, it was concluded that the levels of vorticity, particularly in the lower part of the vortex ring, and the formation of additional vortices in the flow field are dependent on plate inclination and thus, the degree of asymmetry of the interaction. During the die off phase the circulation of the upper part of the vortex ring is inversely proportional to plate angle, while circulation of the lower part of the vortex ring is proportional to plate inclination. The

relationship between plate inclination and vertical displacement of the two parts of the ring was found to be based on the degree of asymmetry.

Table of Contents

Page

Page

Page

List of Figures

Page

Page

Page

Page

Chapter 1 Introduction

1.1 General Introduction

Fluid motion is ubiquitous though not always appreciated in everyday life. A unique form of fluid motion is the rotating body of fluid known as a vortex, which like other fluid flow types, is ever present and constantly impacting our daily lives. There are instances in which we see vortices or their toroidal forms, vortex rings, and take note but are generally not interested in their mechanics. Tornados are prime examples of vortices that we have little difficulty seeing and of which one easily feels the effects. There are however, reasons for scientific interest in the mechanics of vortices that are not as easily visualized and that one might not expect to be affected by.

In some cases vortices are the result of intentional production, such as the means of propulsion or directional control for various forms of aquatic life. These organisms may use the flapping of a fin at different speeds or amplitudes to produce vortices of varying character, to differently affect locomotion (Linden & Turner, 2004). In other cases vortex production may be an unintended consequence of some action, such as the generation of thrust by a ship's propeller. Vortex fluid flow in cases such as this may cause interference with other parts of a system; on a ship generating thrust, the vortex interference with the surface of the rudder may be of concern (Felli & Falchi, 2011). Cycloidal rotor propelled craft also exhibit significant interaction between the propelled structure and the vortices produced for propulsion or directional control. It was shown by Chopra, Parsons, and Sirohi (2007) that these secondary vortex interactions may be exploited to increase the craft's propulsive forces. For reasons such as these, the behavior of

particles in a flow field where vortices are being generated and where existing vortices interact with a body are of scientific and practical interest.

Specifically, this research applies to engineering applications in which vortices are employed as a means of propulsion. The movement of propeller driven ships and cycloidal rotor craft may benefit from increased propulsion efficiency and finer directional control, with further research into the mechanics of the associated vortex interactions. Each of these propulsion methods involves the production of a vortex and post-production interaction of the propelled body with the vortex. Investigations such as those made in this research are significant in that increased fundamental knowledge of vortex production and vortex-body interactions allow for improved efficiency and control, when applied in the design of ships and cycloidal rotor craft.

1.2 Objective

The objective of this work was to provide quantitative analysis and subsequent comparison of flow field and vortex behavior, given varied parameters in both cantilevered plate vortex production and vortex ring-plate interaction experiments. The aforementioned scientific understanding and practical utilization of this understanding are works in progress. This research is intended to build upon the existing knowledge base of flow field phenomena, so that further scientific investigation and real world design of vortex propelled bodies may result in increased propulsion efficiency and directional control.

1.3 Organization

Chapter 1 provides an introduction into the concepts that have been both employed and investigated in this research. This chapter also states the objective of the experimental work.

Chapter 2 is a review of the fundamental mathematical and theoretical principles used to analyze vortices as well as a review of some existing research this study is intended to build on. The experimental methods used to complete this study are described in chapter 3. Specifically, this chapter discusses the physical apparatus used to conduct the experiments, the digital means used to analyze the data, and the data collection method linking experiment and analysis. In chapter 4 the results of the flapping cantilevered plate experiments are presented, discussed, and a conclusion is drawn. Similarly, chapter 5 is a presentation and discussion of the results of the vortex ring experiments, ending in a conclusion specific to this set of experiments. Finally, all references used in this paper are cited in chapter 6.

Chapter 2 Background and Supporting Theory

2.1 Vortices

Though there are many physical and mathematical distinctions between various types, vortices are, very generally, considered to be areas within a flow in which there is rotation of the fluid elements about a center (Reynolds, 1974). While the fluid elements in a vortex may be rotating, vortices can be considered irrotational or rotational and free or forced (Munson, Okiishi, & Young, 1998). The mathematical distinction between these classifications is to follow in the discussion of vorticity. However, in a physical sense an irrotational, or free, vortex is not influenced by solid boundaries but rather develops as the result of shear forces strictly within a fluid; rotational, or forced, vortices are the result of solid body interaction (Reynolds, 1974). When a rotating mass of fluid forms a toroidal vortex it, is known as a vortex ring. These vortex rings generally entrain some of the fluid surrounding them and move perpendicular to the circumference of the toroid (Akhmetov, 2008).

2.2 Velocity Field

Fluid motion is by nature a difficult phenomenon to understand and model. One of the key parts of modeling fluid motion is the velocity field. Approximating the flow of fluid as the aggregate motion of many small fluid elements, one can use a vector field as a representation of motion at distinct points in a volume of fluid. In many cases a two dimensional cross section of a volume of moving fluid, divided along both axes at regular intervals, allows for adequate modeling of the fluid flow with a two dimensional vector field. Each fluid element created by the division of the axes may be assigned a vector representing the average velocity of that

element. In a simplified, two dimensional, cartesian coordinate system the velocity vector is defined as the following (Anderson, 2001).

$$\mathbf{V} = u\mathbf{i} + v\mathbf{j} \tag{1}$$

Where, **i** and **j** are unit vectors along the x and y axis respectively and

$$u = u(x, y, t) \tag{2}$$

$$v = v(x, y, t) \tag{3}$$

Particle image velocimetry (PIV) allows for the quantification of these velocity vectors and with the resulting velocity field a number of useful pieces of information can be obtained. Many of the useful pieces of information that can be derived from a velocity field are the result of further calculations. These include total kinetic energy, vorticity, and circulation. With a reference vector available for scale, looking at the magnitude and direction of vectors in a velocity field allows for visualization of translation of individual fluid elements as well as rotational qualities of groups of fluid elements. In some cases, velocity vectors near the surfaces of solid bodies allow for visualization of boundary layer behavior.

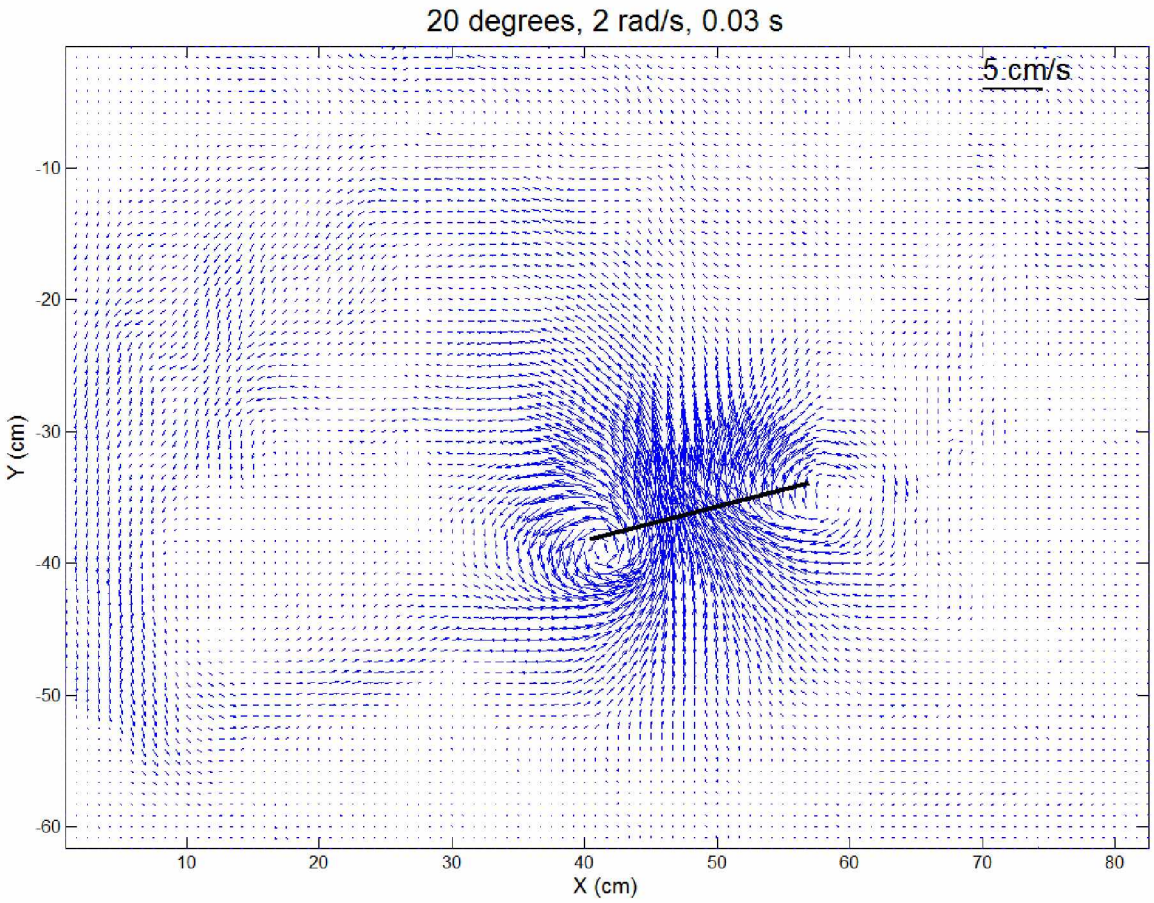

Figure 2.1 Example velocity field plot

2.3 Total Kinetic Energy

When fluid is in motion, even inside a rigid container, it possesses kinetic energy. This kinetic energy may be in the form of translational motion, rotational motion, or a combination of the two. Interaction between fluid and a solid boundary will result in change in kinetic energy of some of the molecules, or fluid elements in the modeling process. After the beginning of the disturbance, viscous forces within the fluid or along the container's surface begin to cause the molecules to exchange kinetic energy. Without further disturbance, the system will return to its former steady state as the relatively uniform kinetic energy of the fluid elements becomes significantly less uniform and kinetic energy is converted into thermal energy which is

transferred to the outside environment (Kondepudi & Prigogine, 2015). Disturbances of similar nature but with somewhat varied parameters will impart different amounts of kinetic energy to the fluid and the variations in fluid flow may result in different rates of conversion of kinetic energy to thermal energy. Changes in kinetic energy are particularly interesting during the formation of vortices as the conditions during formation can be linked to resulting kinetic energy in the fluid and these relationships have much applicability in areas such as biomechanical efficiency (Bandyopadhyay & Leinhos, 2013).

The kinetic energy of a fluid element can be found given its mass and velocity. Total kinetic energy for a complex flow involving many fluid elements is slightly more involved. Given that fluid flow is often analyzed using two dimensional velocity fields, total kinetic energy must be determined in the form of total kinetic energy per unit depth. This allows for the determination of kinetic energy in the fluid field assuming the unit of depth does not reach a point in the flow field where any boundary effects become significant.

$$K = \tfrac{1}{2}\, m\, \mathbf{V}^2 \tag{4}$$

Dividing through by z gives kinetic energy per unit depth and in terms of the fluid element's length and width.

$$K/z = \tfrac{1}{2}\, d\, x\, y\, \mathbf{V}^2 \tag{5}$$

2.4 Vorticity

Vorticity is a descriptor of the rotational nature of a flow field. Most generally vorticity may be zero or finite resulting in the classification of the flow as irrotational or rotational,

respectively (Crowe, Elger, Robertson, & Williams, 2010). More specifically vorticity is defined as the curl of the velocity,

$$\xi = \nabla \times \mathbf{V} \tag{6}$$

$$\mathbf{V} = u\mathbf{i} + v\mathbf{j} + w\mathbf{k} \tag{7}$$

As derived by Anderson (2001) and simplified for the two dimensional case, vorticity is expressed mathematically as,

$$\xi = (\partial v/\partial x - \partial u/\partial y)\mathbf{k} \tag{8}$$

Just as a velocity field can be plotted for visual interpretation, both quantitatively and qualitatively, vorticity plots can be made to interpret areas of rotation. In such plots areas of different vorticity are demarcated by contour lines of constant vorticity as well as colors which correspond to varying levels of vorticity as marked on a reference color bar. As vorticity is a vector quantity normal to the plane of rotation and multiple vortices rotating in opposite directions often develop in the same flow field, vorticity plots employ different colors for positive and negative values of vorticity.

2.5 Circulation

Circulation is a fluid dynamic property that can be derived from a flow field in which either velocity or vorticity are known. Rather than indicating there is some rotation of the fluid in a circular pattern, circulation describes the movement of fluid in any direction with respect to

the boundary of a closed loop or the surface of a contiguous area (Anderson, 2001). In the first case, circulation takes the form of a line integral and is related directly to velocity while in the second case circulation is defined as a surface integral related directly to vorticity; as Chirgwin and Plumpton (1967) showed using Stokes' theorem this statement in mathematical form is as follows:

$$\Gamma = \oint_C \boldsymbol{V} \cdot \boldsymbol{ds} = \iint_S (\nabla \times \boldsymbol{V}) \cdot \boldsymbol{dA} \tag{9}$$

In the first portion of the expression the line integral is taken about a closed contour C on the velocity field with infinitesimal segment **ds** oriented along C. Similarly, the second half of the expression is equal to the circulation calculated as the area integral over area A. This relationship is useful in the sense that areas of interest for calculating circulation are more obvious when looking at vorticity plots than velocity fields. Software exists to create a vorticity plot for easy visualization, selection of an area of interest, and calculation of the area integral over the selected area.

2.6 Vortex Trajectory

When a vortex or vortex ring is formed, interacts with a solid body, or interacts with another vortex its area of highest vorticity changes position. This area of highest vorticity can be considered to be the average location of the vortex. Tracking the path of a vortex can be useful in determining what bodies or other areas of vorticity might be influencing the trajectory of the vortex. The trajectory itself is not as scientifically interesting as what it tells us about the vortex's interactions, which influence such properties as kinetic energy and circulation (Couch &

Krueger, 2011). In addition vortex trajectory is sometimes useful for keeping track of an original vortex when several other vortices may have formed around it.

2.7 Cantilevered Plate Research

The nature of fluid flow around plates has been the subject of numerous studies. The focus of this work has been on such inquiries from measuring the pressure field to investigating span wise flow (Obi & Suryadi, 2011; Kriegseis, Rival, & Wong, 2013). This existing research has been spurred mainly by interest in enhancing hydrodynamic efficiency of lift generating bodies as well as the energy extraction efficiency of power generation devices using plates in a fluid stream.

Many types of plates have been studied including: segmented plates with varying flexibility, plates with segments that are actively controlled and move independently of the rest of the plate, fully rigid, and uniformly flexible. These studies have found differing efficiencies and different vortex production for results for the same plate types when used as lifting bodies when compared to power extraction devices (Lai, Tian, & Young, 2014). Various plate motions have been studied for each application. Among other motions the following have been tested: hinging the plate partially along its chord line, moving the plate at a resonant frequency with the flow, and plunging the plate while flapping it about a fulcrum (Eloy, Paraz, & Schouveiler, 2014; Lai et al., 2014).

A few studies have investigated the vortex production of a fully cantilevered, rigid plate which moves with only a flapping motion. While Obi and Suryadi (2011) and Ishii, Obi, and Suryadi (2010) have conducted experiments with similar a similar setup, their work focused on the pressure field around the plate and the forces acting on the solid bodies. It is the intention of

this study to focus on vortex behavior and quantitative properties, and their correlation to plate speed and flapping amplitude.

2.8 Vortex Ring Research

Vortex ring behavior and interaction with other bodies or fluids have been described in many studies. The application of these studies, like those for flapping plates, is often to increase efficiency or a lifting body, maximize energy extraction for power generation device, or resolution of unintended fluid interaction between a machines components (Felli, Guj, & Roberto, 2009). The focus of vortex ring studies has been on a number of phenomena with a wide range of experimental conditions. In some cases such as the work by Bernal, Song, and Tryggvason (1992) the interaction in question is that of the vortex ring with a free surface and the resulting surface behavior. In other cases the interaction of a vortex plate with a solid body has been investigated, sometimes with the addition of an exotic parameter such as heating of the solid body above the ambient fluid temperature (Arévalo, Hernández, Nicot, & Plaza, 2010).

This conditions and parameters in this study are a combination of the basic elements, of which at least one is usually found in vortex ring studies of any kind. The main condition of interest in this study is the body with which the vortex is to interact is solid and has no fluid density gradient at its surface, as would be the case with a heated plate or if the ring were to interact with a free surface. The parameter to be varied in this study is plate inclination angle. This combines two interaction natures studied in other experiments: symmetrical and asymmetrical. The asymmetrical behavior of vortex rings has been studied not only by interaction with solid bodies, but also with free surfaces (Miloh & Tyvand, 1994).

Here it is sought to combine the basic parameters and conditions commonly seen in vortex ring interaction studies in a single set of experiments. The analysis of these interactions should not only relate to existing vortex ring interaction studies but provide future insight into the nature of these interactions under uncontrived conditions. It is the intention of this study to focus on vortex ring behavior and quantitative properties, and their correlation to fixed plate inclination.

Chapter 3 Methods

3.1 General Setup

In general these experiments consisted of the formation of vortices in a large acrylic tank filled with water. Images of the fluid motion were recorded on a high definition camera. A PIV analysis was performed on these images and the resulting data were then processed using several programs to produce velocity, vorticity, circulation, total energy, and vortex trajectory data.

3.1.1 PIV

The particle image velocimetry technique used to conduct these experiments allows for the visualization and analysis of the fluid moving in a single plane. In order to isolate a single plane within the acrylic tank, a lens is placed in line between the tank and a laser. The laser beam is transformed by the lens into a light sheet that illuminates a vertical plane within the tank and creates a cross sectional view of the fluid under investigation. The light is reflected from tracer particles in the fluid to a camera placed perpendicular to the sheet a few feet from the tank, with a clear view of the area in which the fluid is to move. The tracer particles used in these experiments were 14 micron silver coated hollow glass spheres, produced by Potters Beads. These beads were used because they serve adequately in multiple key areas of PIV analysis; namely the tracer particle must be reflective enough to be clearly distinguished from any foreign debris or haze in the container walls and must also have a density close to that of the fluid so that the tracer particles are neutrally buoyant and closely approximate movement of the actual fluid particles (Kompenhans, Raffel, Wereley, & Willer, 2007).

3.1.2 Image Production

The camera used to record images in these experiments was a Princeton Instruments ES 2020. This camera was chosen as it is able to capture high resolutions images at relatively high speeds: 1600x1200 pixels at 30 frames per second. A PIXCI frame grabber card from Epix was installed in a desktop to be used as an interface between the camera and the XCap camera control software used to record the images. The XCap software produced bitmap image files that could then be reviewed frame by frame to ensure all parts of the apparatus worked properly during the experiment.

3.2 Specific Setup

While the general setup for all experiments remained the same, some components varied between tests. The configuration of the light sheet, tank, camera, and camera control software remained essentially the same for all experiments. The apparatuses used for the cantilevered plate and vortex ring experiments were significantly different.

3.2.1 Cantilevered Plate Experiments

The apparatus used in the cantilevered plate experiments consisted of an acrylic plate (30.5 cm x 30.5 cm x .318 cm) rigidly connected in a cantilevered configuration to an axle. The length of the plate was chosen such that there would be sufficient distance between the plate and any boundaries to prevent significant edge effects. Similarly, the width of the plate was made sufficiently large to prevent interference from fluid motion around its lateral sides. The axle was connected via belt to a stepper motor (Lin Engineering 4118L-07S).

Figure 3.1 Cantilevered plate with inclination markers

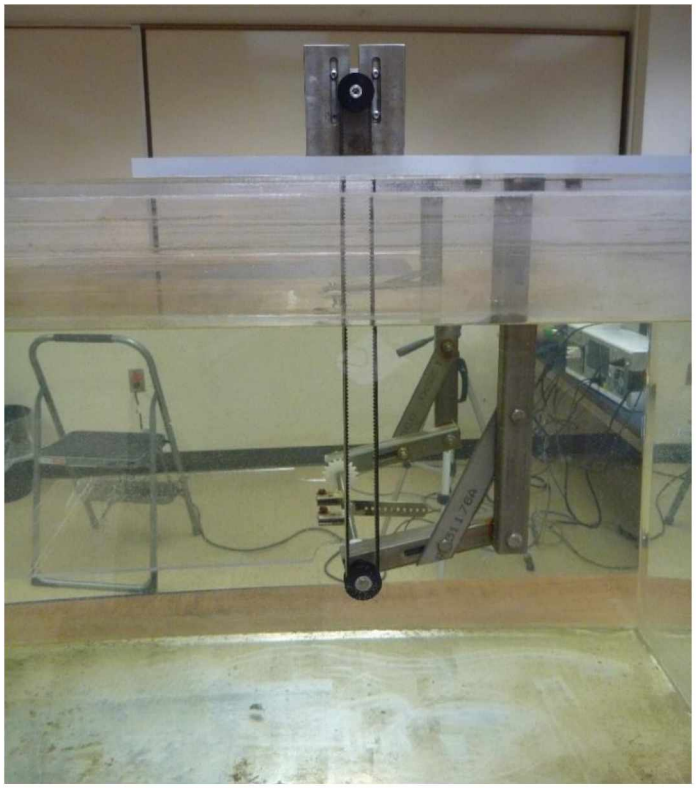

Figure 3.2 Cantilevered plate, pulley system, and motor

A second computer controlled the function of the motor via a LinCommand program in which several parameters could be varied. In this experiment it was sought to vary the amplitude and rotational velocity of the plate independently. This was done via manipulation of the settings within LinCommand for the number of steps, and steps per second. The number of steps could easily be correlated to the number of degrees of amplitude. However, due to the large forces on the motor and the resulting inconsistencies between input speed and actual speed seen during the experiments, trial and error was used to determine appropriate input speeds that resulted in the proper number of images depicting plate movement and thus the appropriate average rotational velocity.

The plate and axle were aligned with a paper on the back side of the tank that showed the plate's inclination. For these experiments the amplitude was defined as the number of degrees from horizontal the plate was rotated. The plate was aligned with the appropriate degree marker below the horizontal and was rotated upward for every experiment. The upward rotation of the plate caused multiple vortices to form and it was their formation that was documented and analyzed in these experiments.

3.2.2 Vortex Ring Experiments

In the vortex ring experiments the plate used for the previous experiments was removed and replaced with a larger acrylic plate (61.0 cm x 45.8 cm x 0.318 cm). In this case the size of the plate was chosen so that the vortices that were to interact with the stationary plate would degrade beyond the point of interest before leaving the surface of the plate; edge effects were considered as in the last experiment. At the other side of the tank an electrically actuated piston

and cylinder acting as a pump were connected to a smaller, hydraulically actuated piston and cylinder which was pointed at the acrylic plate and perpendicular to its axis of rotation.

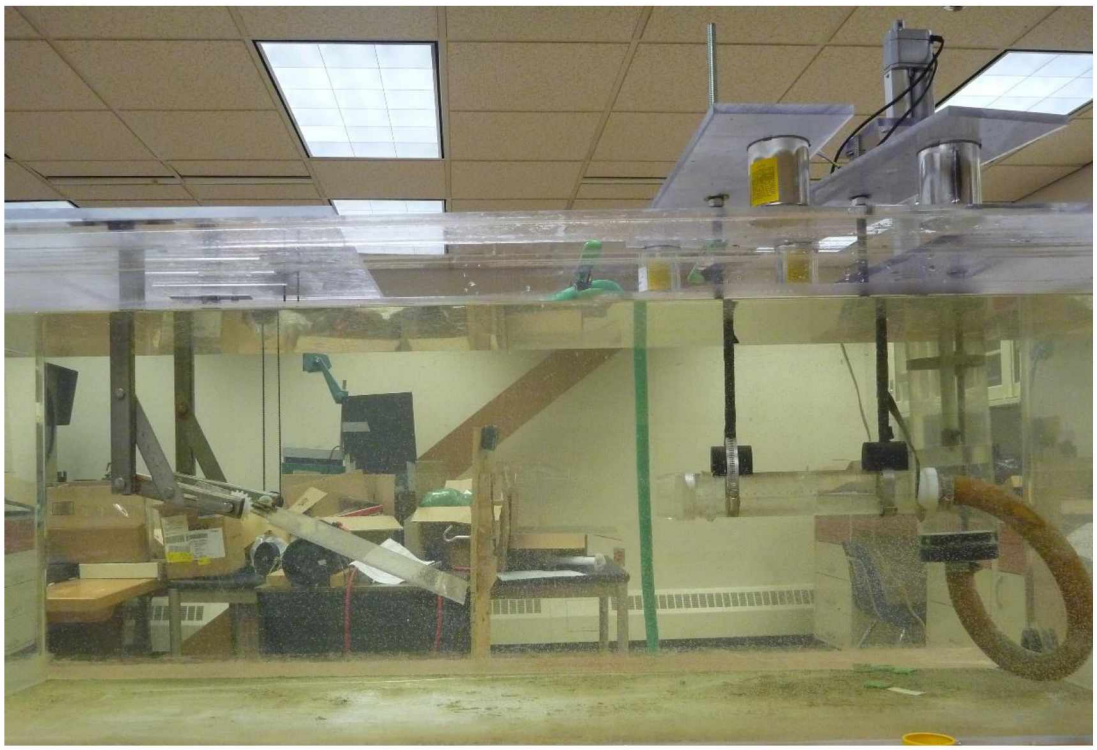

Figure 3.3 Inclined plate, vortex tube, and pump

This system was used to create a vortex ring directed at the plate in different orientations. The actuator controlling the pump was connected to the second computer and manipulated using a LabView control panel. In each experiment the stroke and speed of the piston in the pump remained the same, so as to produce identical vortex rings in each experiment. The inclination of the plate was changed for each experiment; inclinations tested were 30, 60, and 90 degrees. The vortex ring shot at the inclined plate deformed and was deflected from its original path and it was the nature of these interruptions that was documented and analyzed in this set of experiments.

3.3 Data Processing

3.3.1 PIV Processing

The first step in obtaining quantitative data from the bitmap images generated during the experiments was to complete the PIV processing. A Matlab script was used to convert the .bmp files into raw images that could be handled by the PIV software. Next, a parameter file was created for the data set undergoing processing. The window (32x32 pixels), step size (16 pixels), and resolution (1600x1200 pixels) remained the same for all data sets. However, because components such as the plate or camera were shifted slightly between experiments a different scaling factor had to be entered into each parameter file; these scaling factors were determined based on a reference image created by holding a ruler in the camera's plane of focus and counting the number of pixels used to depict 1 centimeter or the ruler. With the parameter file saved the PIV software was run, velocity (.vel) and vorticity (.vor) files were generated.

3.3.2 Quantitative Data Processing

The .vel files were converted using a Matlab script to Matlab data files which could then be plotted in a velocity field using a separate script. These files were smoothed in a script that performs some averaging of the data to reduce noise. The velocity files were next called on by a program that calculated vorticity over the field of view and produced vorticity Matlab data vorticity files. A set, one for each of the two types of experiments, of fairly comprehensive processing script was written in Matlab that served to: record the location of the plate in each image, plot the velocity and vorticity data with the plate superimposed on these images, record the location of the vortices in each images, create a trajectory plot of the vortex locations, calculate the total kinetic energy associated with each image, and create a scatter plot of the total

kinetic energy for all images in the trial. The script for the vortex ring experiments did not calculate or plot total kinetic energy as this was not a data type of interest. Finally Matlab was used to compile the data into respective plots for comparisons between data sets.

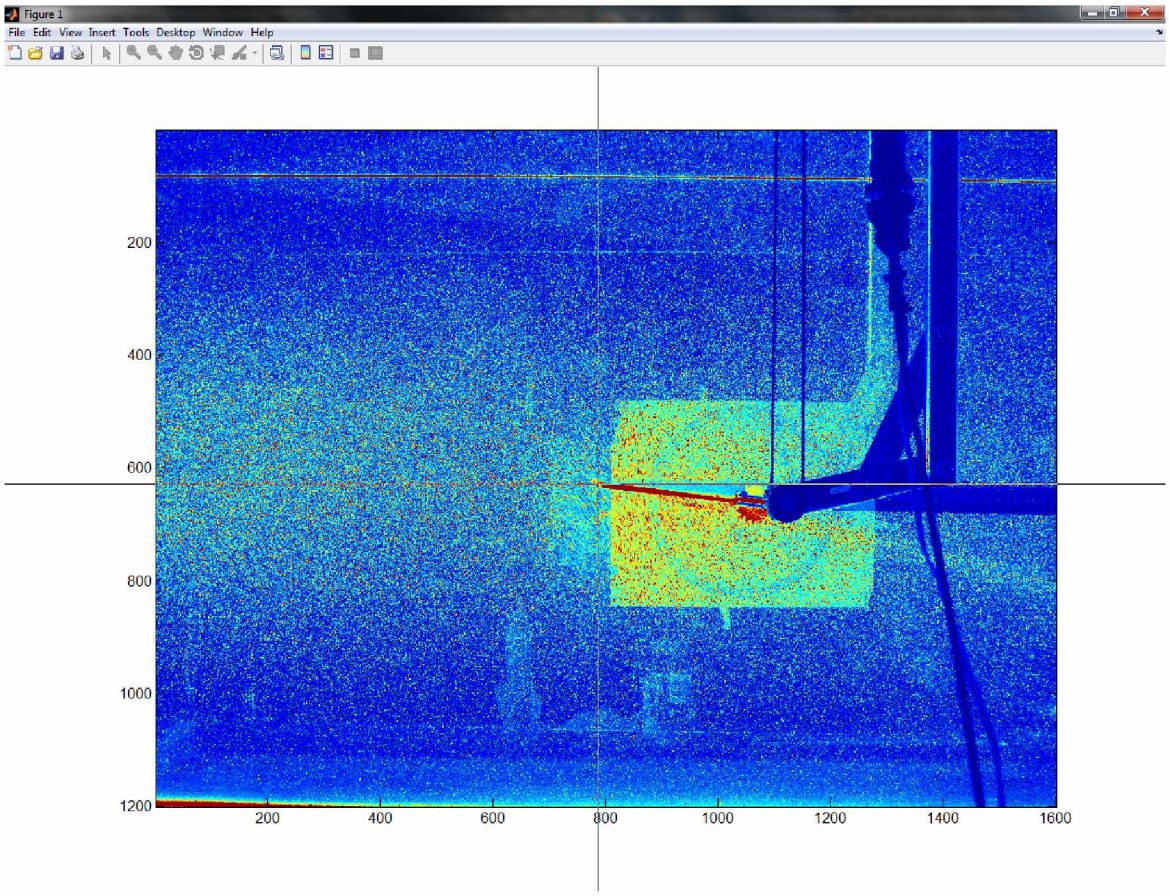

Figure 3.4 Tracking of plate tip

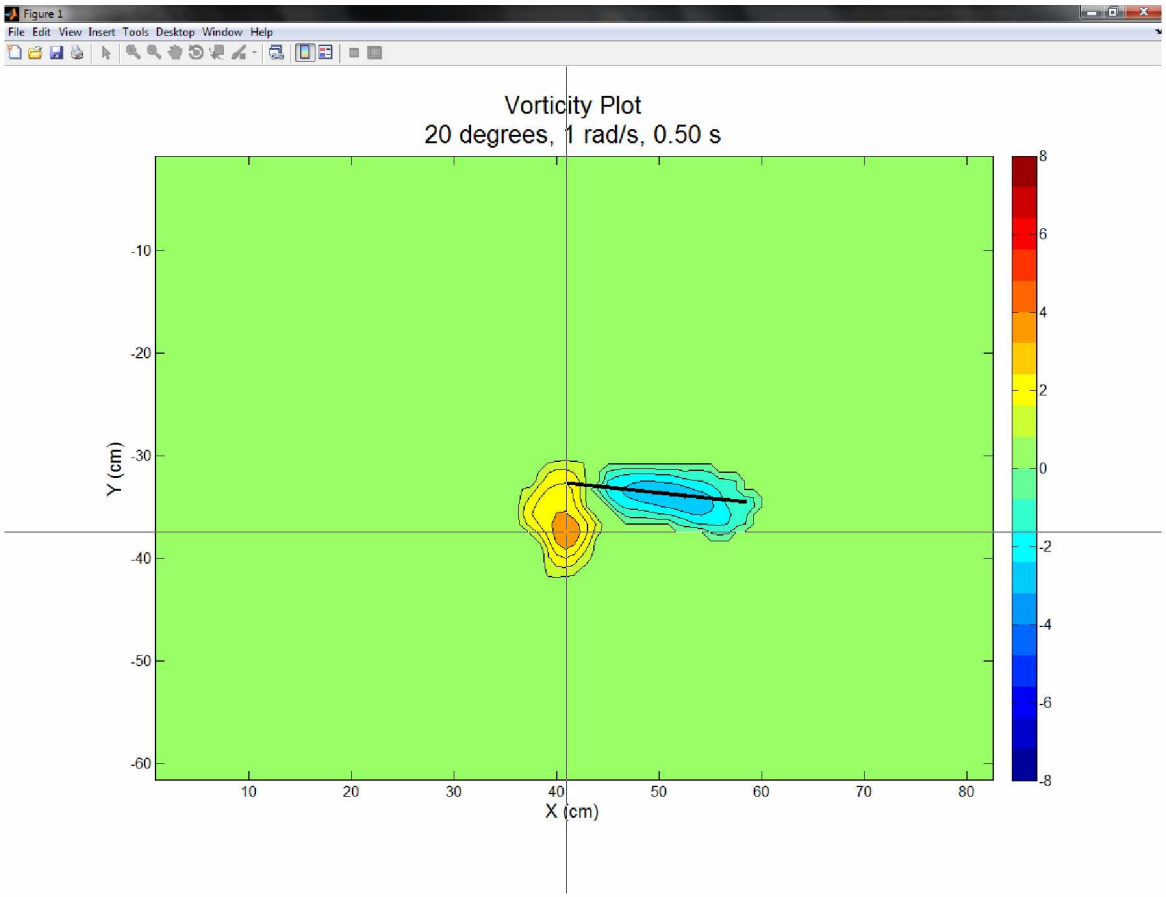

Figure 3.5 Tracking of vortex

Circulation was the only data type not determined using a Matlab script. Instead a software that performs the area integration process described earlier was used. The area for which the vorticity was to be calculated was manually selected for every image in every experiment. The circulation value returned by the software was recorded in Excel. Individual and comparative plots of circulation were made for the appropriate data sets.

Chapter 4 Cantilevered Plate Results

4.1 Investigation

The investigation into the vortex production by a cantilevered plate focuses on the relationship between the vortex produced and the kinematic parameters of the plate. This research explores the question of what relevance amplitude and speed of a rigid flapping plate have to the nature of the vortices produced. Similar experimental setups have been used in other research but these experiments leave questions, as to how the vortex evolves, unanswered.

4.2 Cantilevered Plate Experiments

The following experiments use a PIV analysis and susbsequent data processing to quantitatively and qualitatively describe the formation of vortices around a rigid flapping plate. The parameters of the plate varied in these experiments were the range of rotation and the rotational velocity. Six test were conducted, using two speeds and three amplitudes. In these experiments amplitude was considered to be the number of degrees the plate was oriented from the horizontal and thus the full range of motion in each experiment was twice the value of the amplitude. Amplitudes used in these experiments were 20, 30, and 40 degrees. At each amplitude two rotational velocities were tested. The rotational velocities were 1 and 2 rad/s and these values represent average speed over the full range of motion. This means the plate started and stopped during the time period being analyzed, rather than maintaining a constant velocity through the full range of motion.

4.3 Amplitude: 20 degrees, Speed: 1 rad/s

4.3.1 Vorticity Evolution

The following images depict the vorticity for each image used in the analysis. The plate is superimposed over the plot for reference. Areas of different vorticity are demarcated by contour lines of constant vorticity as well as colors which correspond to varying levels of vorticity as marked on the reference color bar. In this trial the plate moves from twenty degrees below the horizontal to twenty degrees above, with an average speed of 1 rad/s. The first image which captures motion of the plate clearly shows two areas of vorticity. The vortex at the tip has positive vorticity, indication that the fluid is beginning to rotate counter clockwise around the tip of the plate. The second area of vorticity is rotating in the opposite direction and rest on the upper surface of the plate, indicating the shear layers

The plate continues to rotate and each vortex become more developed, with the maximum vorticity increasing at the center. This process stops near time 0.33 seconds, as in the next image there is a slight decrease in maximum vorticity of the tip vortex. Also near t = 0.33 s, the area of nonzero vorticity begins increasing and the tip vortex begins to stretch. Between t = 0.67 s and t = 0.73 s the tip vortex begins to diminish significantly. The lack of a stopping vortex or splitting of the tip vortex suggests the kinetic energy is not sufficient for abundant turbulence to develop.

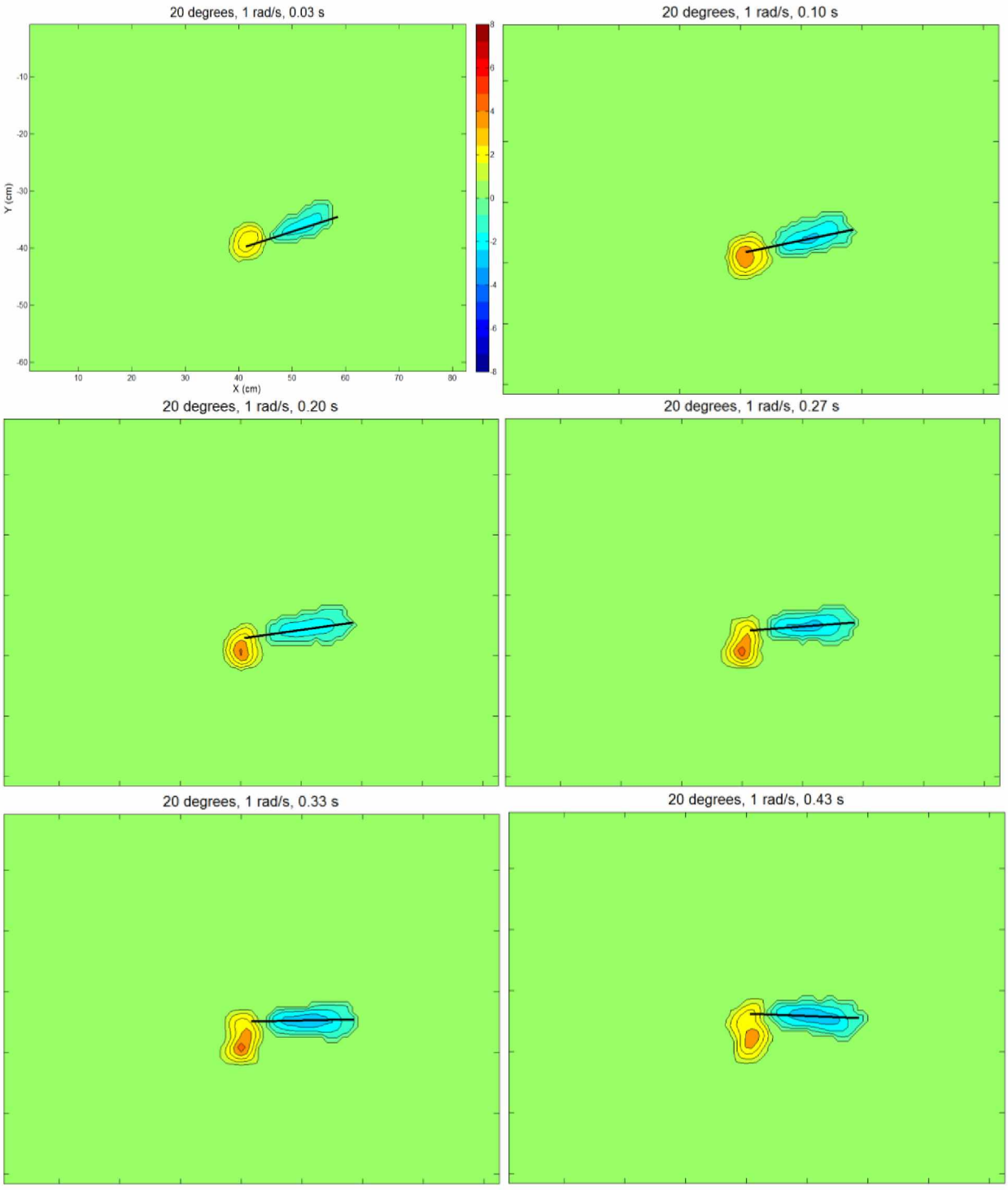

Figure 4.1 Vorticity plots: 20 degrees, 1 rad/s

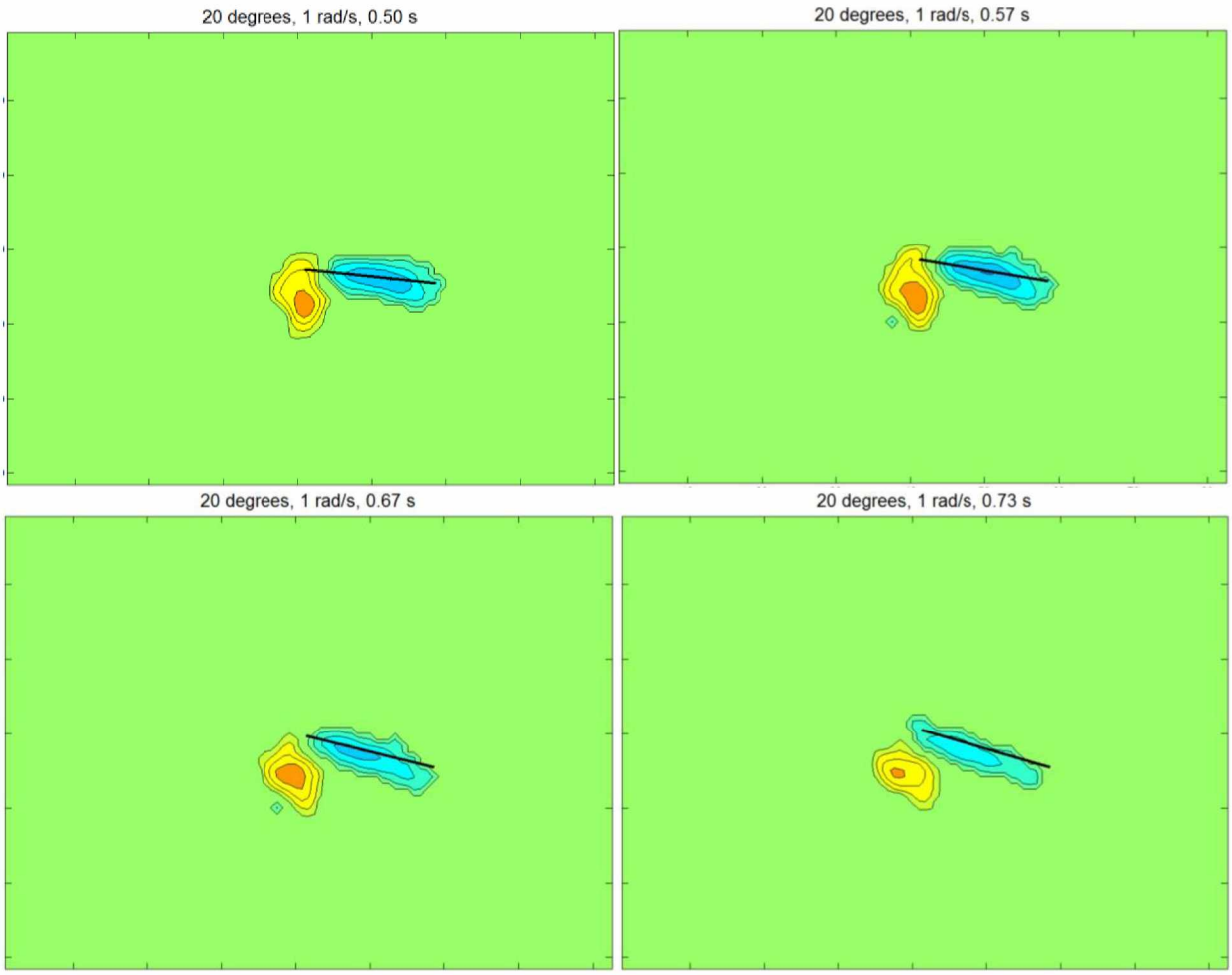

Figure 4.1 continued Vorticity plots: 20 degrees, 1 rad/s

4.3.2 Circulation and Total Kinetic Energy

In the following plot the circulation of both the tip vortex, Vortex A, and the vortex on the upper surface of the plate, Vortex B, are shown for each image used in the analysis. A clear trend is seen in which the circulation of both vortices increases, reaches a peak and begins to decrease. This result makes sense, as the plate begins decelerating and less energy is being added to the flow the levels of circulation begin to decrease, in this case circulation peaks at t = 0.57 s. The small vortex seen developing at this time in the vorticity plots is likely not the cause of the drop in circulation for the tip vortex as the circulation for both Vortex A and Vortex B begins to decrease at this point. The plot of total kinetic energy demonstrates the close

relationship between kinetic energy in the flow and the circulation levels of the developing and fully formed vortices. The maximum value of kinetic energy is lowest in this experiment and this supports the idea that additional vortices did not form due to a lack of energy in the flow.

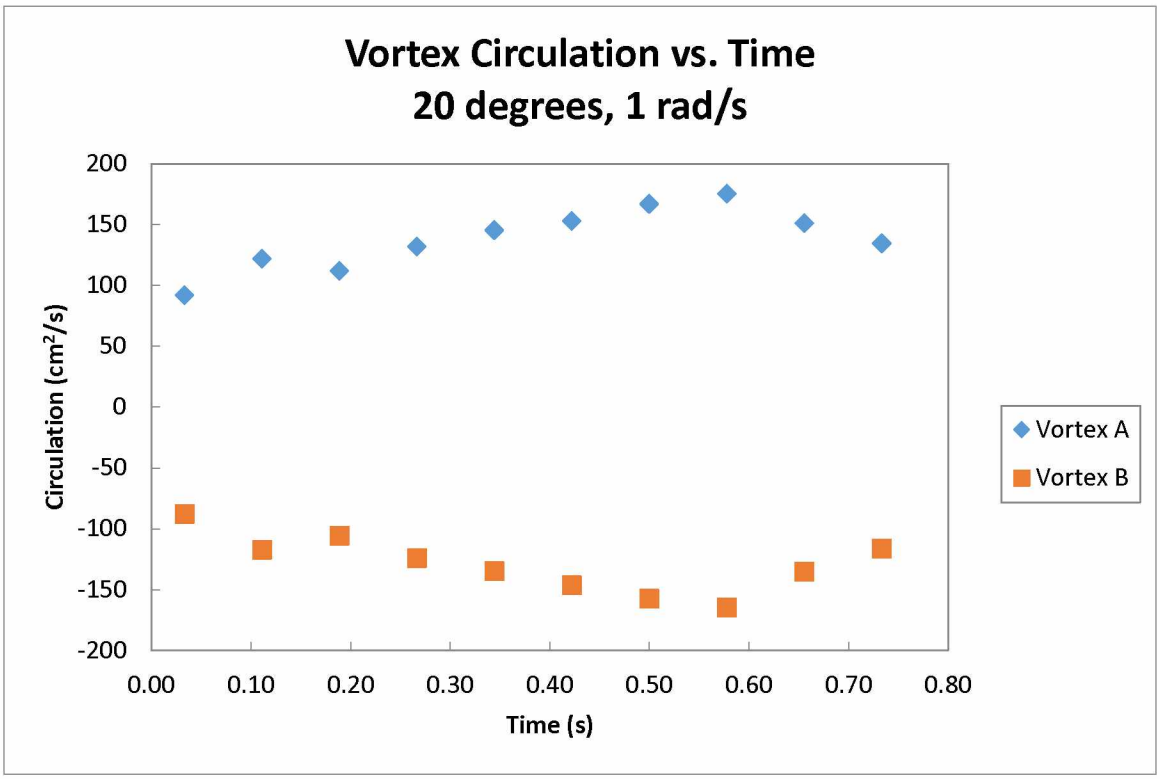

Figure 4.2 Vortex circulation vs. time: 20 degrees, 1 rad/s

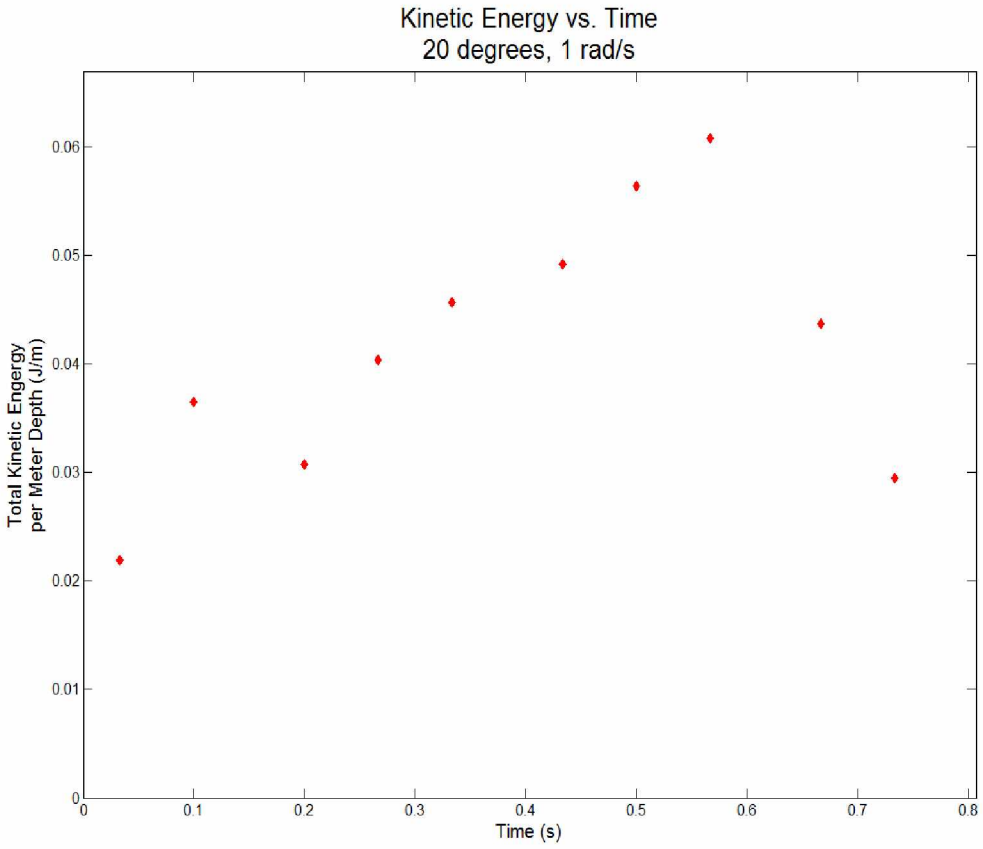

Figure 4.3 Kinetic energy vs. time: 20 degrees, 1 rad/s

4.3.3 Vortex Trajectory

The following plot shows the path of the tip vortex during the time frame being analyzed. The general direction of travel was up and to the left. However at the early stages of vortex development the vortex center primarily moved away from the plate. Though this appears to be an extreme example, it is roughly in keeping with other trajectory plots which show that the travel of the tip vortex is limited during the first few time periods.

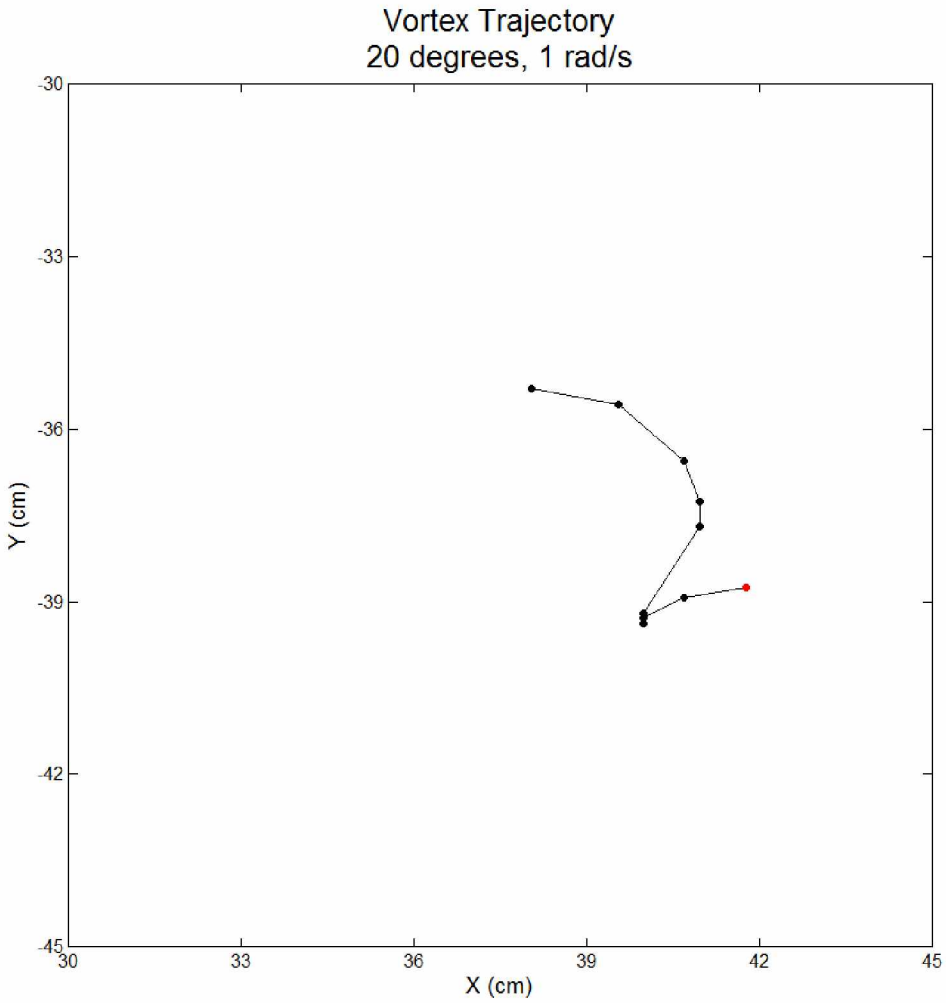

Figure 4.4 Vortex trajectory: 20 degrees, 1 rad/s, red marker indicates starting point

4.4 Amplitude: 20 degrees, Speed 2 rad/s

4.4.1 Vorticity Evolution

The following plots show the vorticity evolution for the higher speed test at an amplitude of 20 degrees. The tip vortex develops much as it did in the test at 1 rad/s but the area of non-zero vorticity at early time periods is significantly larger. At t = 0.17 s the area of vorticity at the tip begins a necking process that continues until t = 0.30 s. By this time the lone tip vortex has begun to split into two distinct areas, but does not completely shed. At t = 0.33 s a stopping

vortex has formed slightly above the tip. This stopping vortex has opposite rotation and thus opposite vorticity as the tip vortex. In the final image the tip vortex has lost some vorticity while the stopping vortex has experienced a rise in peak vorticity.

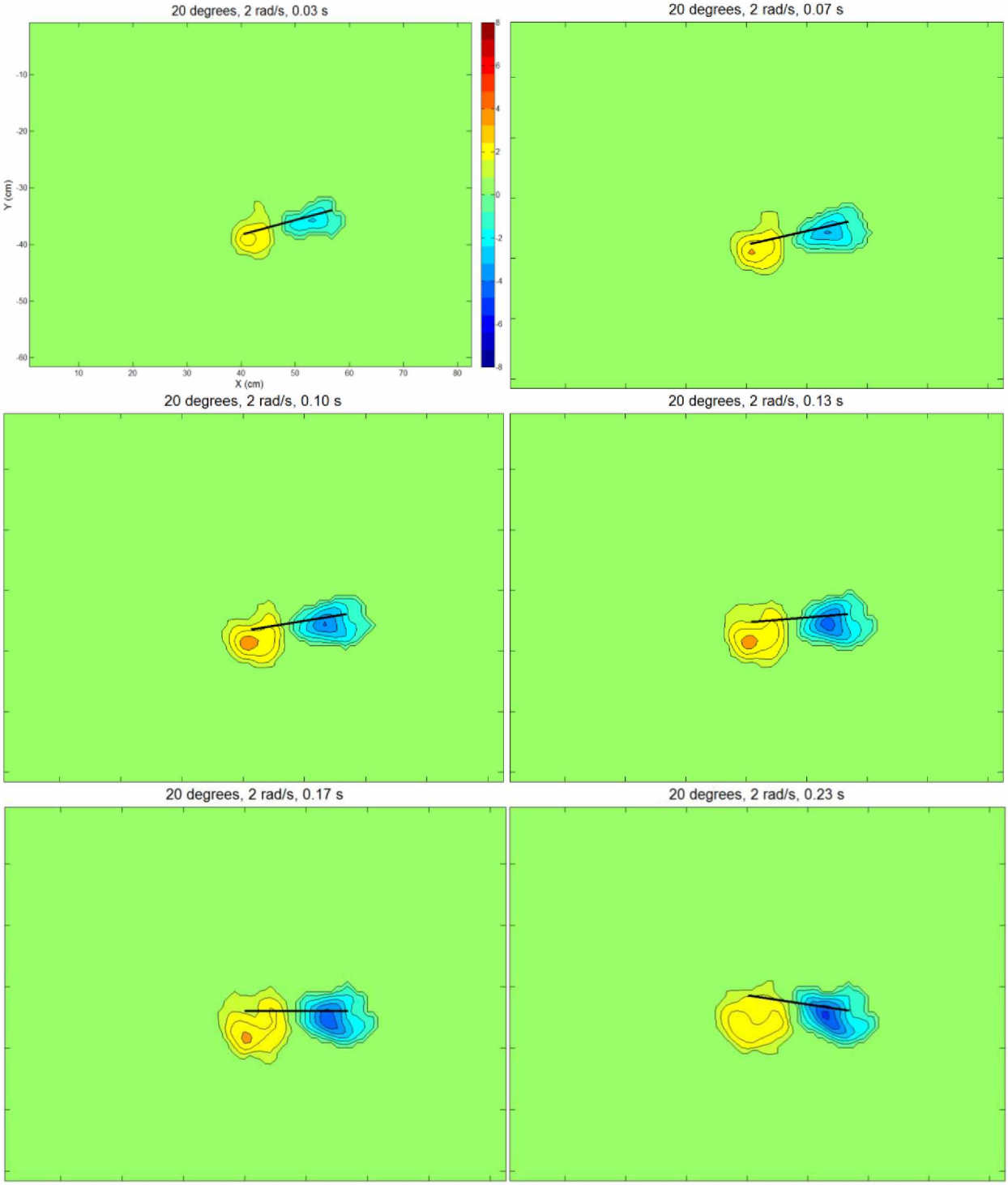

Figure 4.5 Vorticity plots: 20 degrees, 2 rad/s

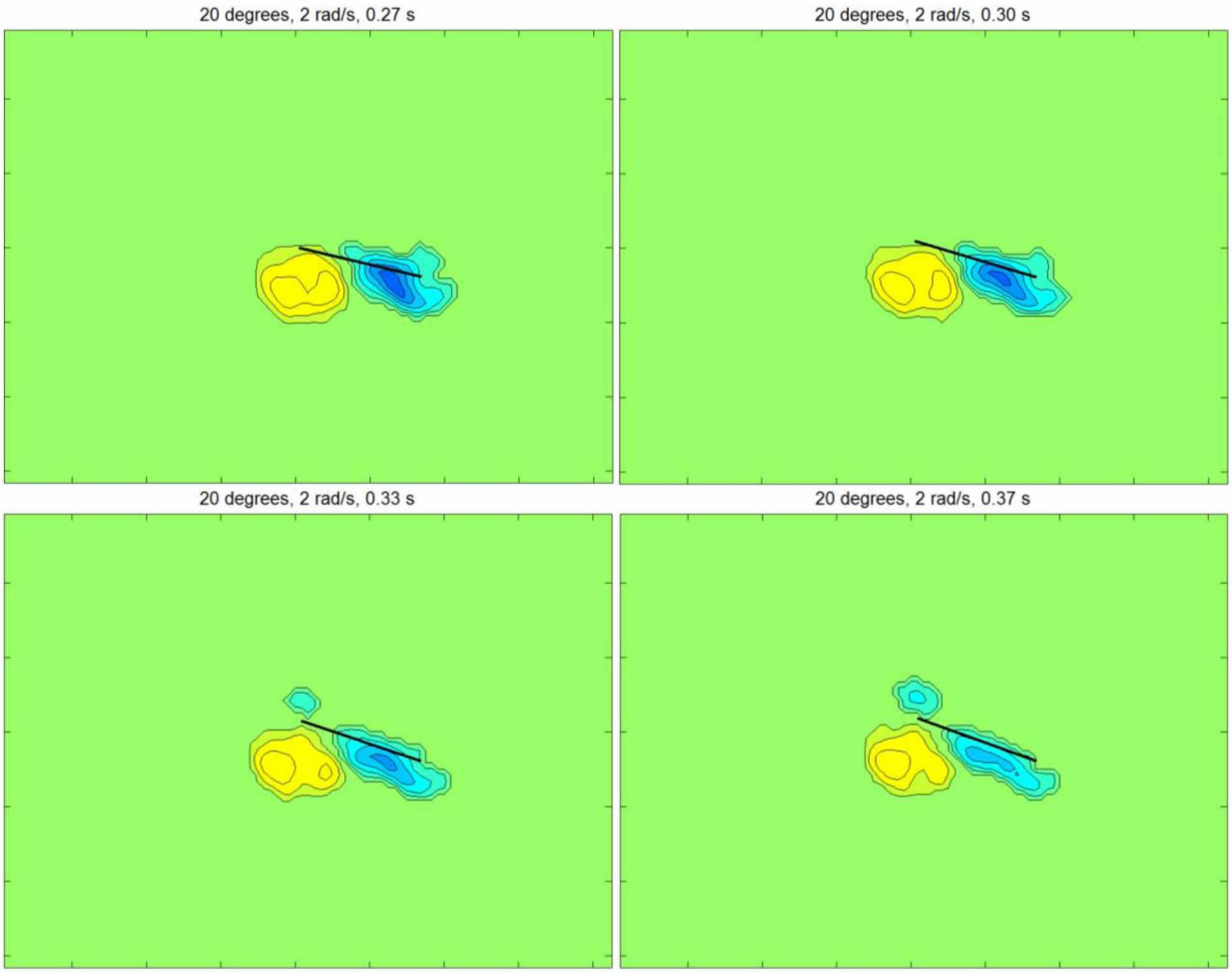

Figure 4.5 continued Vorticity plots: 20 degrees, 2 rad/s

4.4.2 Circulation and Total Kinetic Energy

The circulation plot for this trial shows the expected, gradual increase, peak, and decrease in vorticity for both the tip vortex and the vortex that clings to the plate. The plot of kinetic energy shows a similar trend. In this case peak kinetic energy was significantly greater than the trial a 1 rad/s, which correlates to the formation of the stopping vortex seen in this experiment.

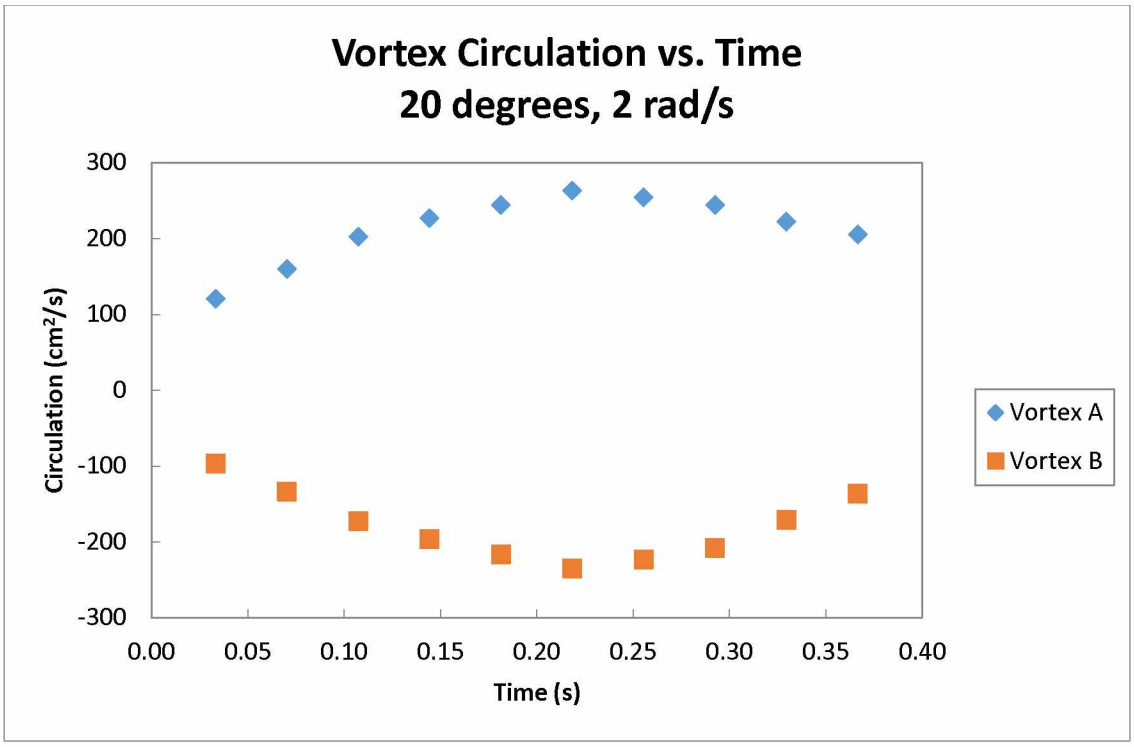

Figure 4.6 Vortex circulation vs. time: 20 degrees, 2 rad/s

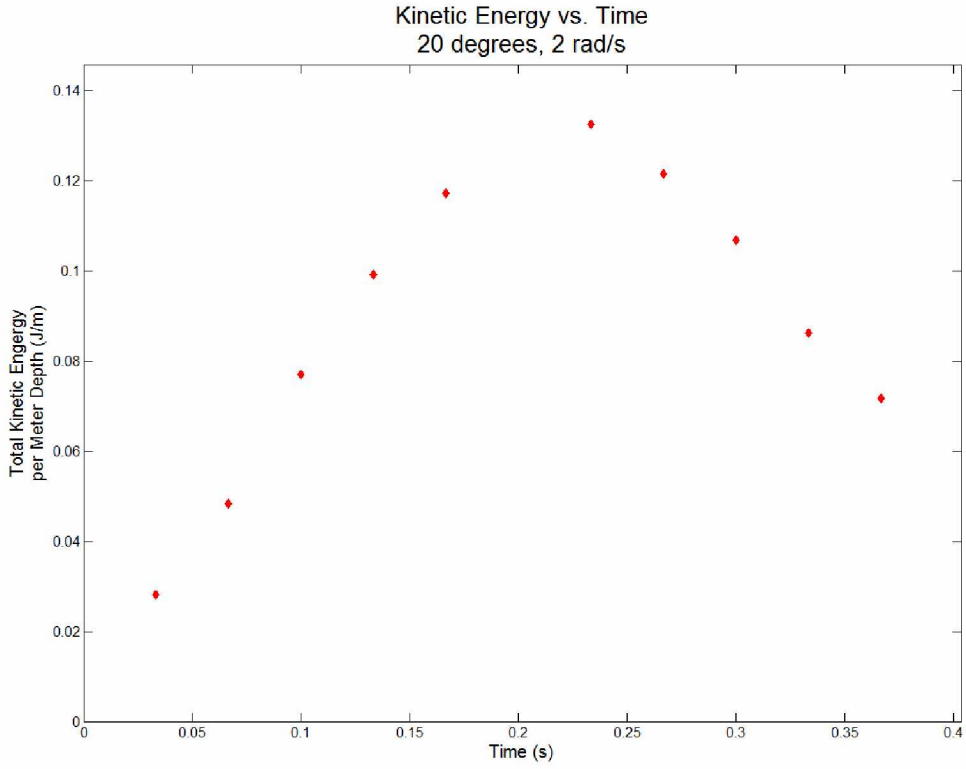

Figure 4.7 Kinetic energy vs. time: 20 degrees, 2 rad/s

4.4.3 Vortex Trajectory

The trajectory of the tip vortex in this trial is generally up and to the left. Again, as indicated by the closely spaced points in the lower right hand area of movement, it appears that the vortex is slow to begin traveling. However, after this intial period the vortex makes a consistant move up and to the left, trailing the tip of the plate in its generally upward path.

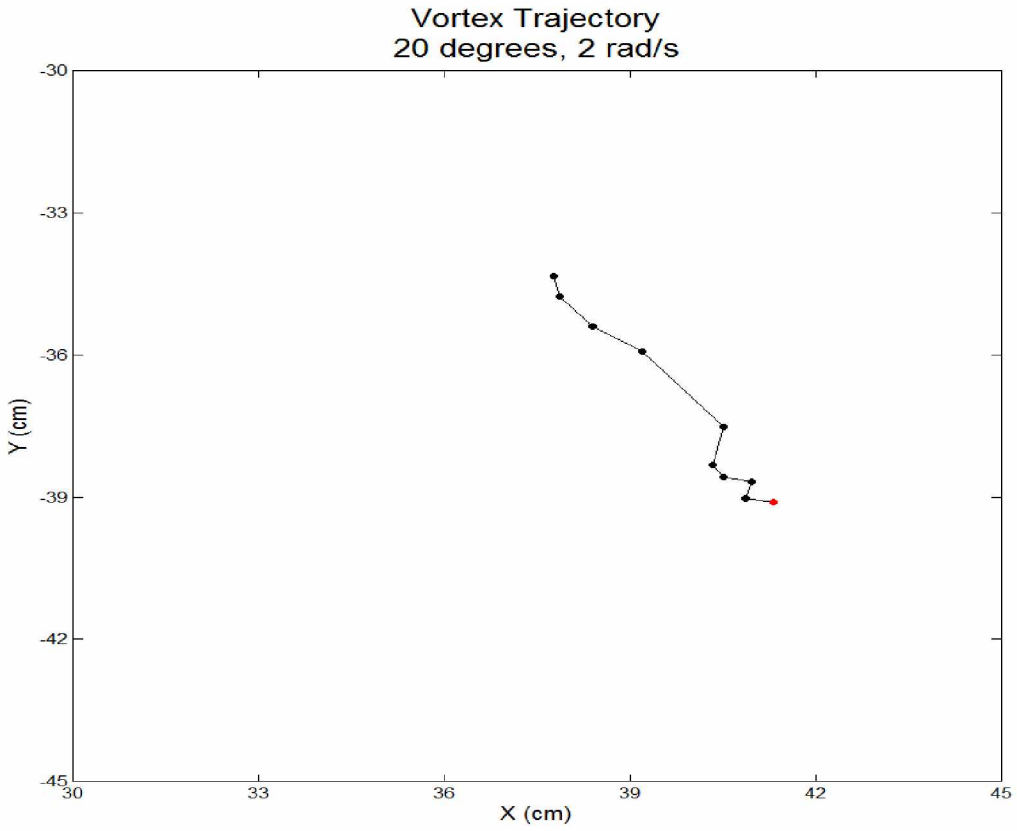

Figure 4.8 Vortex trajectory: 20 degrees, 2 rad/s, red marker indicates starting point

4.5 Amplitude: 30 degrees, Speed 1 rad/s

4.5.1 Vorticity Evolution

The evolution of the vortices in the trial at 30 degrees amplitude and a speed of 1 rad/s is the first to show a significant tendancy of the tip vortex to shed. From the first time period until t = 0.50 s both vortices develop normally, but at this time an area of vorticity can be seen closely surrounding the tip of the plate and necking off of the tip vortex. Some form of necking of the tip vortex toward the tip of the plate is seen until t = 1.10 s. Here the tip vortex has formed two centers of vorticity but is no longer necking with the plate's tip. A stopping vortex is also seen at this point, it has begun to interact with the secondary vortex that remains close to the plate.

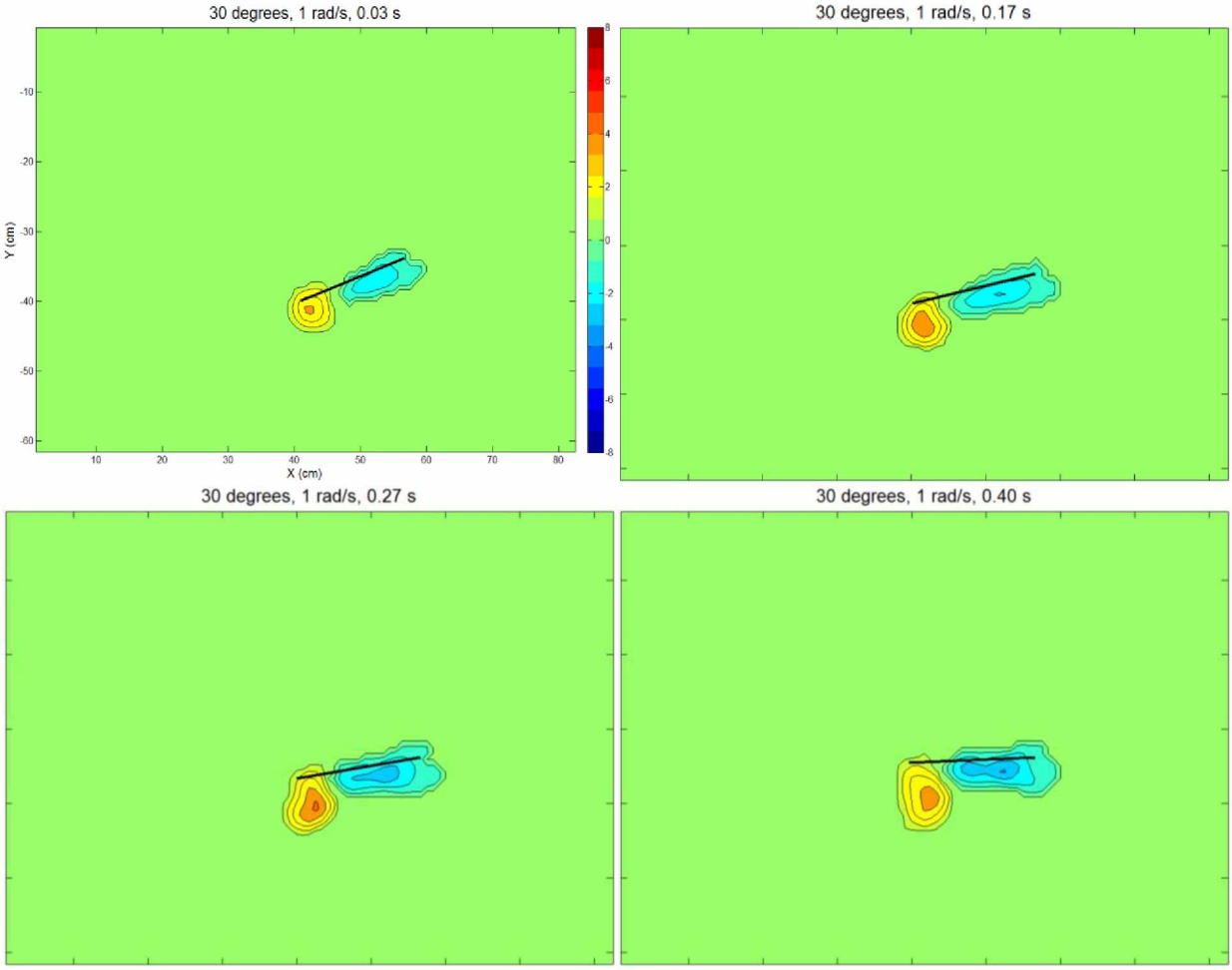

Figure 4.9 Vorticity plots: 30 degrees, 1 rad/s

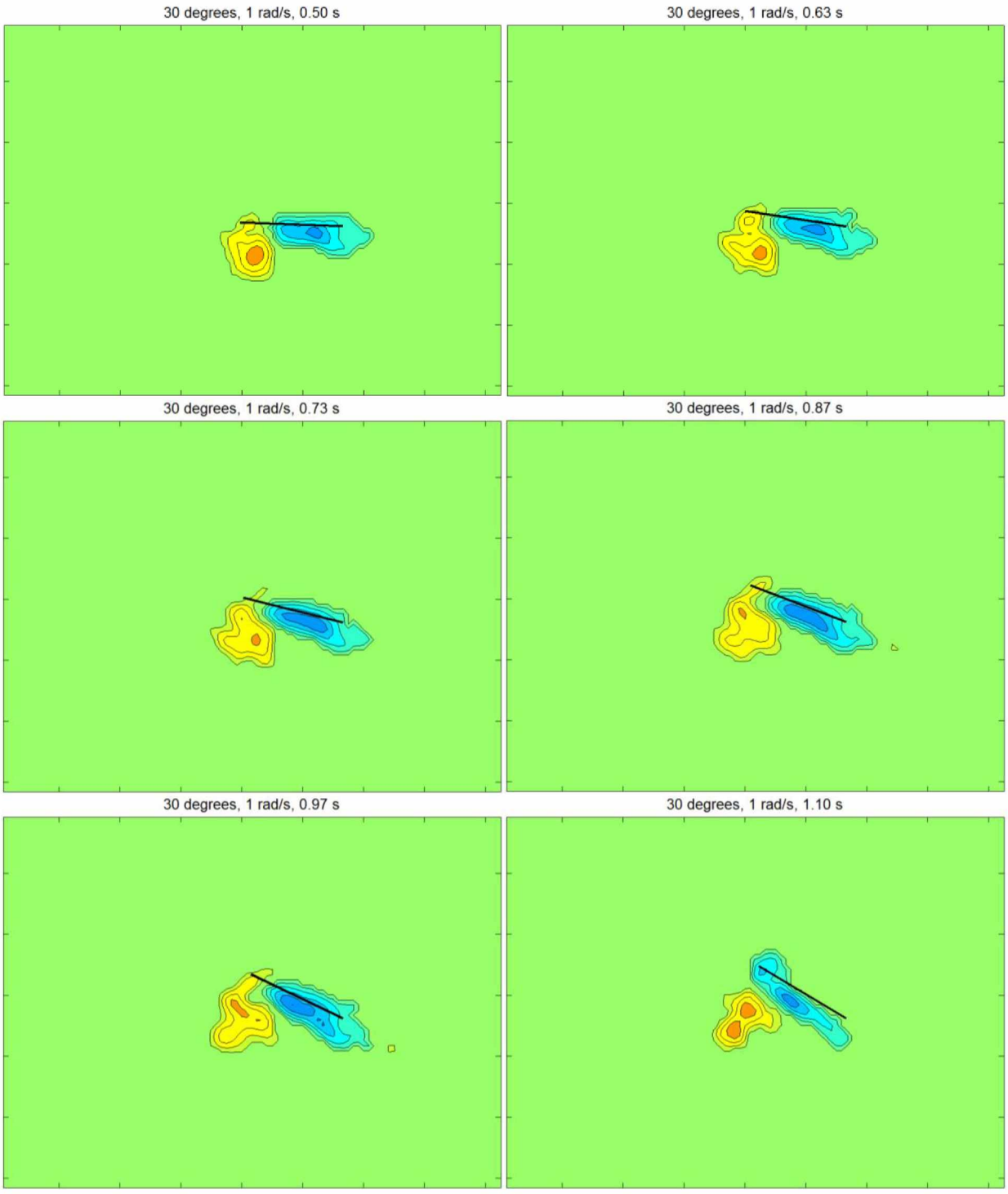

Figure 4.9 continued Vorticity plots: 30 degrees, 1 rad/s

4.5.2 Circulation and Total Kinetic Energy

The circulation and kinetic energy plots for this trial both show a steady increase followed by a sharp drop when the plate comes to rest. This indicates that enough energy is added to the flow early on to allow the two original vortices to continue entraining fluid until the plate's motion has nearly stopped. When the plate is no longer being forced to move and kinetic energy is not being added to the flow, the original vortices rapidly lose circulation, though the vortex that remains near the plate seems to lose more circulation in the final time period. This is because wall-bounded vorticity disippates faster due to larger viscous effect near the solid-fluid interface.

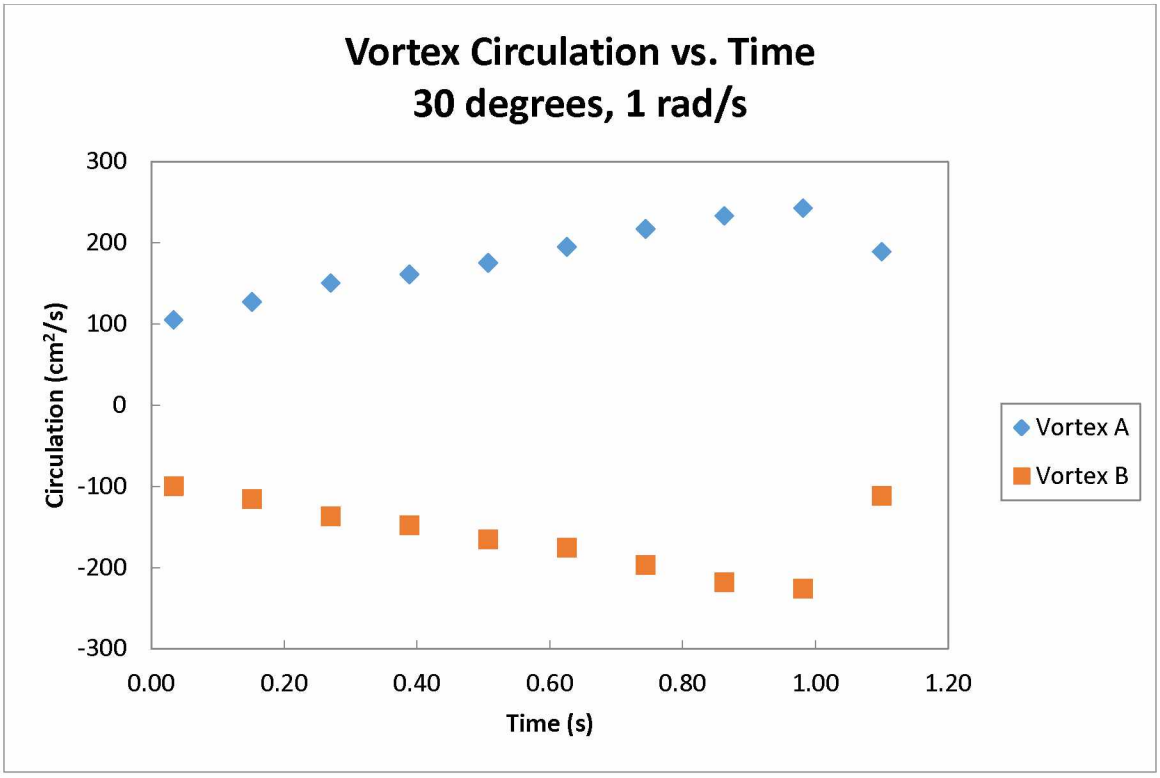

Figure 4.10 Vortex circulation vs. time: 30 degrees, 1 rad/s

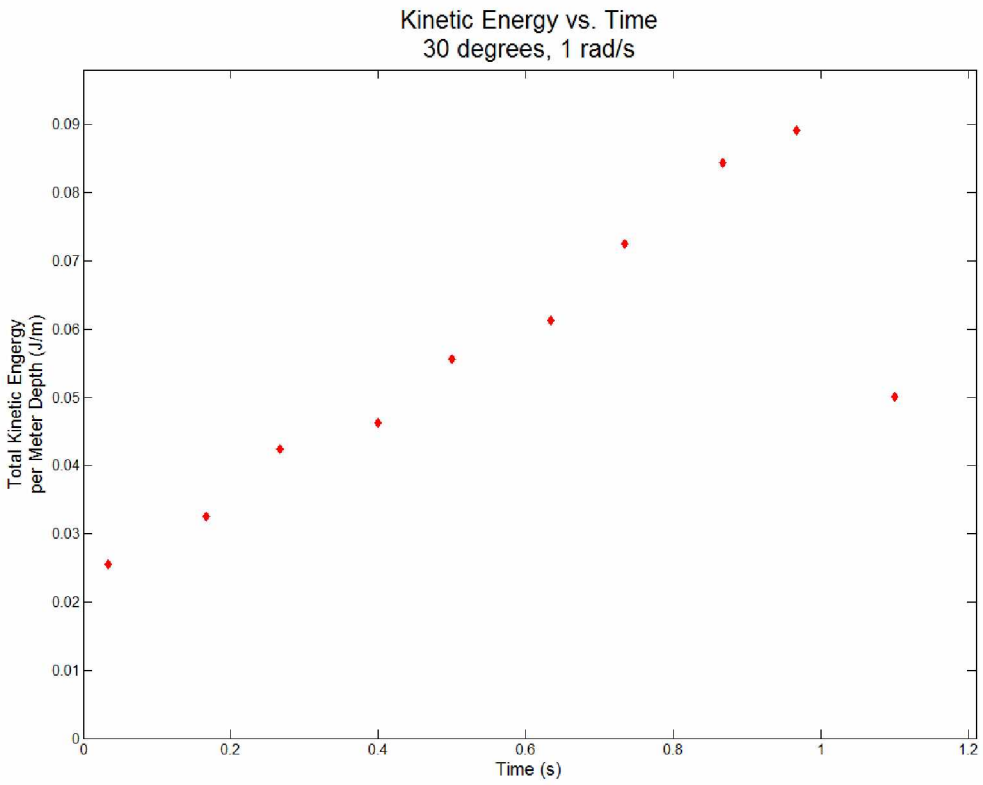

Figure 4.11 Kinetic energy vs. time: 30 degrees, 1 rad/s

4.5.3 Vortex Trajectory

This trajectory plot shows primarily upward movement of the tip vortex. After making a large jump in the last few time periods the vortex is shifted slightly to the left of its previous path. This is corresponds to the dissipation of the area of highest vorticity in the vortex and growth of another area of vorticity up and to the left of the original center.

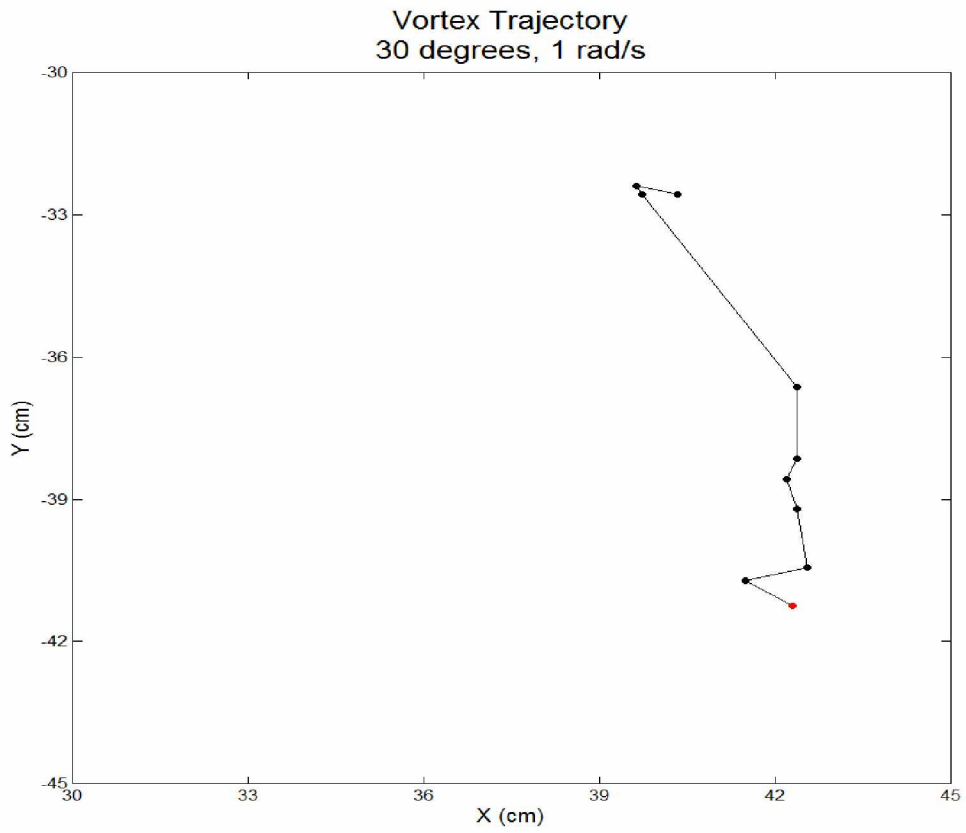

Figure 4.12 Vortex trajectory: 30 degrees, 1 rad/s, red marker indicates starting point

4.6 Amplitude: 30 degrees, Speed 2 rad/s

4.6.1 Vorticity Evolution

The evolution of the vortices in this trial is similar to that of the other trial at 30 degrees amplitude. However, in this experiment the vortex that hugs the surface of the plate demonstrates significant necking, and at time t = 0.27 s a second center of vorticity has appeared in the vortex. A stopping vortex forms above the tip of the plate at t = 0.43 s and eventually merges with the vortex of similar rotation. The tip vortex, again, necks and eventually sheds at t = 0.53 s.

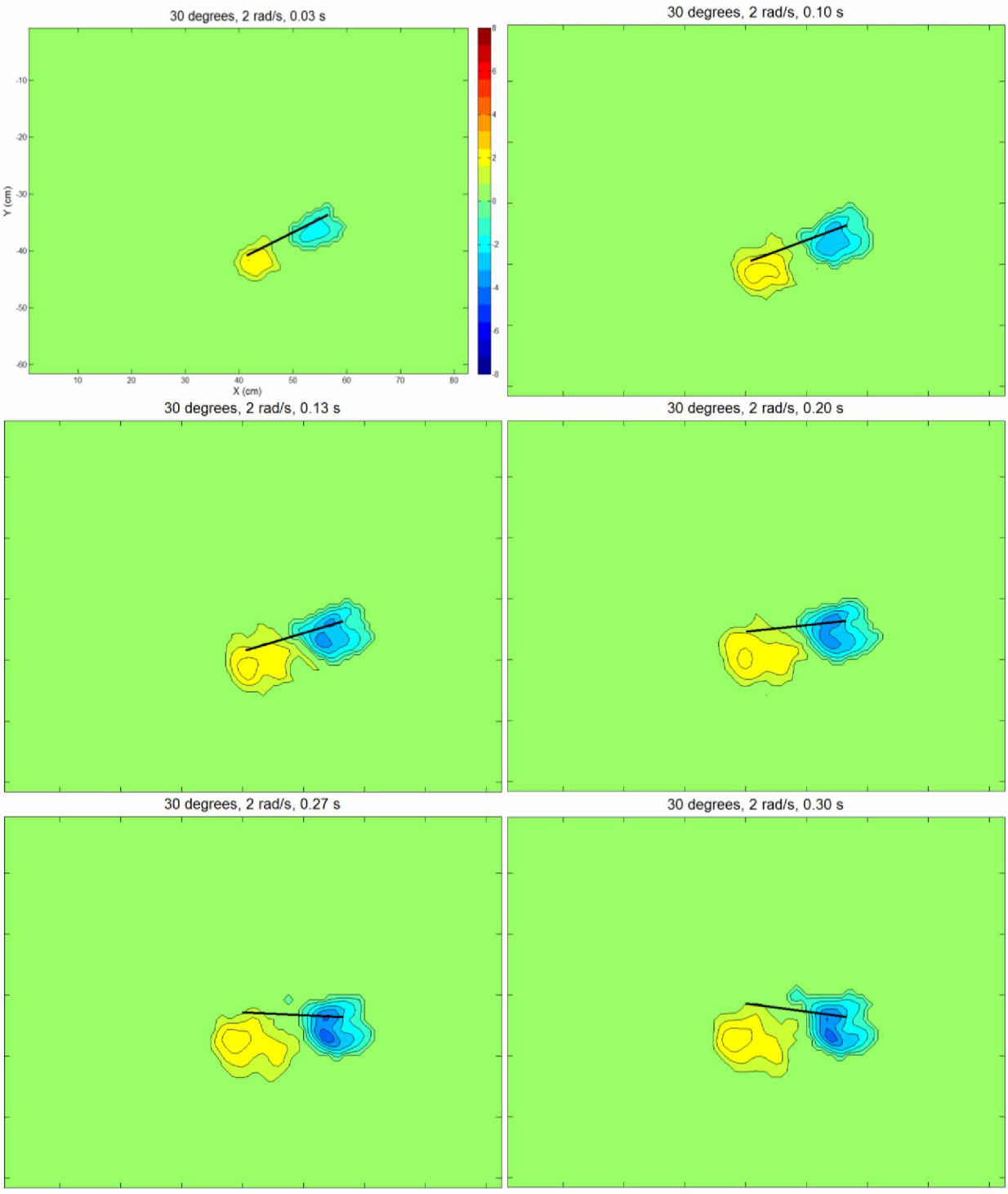

Figure 4.13 Vorticity plots: 30 degrees, 2 rad/s

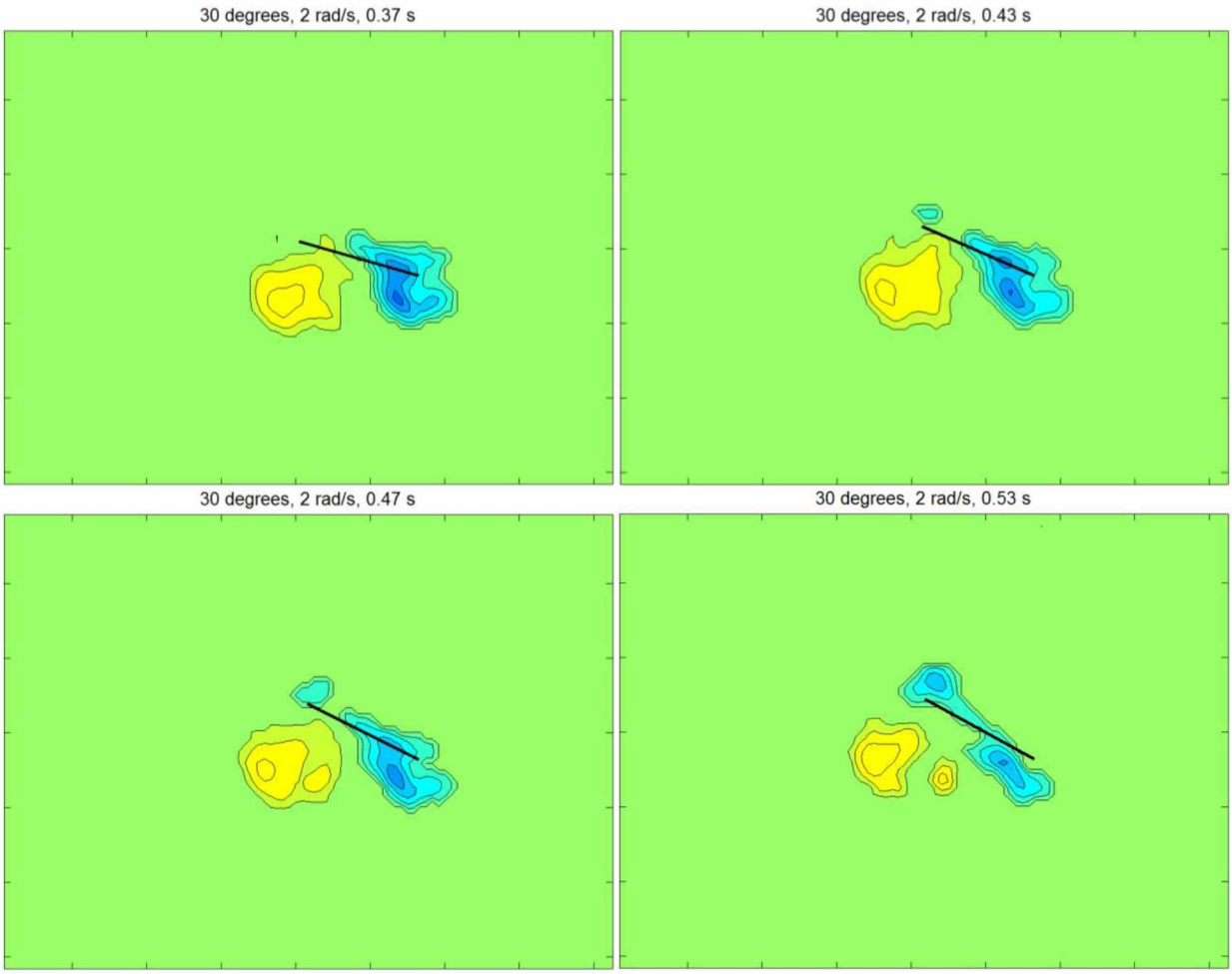

Figure 4.13 continued Vorticity plots: 30 degrees, 2 rad/s

4.6.2 Circulation and Total Kinetic Energy

The circulation and kinetic energy plots below show the typical trend. A comparison of the circulation of the two vortices at the same points in time shows that the plate hugging vortex loses circulation more rapidly after the point of maximum circulation than the tip vortex. This occurs despite the circulation levels being near equal in magnitude and trend for the rest of the time periods. This is because wall-bounded vorticity disippates faster due to large viscous effect near the solid-fluid interface. Though the vorticity plots show the tip vortex shedding as the plate comes to a stop, the circulation of the original tip vortex is not reduced at the same rate as the plate hugging vortex.

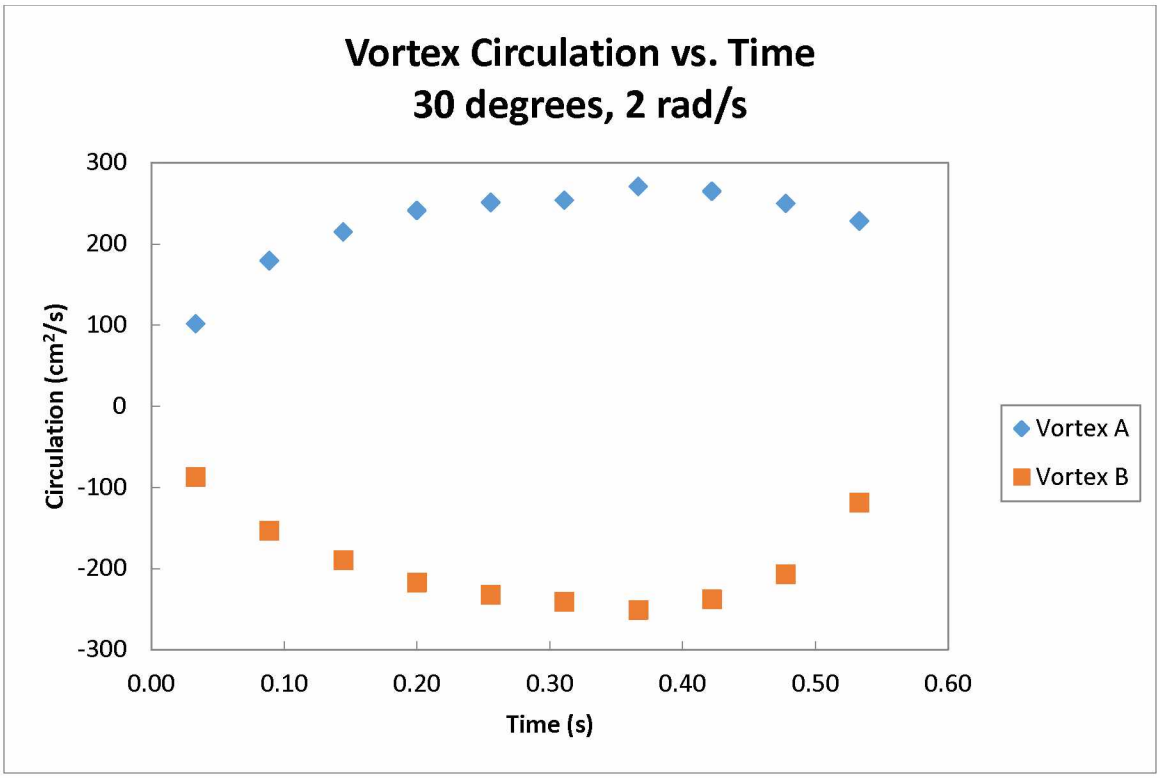

Figure 4.14 Vortex circulation vs. time: 30 degrees, 2 rad/s

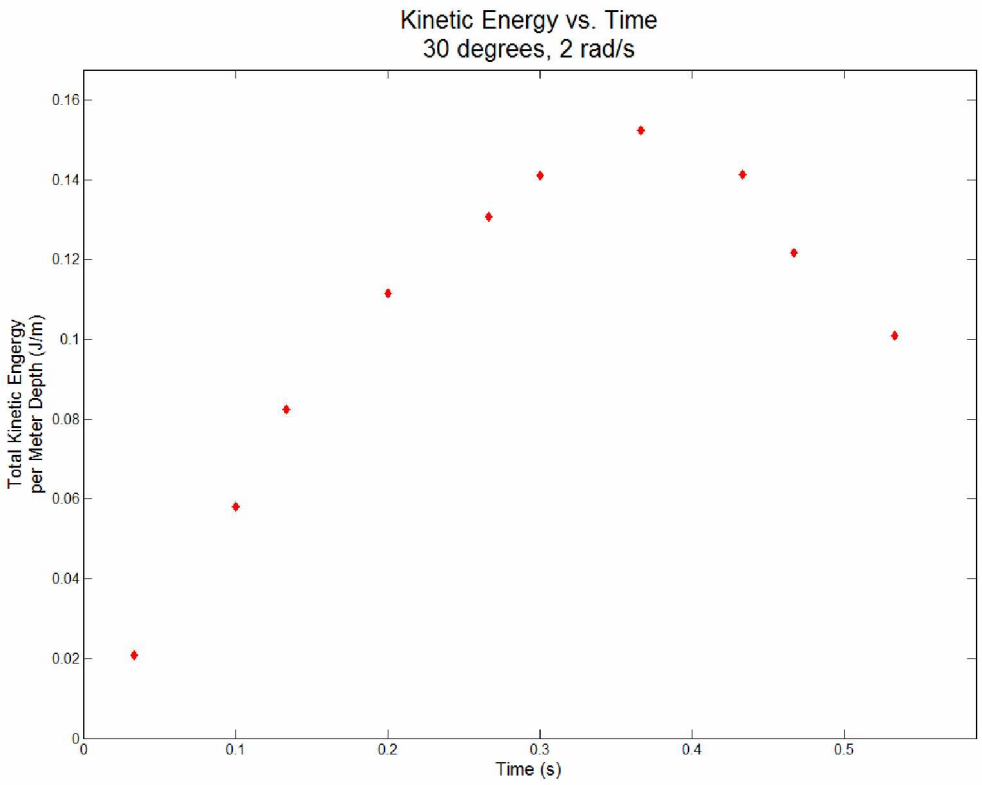

Figure 4.15 Kinetic energy vs. time: 30 degrees, 2 rad/s

4.6.3 Vortex Trajectory

The trajectory of the tip vortex in this experiment was along a nearly straight path. The direction of this path is up and to the left. While mainly consistent in direction the tip vortex does not always move a consistent distance during each time period. This is due to a shallow gradient of vorticity seen in the tip vortex, which maked determining the true center of vorticity difficult.

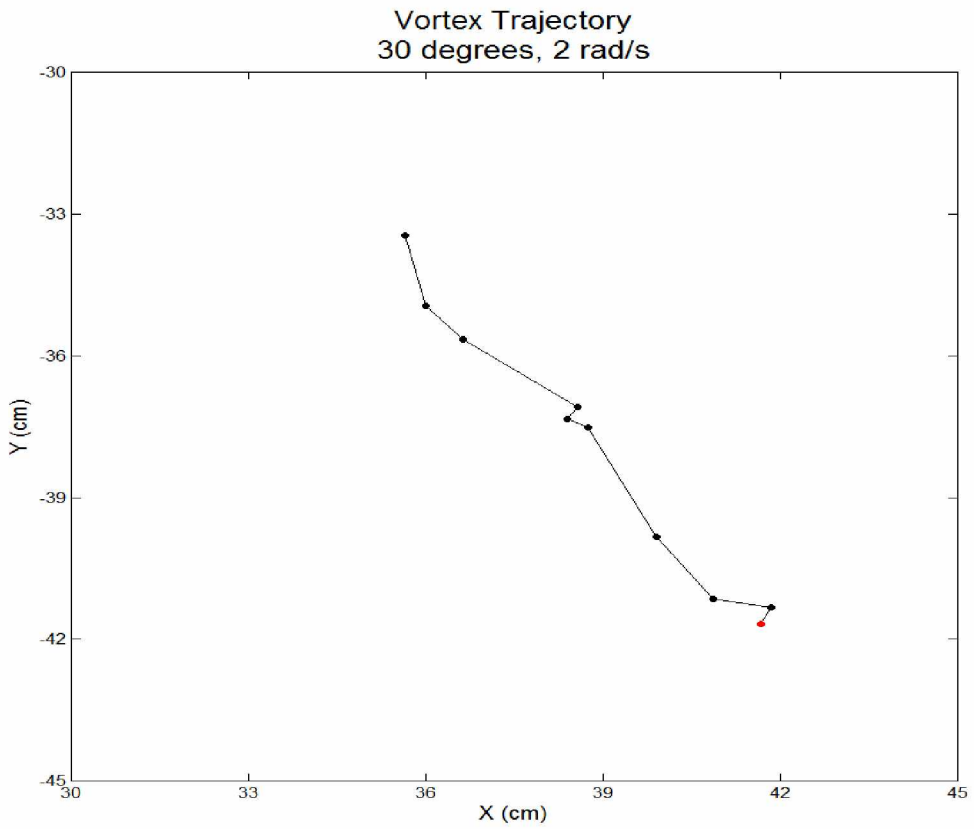

Figure 4.16 Vortex trajectory: 30 degrees, 2 rad/s, red marker indicates starting point

4.7 Amplitude: 40 degrees, Speed 1 rad/s

4.7.1 Vorticity Evolution

The evolution of the vortices in this trial shows a feature unseen in the experiments with lower amplitudes; the tip vortex necks at two different locations. The vortices develop uniformly until t = 0.87 s where the tip vortex begins necking toward the tip of the plate. At t = 1.20 s the neck still exists and a second has formed to the right of the first. At this point the maximum vorticity of the tip vortex has decreased slightly. The necking and reduction in maximum vorticity continue into the next time period, but at t = 1.53 s the secondary neck has retracted and the maximum vorticity of the tip vortex has increased slightly.

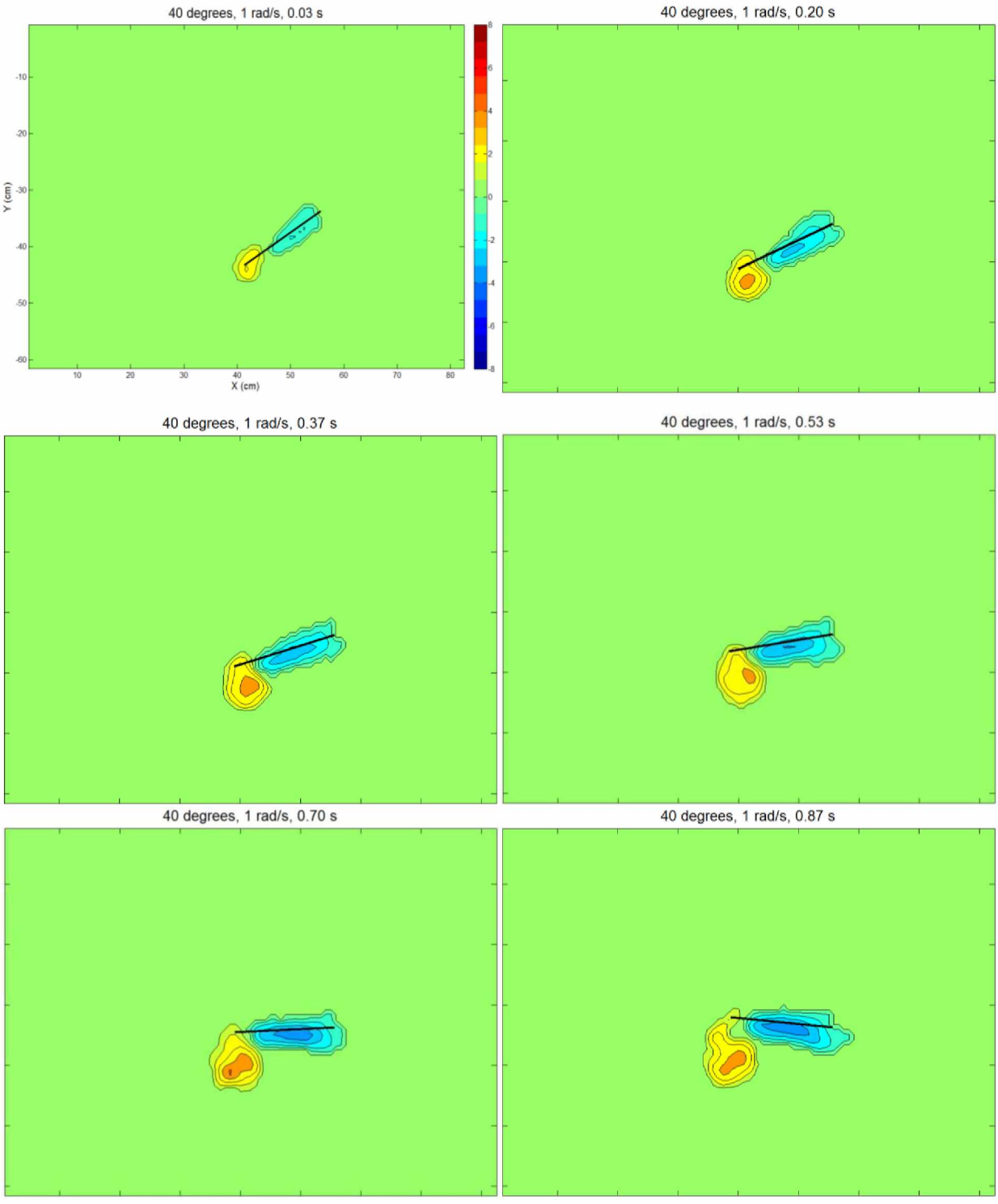

Figure 4.17 Vorticity plots: 40 degrees, 1 rad/s

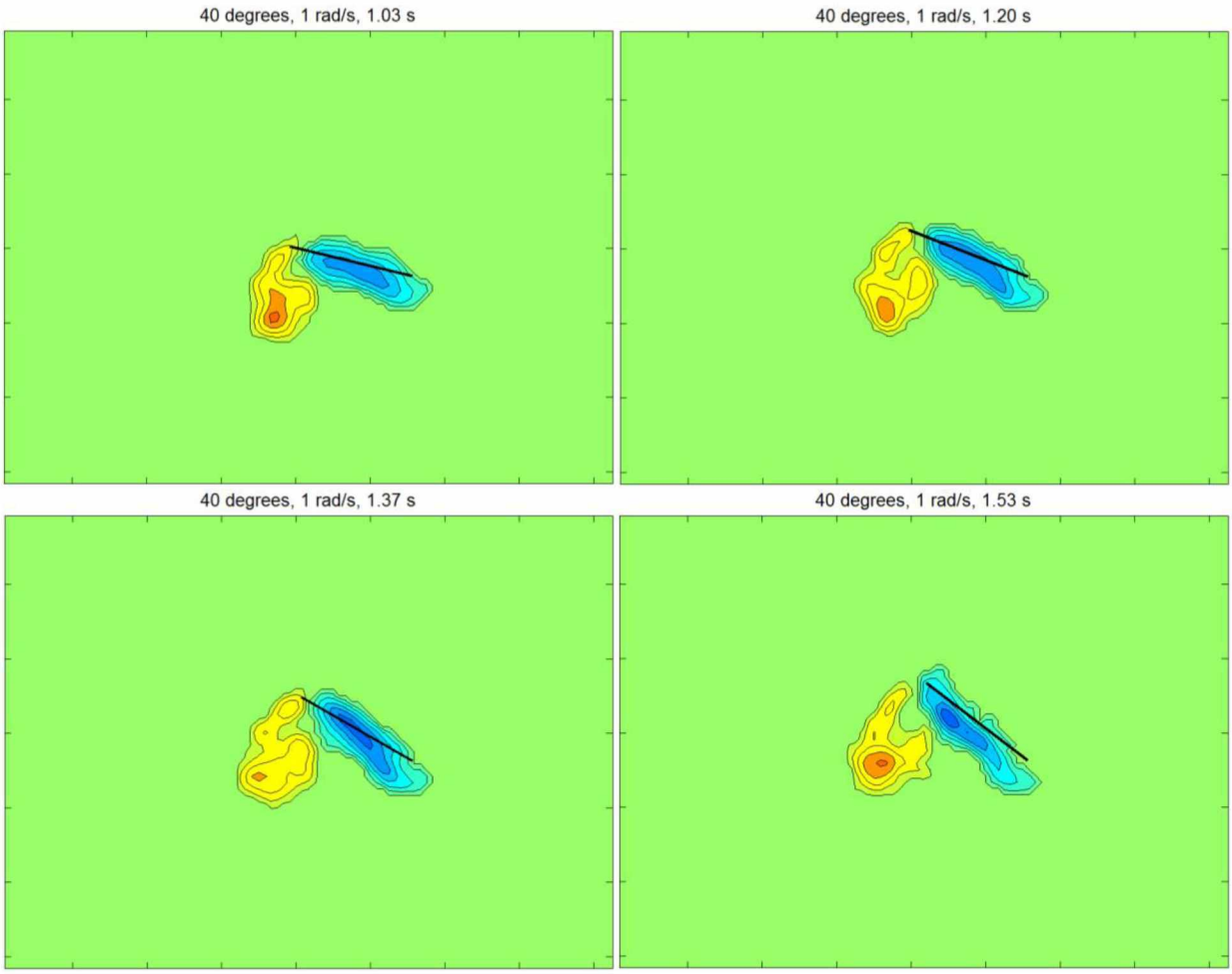

Figure 4.17 continued Vorticity plots: 40 degrees, 1 rad/s

4.7.2 Circulation and Total Kinetic Energy

The circulation and kinetic energy plots show expected behavior. The trend of each data set remains consistent and the drops in circulation and kinetic energy occur in the same time period. This is the expected behavior for these data sets as neither vortex experienced complete shedding or significant splitting of its center of vorticity.

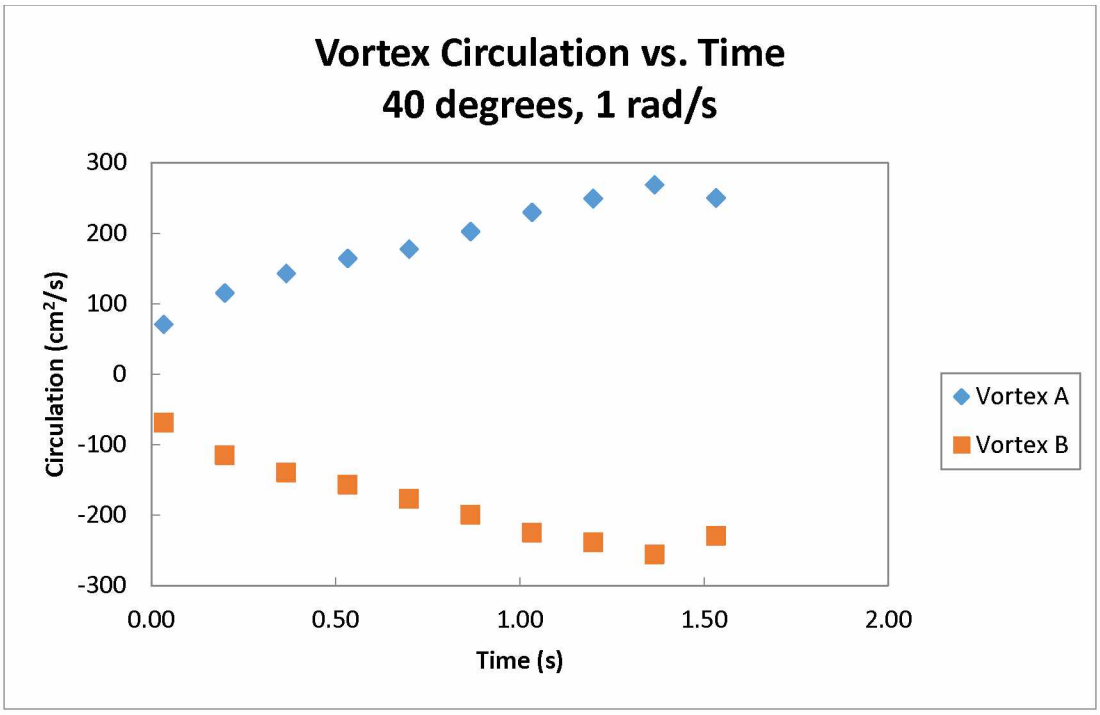

Figure 4.18 Vortex circulation vs. time: 40 degrees, 1 rad/s

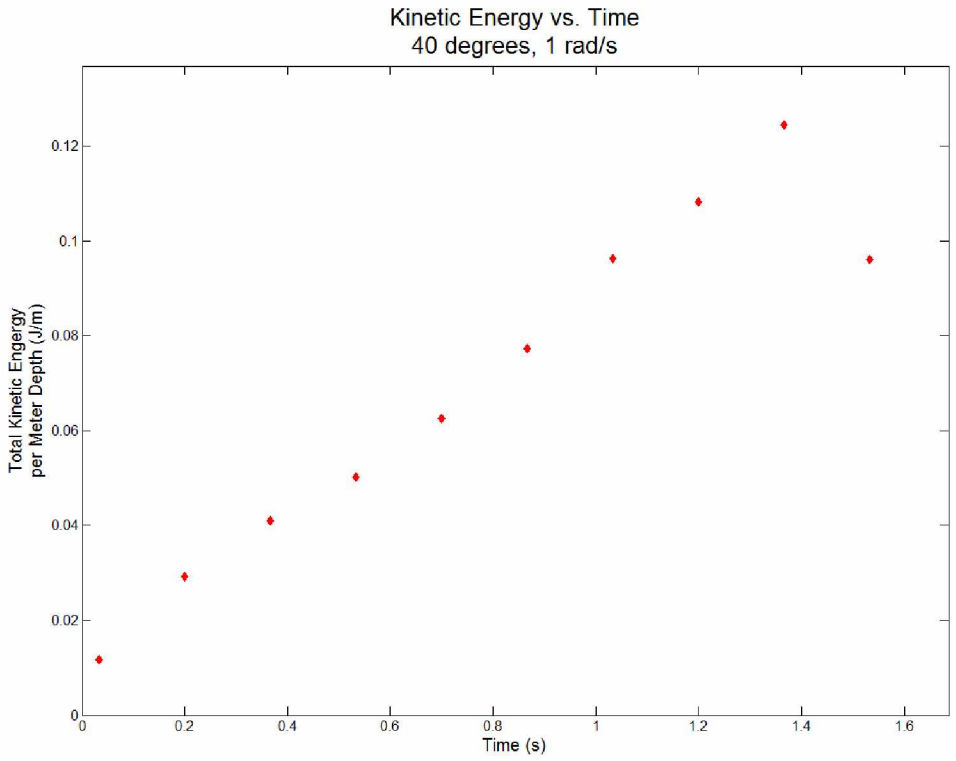

Figure 4.19 Kinetic energy vs. time: 40 degrees, 1 rad/s

4.7.3 Vortex Trajectory

The trajectory of the tip vortex maintains a path that is generally directed up and to the left. The distance between tracking points along the path is fairly uniform. However, there are some deviations to the right of the general path. As can be confirmed by referencing the vorticity evolution plots, these deviations are the result of some shifting of the area of maximum vorticity within the general center of the total area of vorticity.

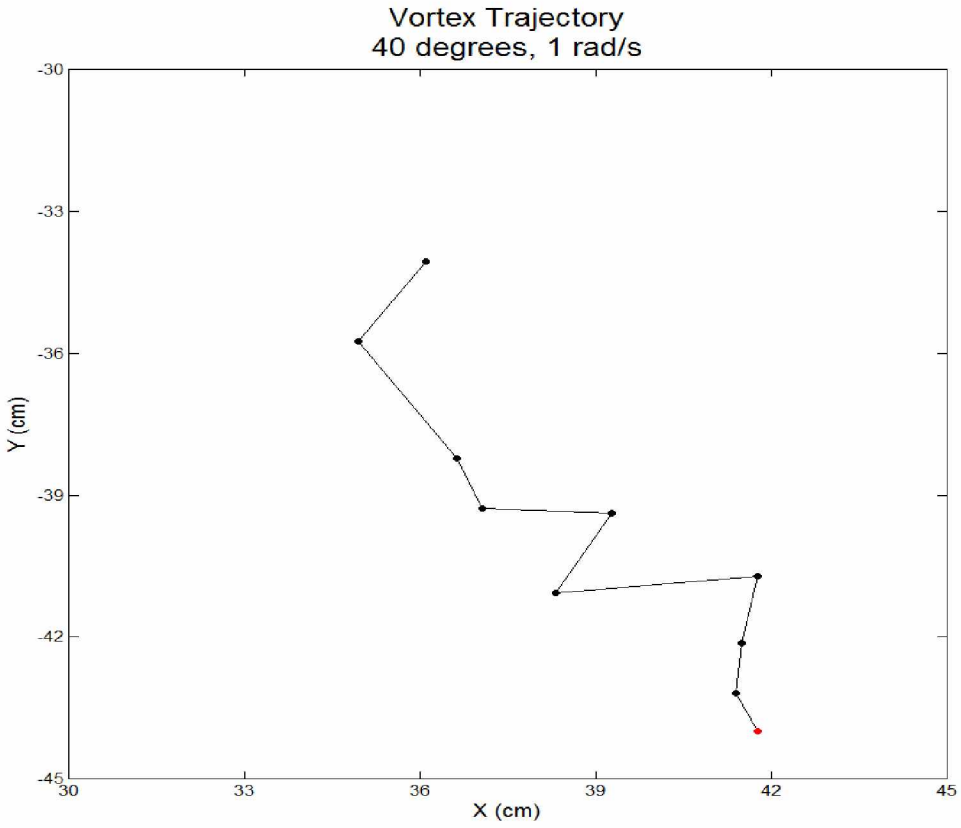

Figure 4.20 Vortex trajectory: 40 degrees, 1 rad/s, red marker indicates starting point

4.8 Amplitude: 40 degrees, Speed 2 rad/s

4.8.1 Vorticity Evolution

The experiment conducted at an amplitude of 40 degrees and speed of 2 rads/s was the most energetic experiment performed. This is reflected in the complex nature of the vortex evolution. The tip vortex begins necking early on at t = 0.17 s, repeatedly necks, and develops a strong area of vorticity on its right side, most notable at t = 0.60 s. A vortex of opposite rotation but similar vorticity has formed next to the shed vortex having resulted from the earlier turbulence in the region. In the final image the plate has come to rest and the area to the right of the tip vortex that has been intermittently deforming has finally shed. A stopping vortex has formed at t = 0.40 s and the plate hugging vortex has developed a second strong central area of vorticity; the two vortices grow closer together and ultimately merge at t = 0.60 s.

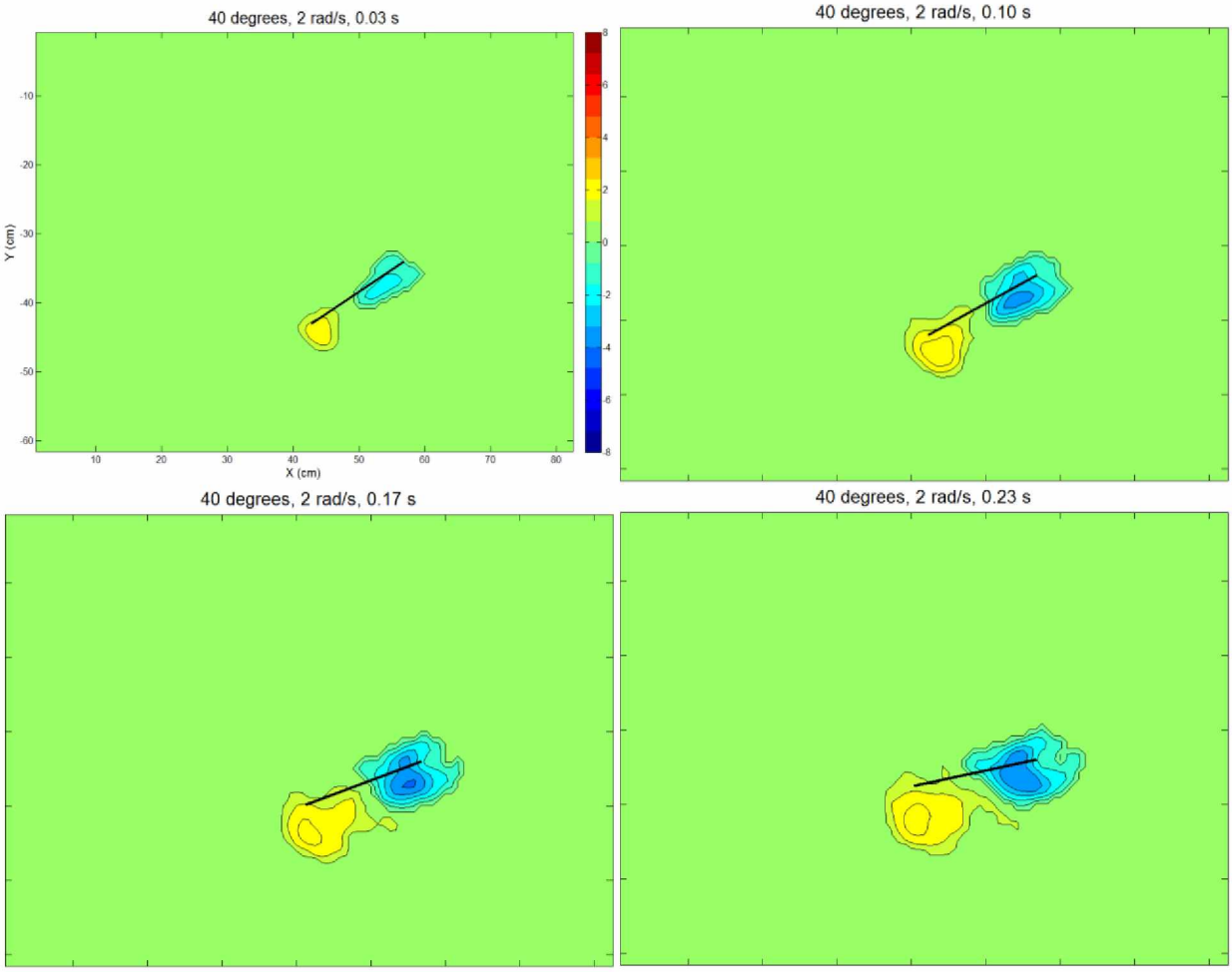

Figure 4.21 Vorticity plots: 40 degrees, 2 rad/s

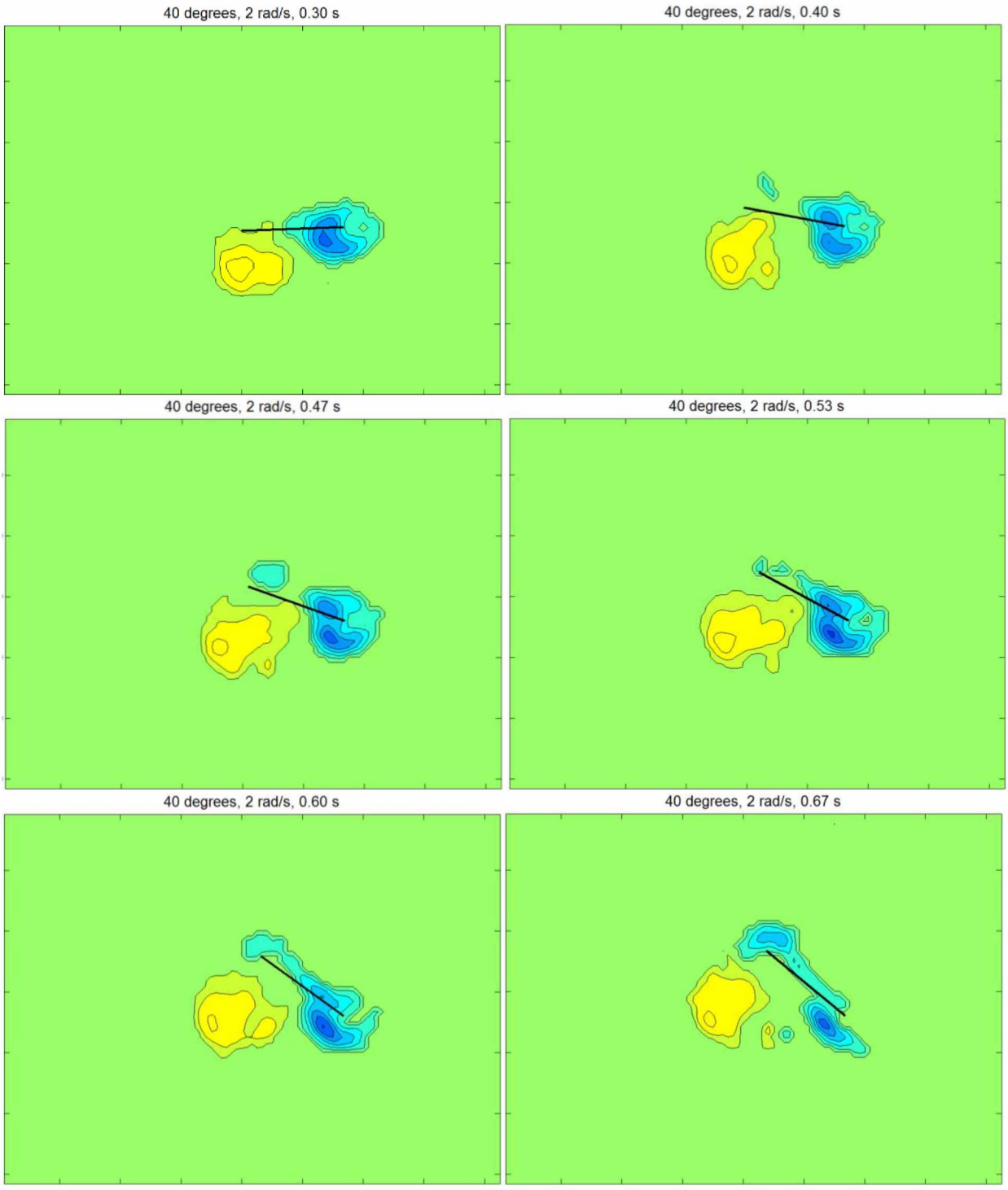

Figure 4.21 continued Vorticity plots: 40 degrees, 2 rad/s

4.8.2 Circulation and Total Kinetic Energy

The circulation plot shows that the plate hugging vortex struggled to reach the same magnitude of circulation as the tip vortex. This is due to the high acceleration and deceleration of the plate in this experiment. The plate hugging vortex is very energetic and is perturbed by the suface of the plate. These factors add to its instability and account for the constant loss of circulation. This is not depicted by the kinetic energy plot because the loss of circulation in this vortex, though disproportionate to the other, does not cause a loss of kinetic energy from the fluid volume as a whole.

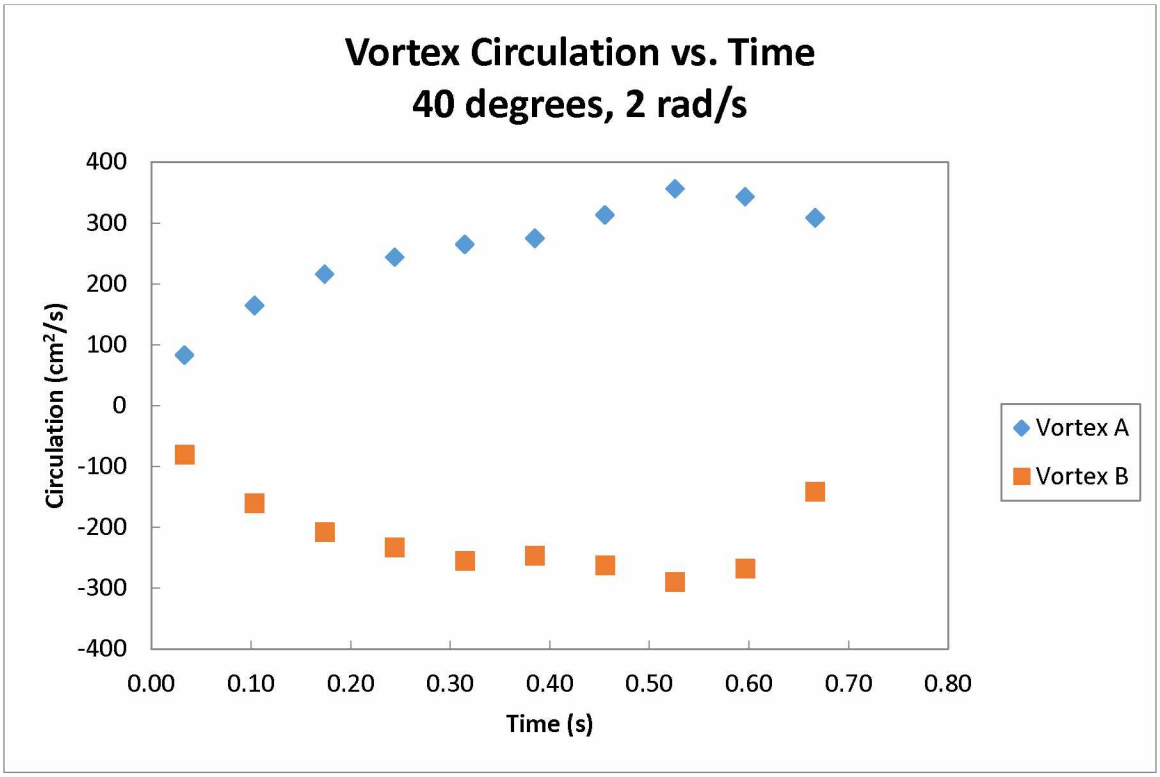

Figure 4.22 Vortex circulation vs. time: 40 degrees, 2 rad/s

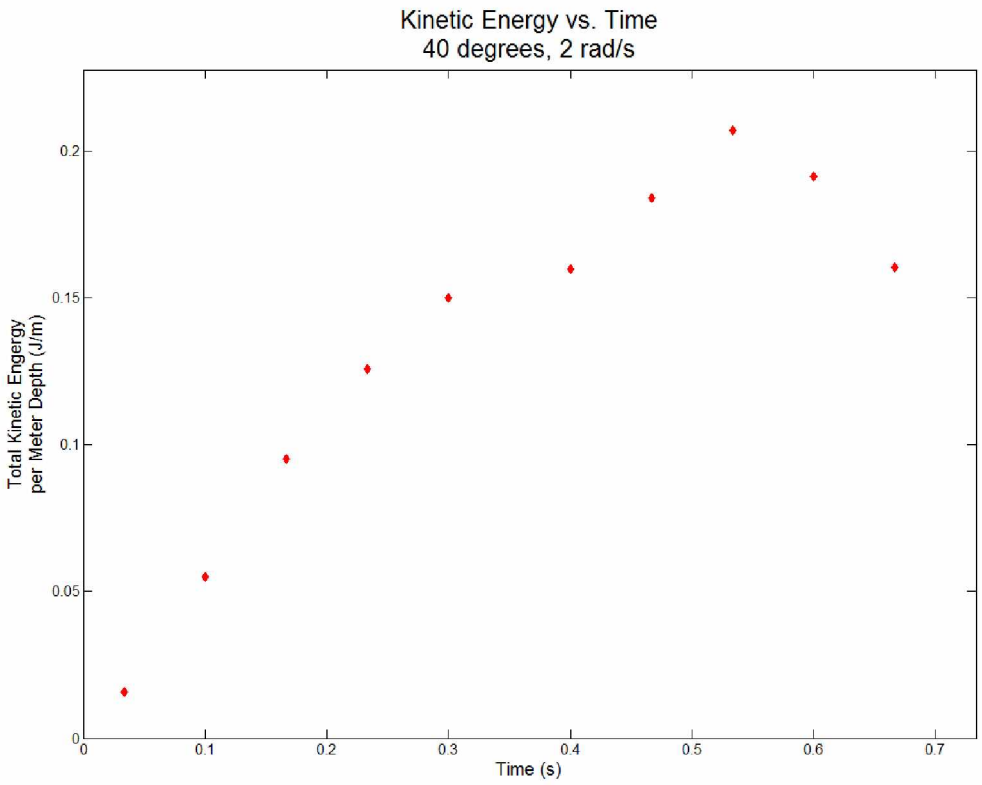

Figure 4.23 Kinetic energy vs. time: 40 degrees, 2 rad/s

4.8.3 Vortex Trajectory

Despite the instability of the tip vortex, its trajectory was fairly uniform. The vortex remained at the lower right at the very early stages of development, but quickly began moving up and to the left with a consistent distance between time periods. The vortex maintains a nearly straight track as the unstable portion of the area of vorticity remains on the upper right hand side while the center of maximum voticity remains on the lower left. The separation between these areas can be seen in the vorticity plots and the trajectory plot demonstrates that this separation is adequate to prevent the unstable area from significantly altering the path of the vortex.

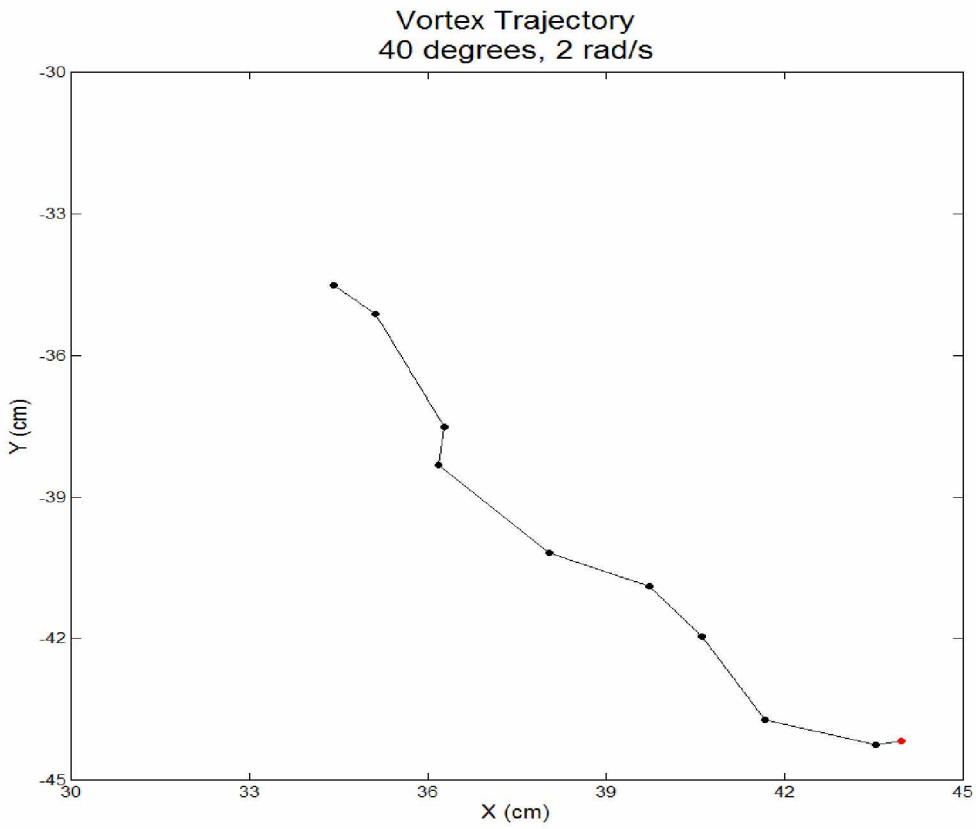

Figure 4.24 Vortex trajectory: 40 degrees, 2 rad/s, red marker indicates starting point

4.9 Constant Amplitude Data Comparisons

4.9.1 Amplitude: 20 degrees

The circulation plot below shows a comparison of the circulation levels for the tip vortex and plate hugging vortex in the experiments performed at 20 degrees amplitude and at both 1 rad/s and 2 rad/s. It is clear that the circulation reached greater magnitude in both vortices in the experiment at 2 rad/s. This suggests a more energetic flow field in the higher speed experiment and is confirmed with a reference to the comparison plot for kinetic energy. The kinetic energy in the 2 rad/s trial peaked at roughly twice the value seen in the 1 rad/s trial, this allowed the vortices in the higher speed trial to develop greater circulation and entrain more fluid. The

trends in both plots indicate that at a higher speed, given the same amplitude, the peak values of circulation and kinetic energy are reached sooner but this does not affect the dissipation trend. The trend seen in dissipation of circulation and kinetic energy is a decrease in value at a very similar rate to that of the increase before the maximum value is reached.

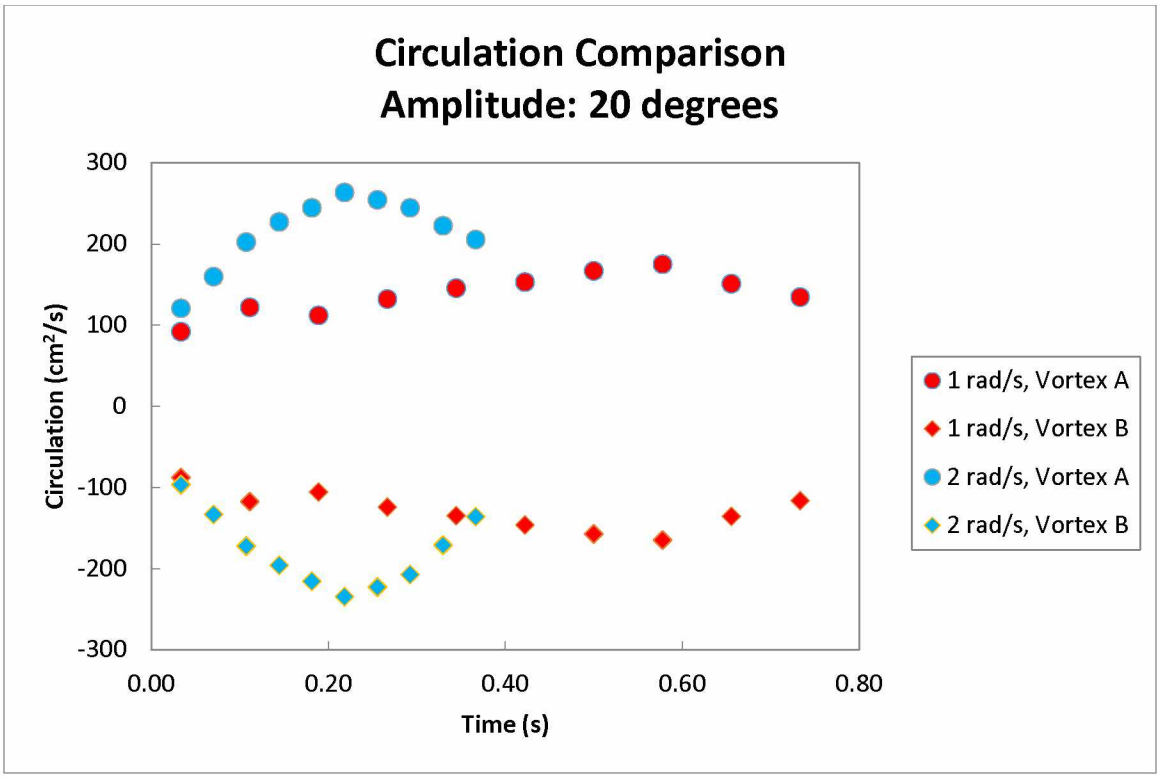

Figure 4.25 Circulation comparison, amplitude: 20 degrees

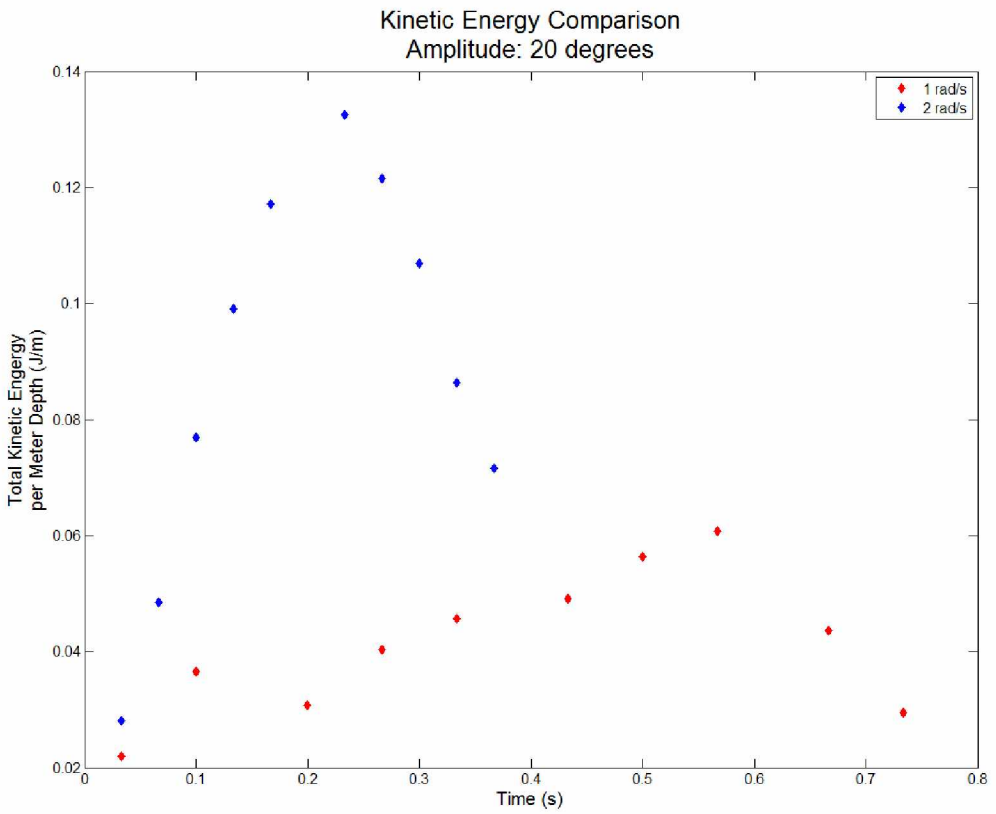

Figure 4.26 Kinetic energy comparison, amplitude: 20 degrees

The trajectory plot below is a comparison of the vortex paths for the experiments in which amplitude was fixed at 20 degrees and speeds of 1 rad/s and 2 rad/s were tested. Despite the difference in speed between the two experiments the vortex trajectories are fairly similar. Both tip vortices traveled up and to the left at roughly the same angle. In addition, while both data sets differ in their spacing in the lower right hand section of the track it is clear that there is less vertical motion at this point in comparison to the mid and upper portions of the trajectories. This suggests that in the early phase of the plate movement the center of maximum vorticity for both vortices does not follow the vertical motion of the plate's tip as closely as it does when the circulation and separation from the plate tip have increased.

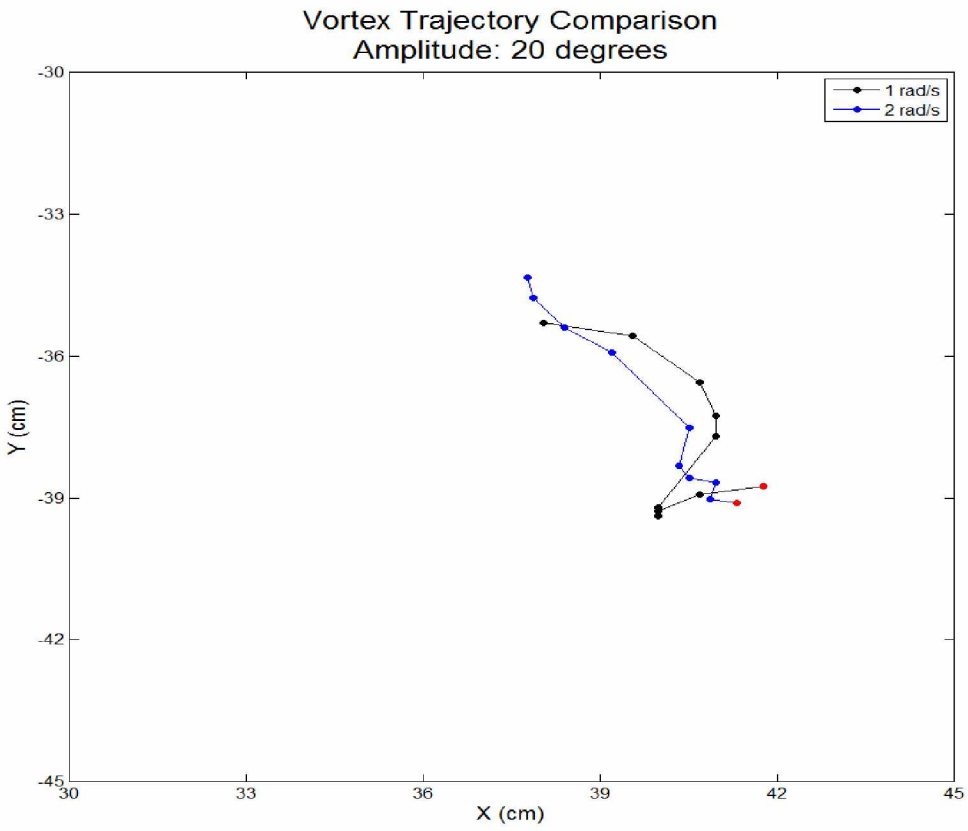

Figure 4.27 Vortex trajectory comparison, amplitude: 20 degrees, red marker indicates starting point

4.9.2 Amplitude: 30 degrees

The folowing two plots depict comparisons between circulation levels and kinetic energy levels during the experiments conducted at 1 rad/ and 2 rad/s, at a fixed amplitude of 30 degrees. In this comparison we again see that the higher speed experiment results in peak circulation and kinetic energy occurring earlier in the total time period than in the experiment at 1 rad/s. This means that the vortices in the higher speed experiment have a longer relative time to degrade and lose circulation. This is reflected in the kinetic energy comparison plot where it is evident that the total kinetic energy for the higher speed experiment has more data points after the peak. The significance of this behavior is that at higher speeds given the same amplitudes the vortices

develop circulation to the full potential warranted by the movement of the plate and then quickly lose circulation due to their higher energy and reduced stability, when compared to those formed at 1 rad/s. The gain and loss of circulation and kinetic energy relative to their peaks appears to be disproportionate between the two speeds.

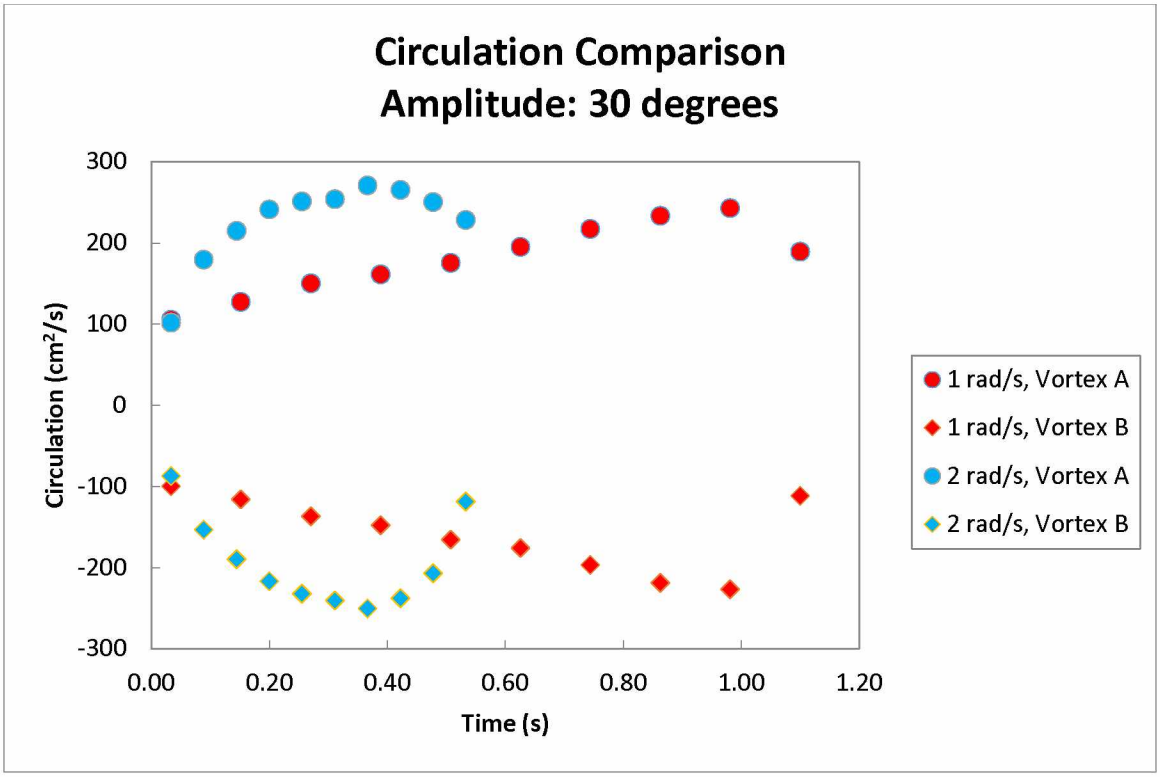

Figure 4.28 Circulation comparison, amplitude: 30 degrees

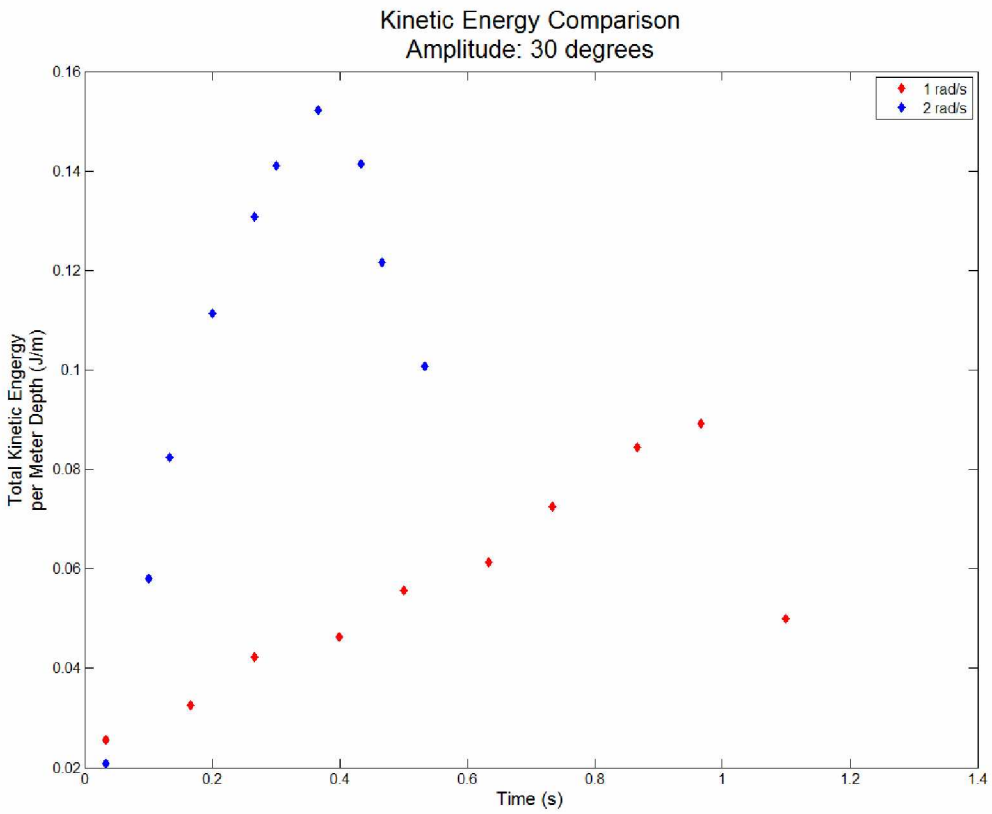

Figure 4.29 Kinetic energy comparison, amplitude: 30 degrees

In the vortex trajectory comparisons below the vortices are produced by the plate sweeping the same total distance but at different speeds. Both vortices follow a relatively straight path that is generally directed up and to the left. There first several tracking points in both data sets show that the vortex does not travel as great a distance in each time period during the early stages of plate movement. This can be attributed to the small displacement of the plate and thus lack of kinetic energy in the first few time periods.

There is a significant difference in the trajectory of the two tip vortices. The vortex resulting from the 1 rad/s plate movement does not travel as far to the left as the vortex in the higher speed trial. This is due to the reduced rotational motion of the fluid displaced by the plate in the 1 rad/s trial, which causes the vortex to remain closer to the tip of the plate so that it can be

sustained at lower levels of circulation. The fluid displaced by the tip of the plate in the 2 rad/s trial has greater rotational motion and is entrained by the tip vortex more easily, allowing for travel further from the tip of the plate.

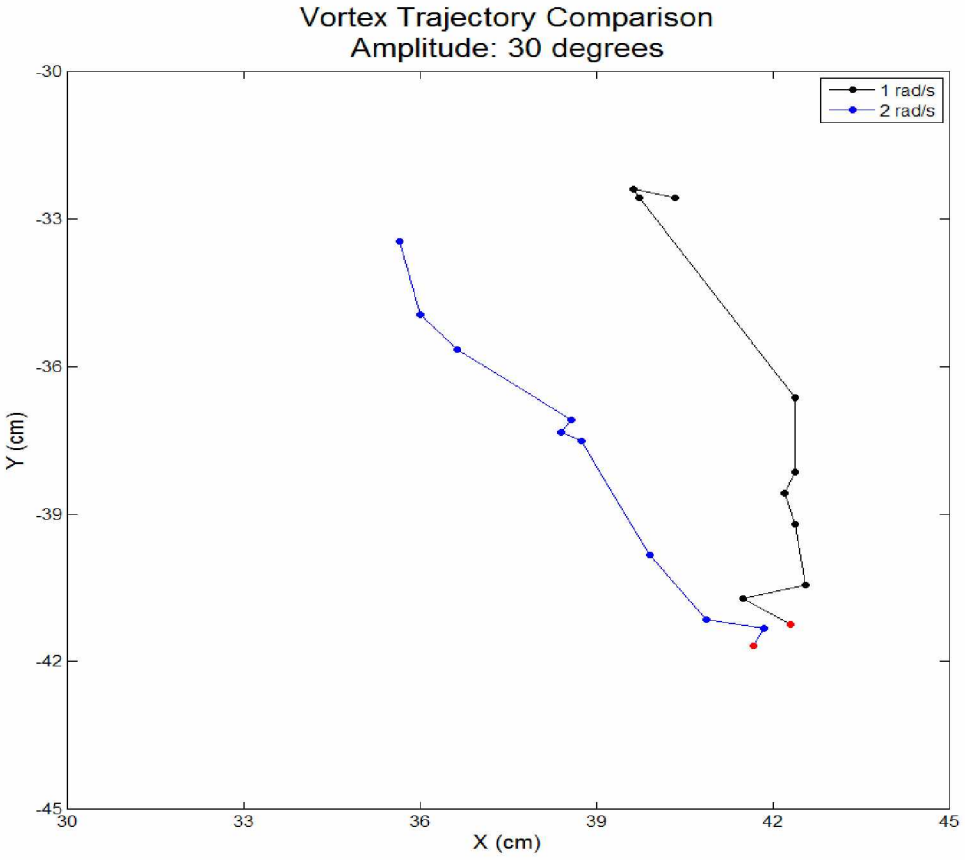

Figure 4.30 Vortex trajectory comparison, amplitude: 30 degrees, red marker indicates starting point

4.9.3 Amplitude: 40 degrees

The following plots compare the circulation and kinetic energy data for the 1 rad/s and 2 rad/s trials at an amplitude of 40 degrees. The increase, peak, and decrease of the circulation and kintic energy levels are closely matched in general trend. The most prominent difference between the two experiments is the earlier peak in kinetic energy and circulation in the higher

speed test. This is seen in the other comparisons of trials at the same amplitude. A more interesting difference between data sets in this comparison is the slightly irregular rate of increase in circulation and kinetic energy before their peak values, for the 2 rad/s trial. This may be attributed to early deformation and unstable nature of the highly energetic vortices in the 2 rad/s, 40 degree experiment, as they are the most energetic seen in this study. However, it is also possible that, because there is a decrease in the rate of kinetic energy increase, the irregularity in the circulation trend is due to the motor struggling to supply energy at the same rate, given increased loads.

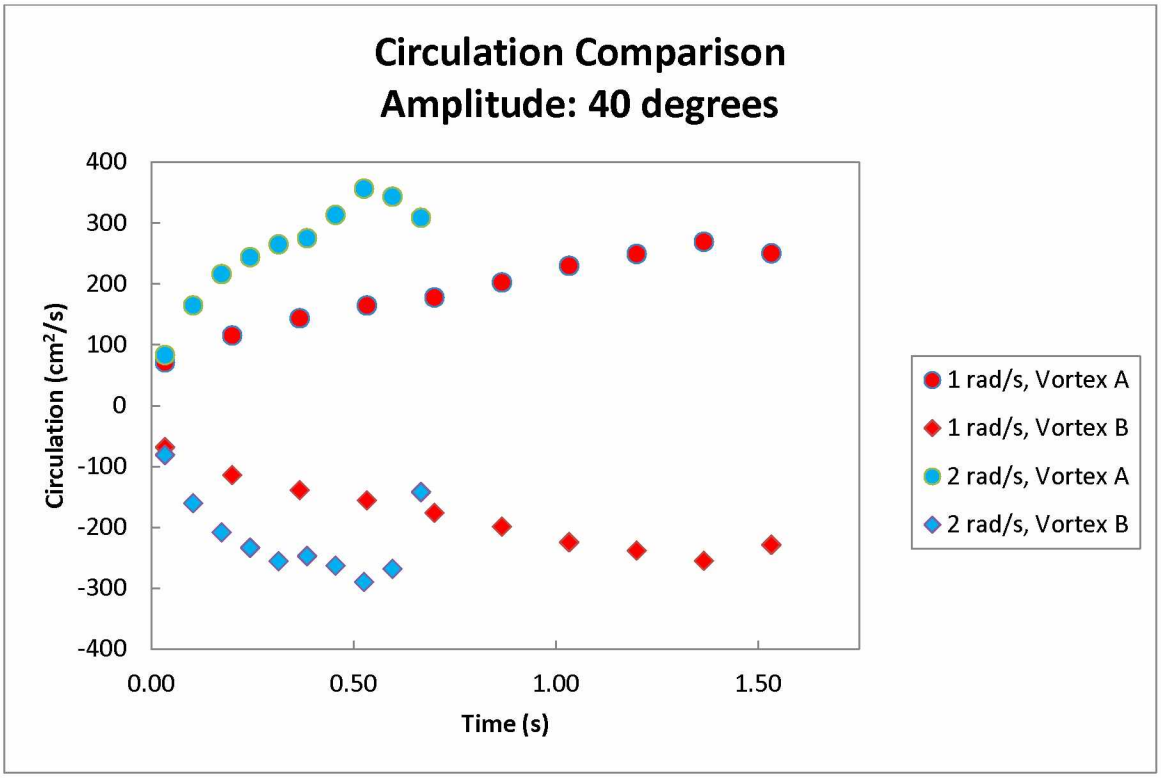

Figure 4.31 Circulation comparison, amplitude: 40 degrees

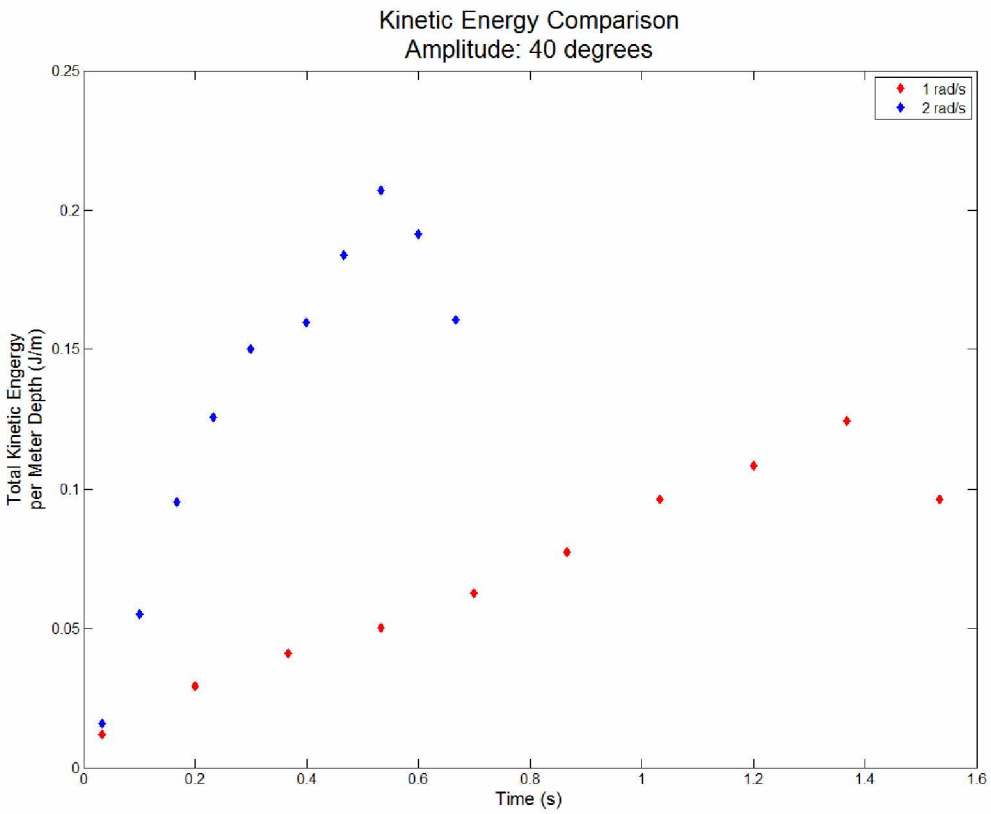

Figure 4.32 Kinetic energy comparison, amplitude: 40 degrees

The comparison of trajectories for the tip vortices produced during trials in which amplitude was 40 degrees shows close correlation between the two data sets. In both the 1 and 2 rad/s trials the vortex moved up and to the right at about the same angle. In addition the total distance traveled by the two vortices closely matches, especially in total vertical displacement. The vortex produced in the 1 rad/s trial strays from the general trend line somewhat more than the one produced in the 2 rad/s trial. This is attributed to the close proximity of the center of maximum vorticity in the slower trial's vortex to the area of instability. In the higher speed trial the center of maximum vorticty hovers in the area opposite the necking and shedding area on the right of the vortex, preventing the center of the vortex from being displaced from its natural track to the same degree as the center of the vortex in the 1 rad/s trial.

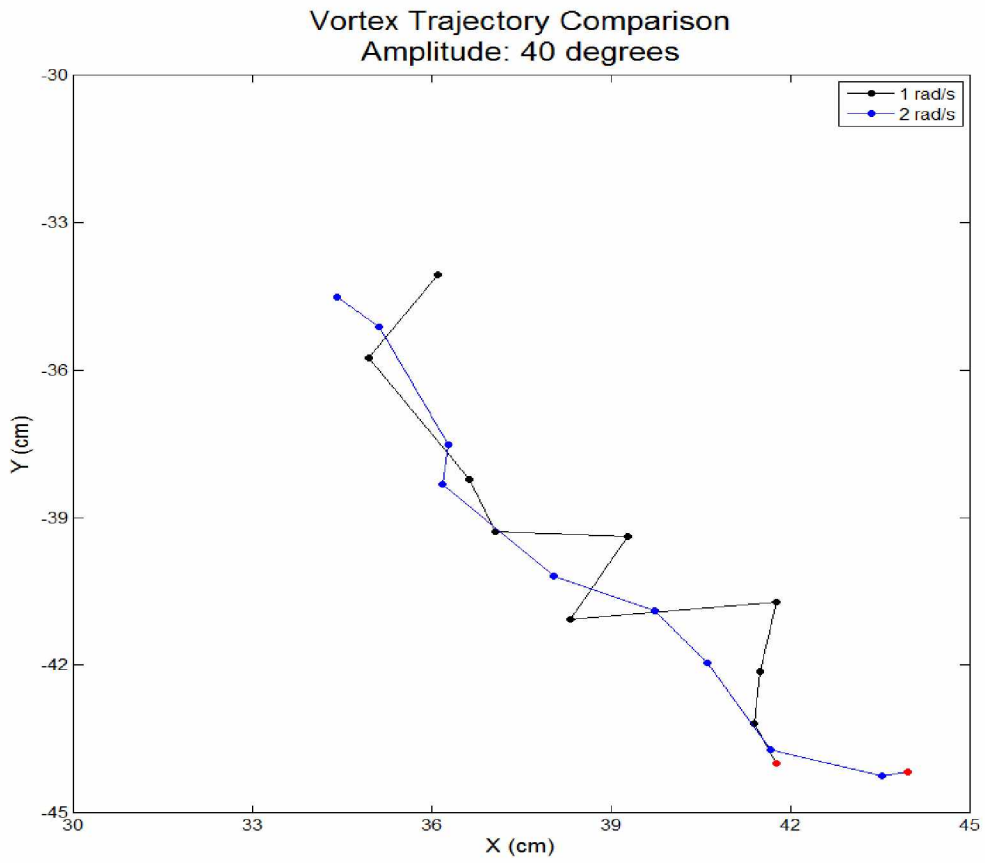

Figure 4.33 Vortex trajectory comparison, amplitude: 40 degrees, red marker indicates starting point

4.10 Constant Speed Data Comparisons

4.10.1 Speed: 1 rad/s

The following two plots represent comparisons between data sets for trials at all amplitudes and a speed of 1 rad/s. In the first figure a comparison of circulation levels throughout each of the three trials is made. The general form of each circulation data set matches that of the other experiments. The slope and values of the circulation for both the tip vortex and plate hugging vortex match closely for each data set, up to the point of peak circulation. Beyond the point of peak circulation the agreement between trends is less clear but appears to be roughly the same. The circulation for the trial at 30 degrees amplitude rises at the

same rate and to the same value as that of the 20 degree trial, but continues at the same rate until reaching a peak. At this peak the circulation of the 40 degree trial continues increasing at the same rate, although from a value slightly less in magnitude. The continuation of the data trend from roughly the same values and at the same rate suggests that the formation of the vortex produced by a rigid flapping plate, with respect to circulation, is independent of the flapping amplitude at least up to peak circulation.

The second figure depicts a similar comparison of data sets, but for total kinetic energy. The comparative results are similar to those for circulation. For increasing amplitudes, the successive data sets for kinetic energy continue from similar values and at the same rate, up to the point of peak kinetic energy. Like circulation, the trends after the peaks in kinetic energy have few data points and a thorough comparison of this portion of the data set cannot be made. However, the trend for kinetic energy after reaching a peak value seems to be similar for all three amplitudes tested. The rise in kinetic energy appears to be independent of the amplitude tested and the decrease after the peak is likely independent as well.

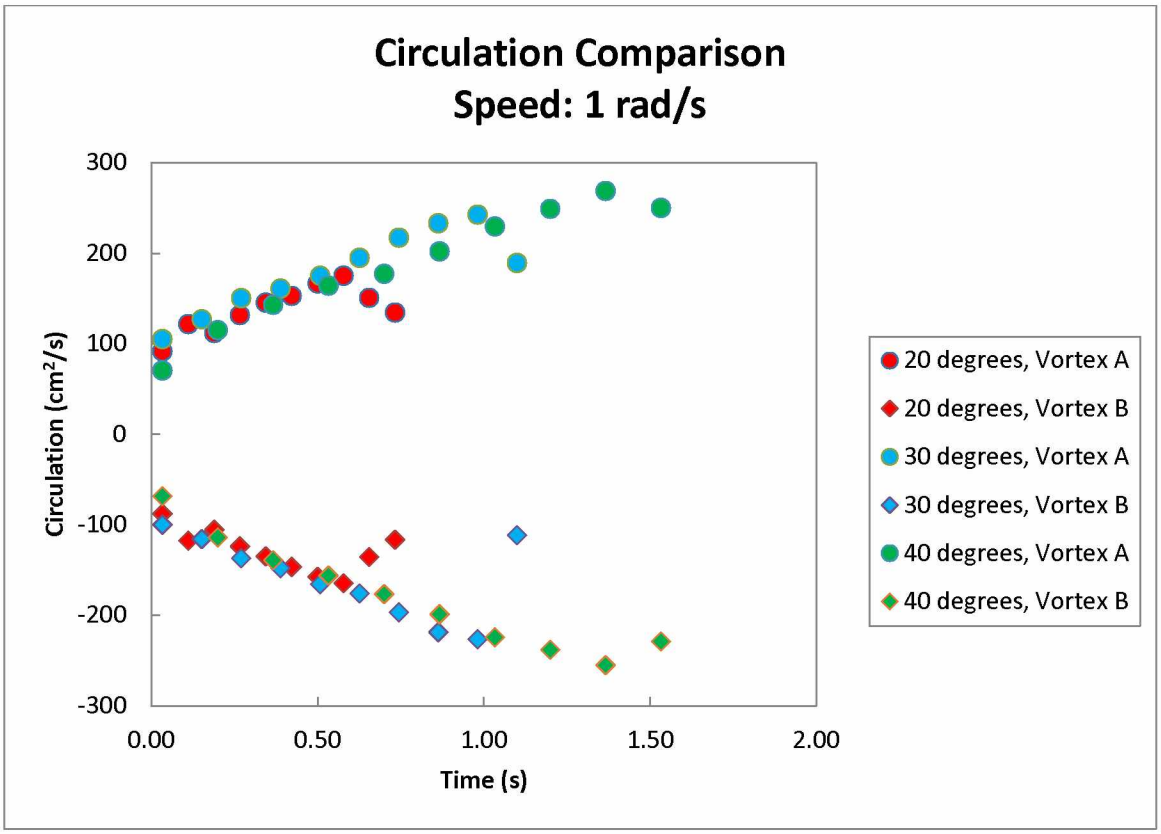

Figure 4.34 Circulation comparison, speed: 1 rad/s

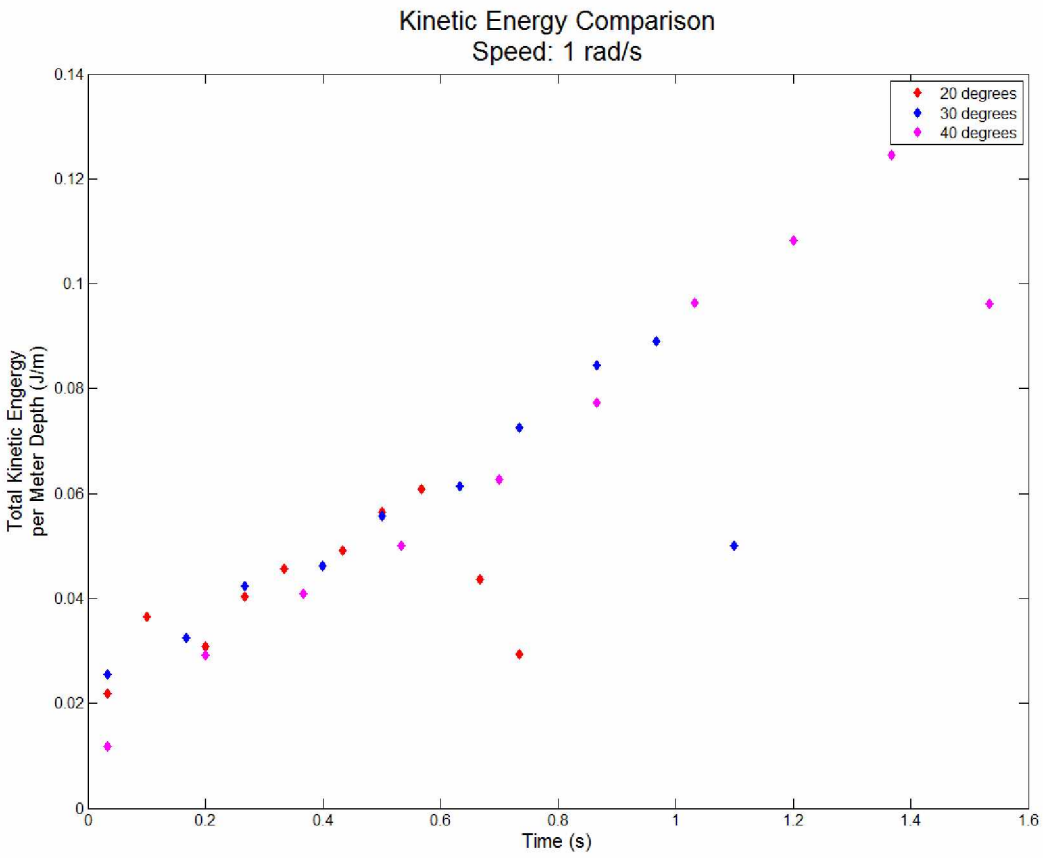

Figure 4.35 Kinetic energy comparison, speed: 1 rad/s

The following figure is a comparison of the trajectories of the tip vortices at amplitudes of 20, 30 , and 40 degrees and a speed of 1 rad/s. The clearest correlation in this data set is that of starting point with amplitude. The data sets begin at progressively lower locations as the amplitude increases. This is a somewhat trivial observation as increasing amplitude means that the plate begins at a lower point in the field of view for each test, and the tip vortex is expected to form at roughly the same location. The three trajectories are generally oriented up and to the left. There does not appear to be a strong correlation between change in amplitude and the angle of trajectory, nor does there seem to be a correlation between total lateral travel and amplitude.

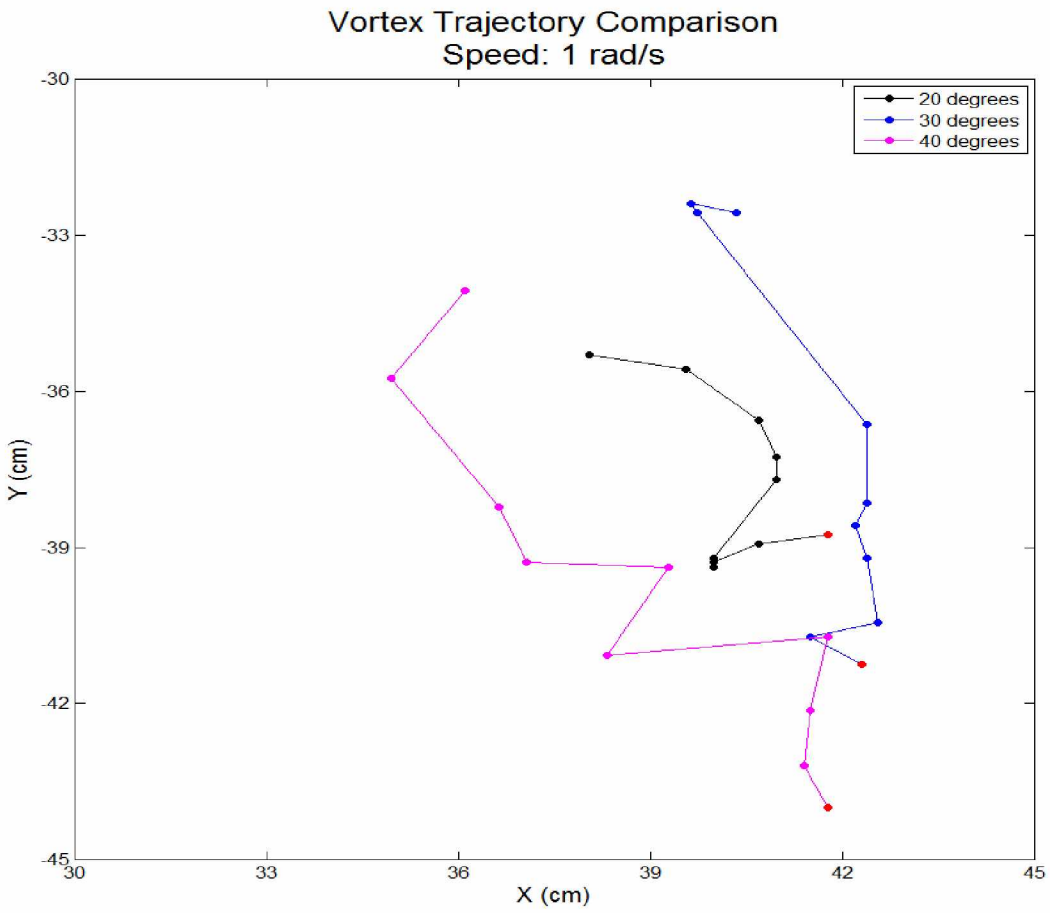

Figure 4.36 Vortex trajectory comparison, speed: 1 rad/s, red marker indicates starting point

4.10.2 Speed: 2 rad/s

The figure below compares the circulation data for the three experiments conducted at a speed of 2 rad/s. As in the comparison of circulation at 1 rad/s the three data sets appear to match in both slope and value up to the point of peak circulation. In this comparison however, there are two noteworthy differences. First, rather than increasing along a straight line to their peak the circulation values follow a very slight arc. This is attributed to the higher speed than in the 1 rad/s comparison; the higher speed results in a more energetic vortex with less stability and a greater tendency to lose circulation by shedding vorticity in the surround fluid. Though this

result is slightly different from that of the 1 rad/s comparison the nature of the correlation is the same. That is, the form of the arc and the values attained are consistent for each amplitude, up to the point of maximum circulation. Again, suggesting that vortex forms with circulation levels independent of the flapping amplitude.

The second noteworthy difference between this comparison and that of the 1 rad/s experiments is that there are enough data points to make reasonable assumptions about the post-peak circulation trend. The arc of the circulation data after the peak appears to be the same for the 20 and 30 degree trials. The trial at 40 degrees does not include enough data to adequately compare it with the lower amplitude trials. The clear agreement of the 20 and 30 degree trials in the 2 rad/s supports the idea that the evolution of the vortex circulation after reaching its maximum value, is independent of amplitude.

The kinetic energy comparison in the second figure shows similar results to those of the circulation comparison at the same speed. The accumulation rate of kinetic energy appears independent of flapping amplitude as the trend and values of the three data sets, up to their maximum kinetic energy value, match closely. Another important result from this comparison is the post peak behavior of the kinetic energy data. The figure shows sufficient data points lie after peak kinetic energy to determine that the rate of decrease in energy is the same between the three data sets and thus independent of amplitude. This result strongly supports that found in the circulation comparison for the 1 rad/s trials, in which the independence of the kinetic energy dissipation rate from amplitude was suspected, but enough data to support the idea was lacking.

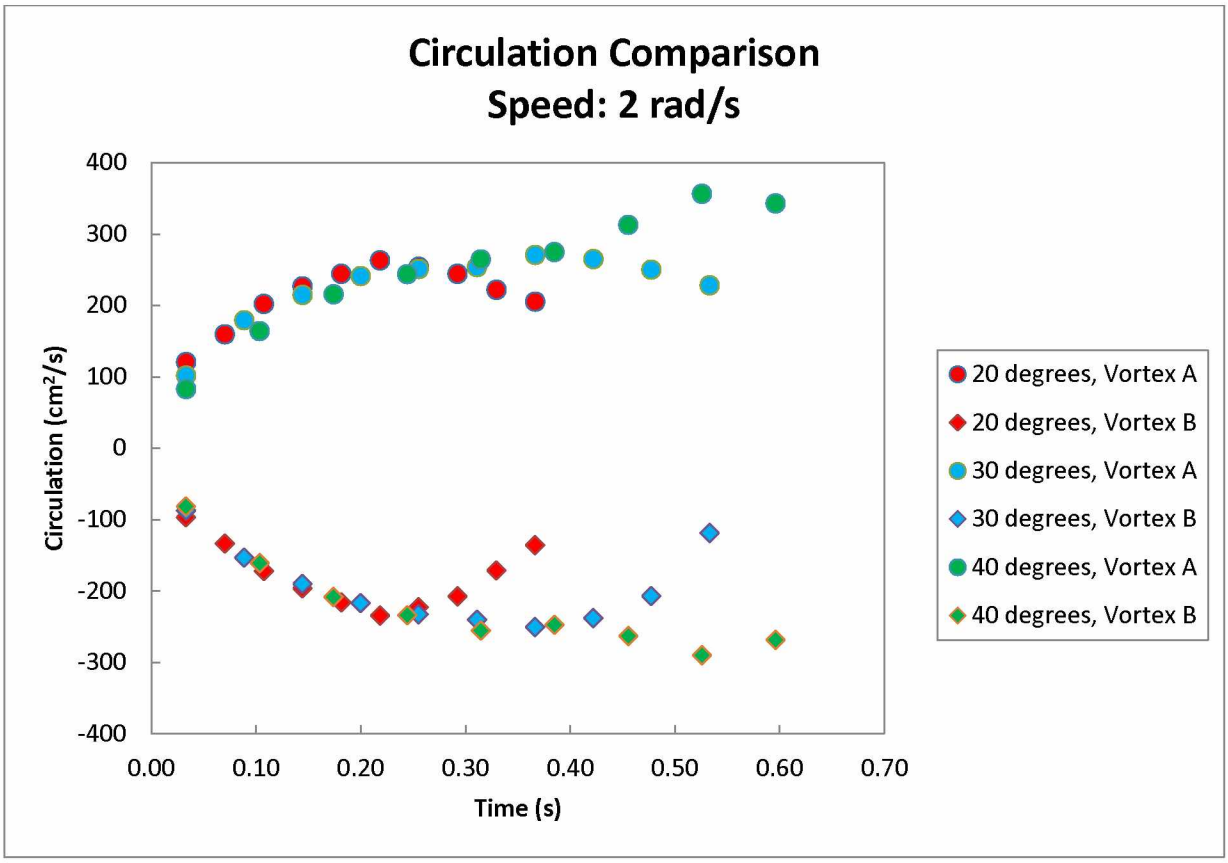

Figure 4.37 Circulation comparison, speed: 2 rad/s

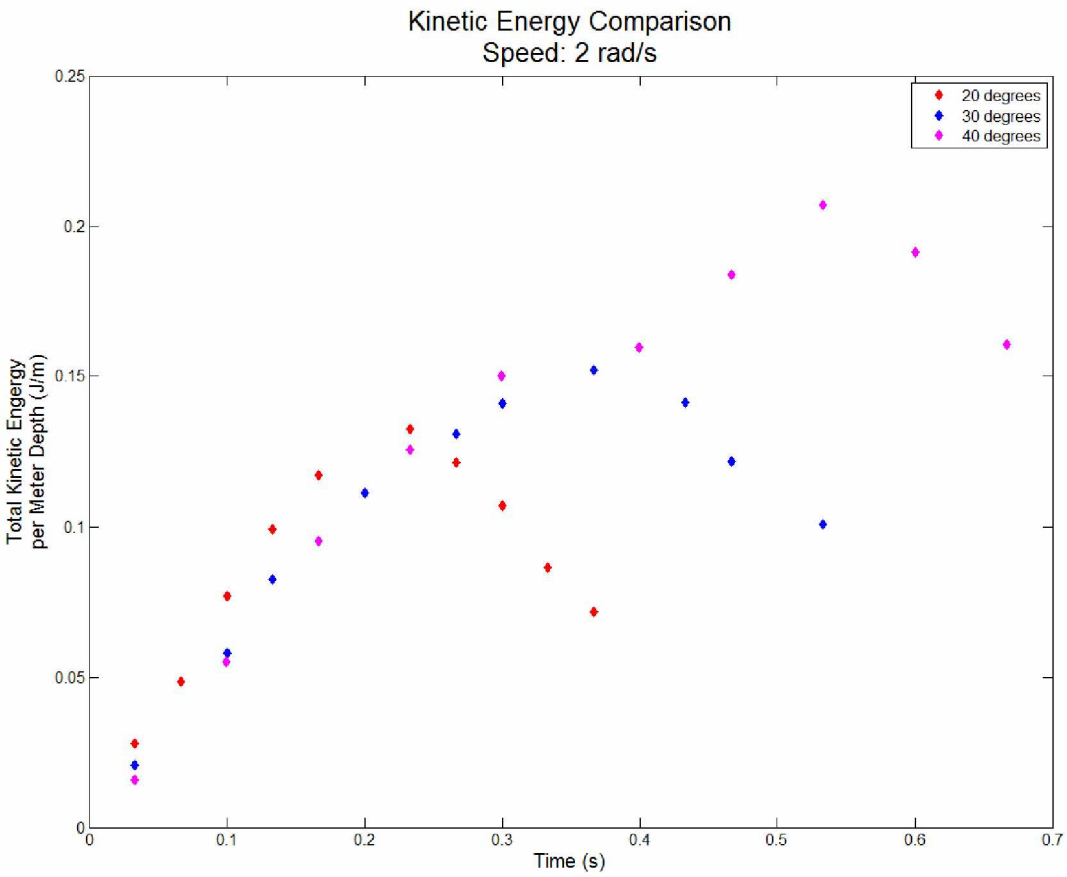

Figure 4.38 Kinetic energy comparison, speed: 2 rad/s

The trajectory comparison plot below shows the trajectories of the tip vortices for the experiments conducted at 2 rad/s. In this comparison several characteristics of the correlation between vortex trajectory and flapping amplitude are clear. In general each trajectory has similar characteristics, that the direction of travel is up and to the left. In this plot is is evident that the angle of the trajectories is consistent between amplitudes. Despite starting at progressively lower positions, corresponding to the starting position of the plate's tip, the vortices were at roughly the same vertical location at the time the plate stopped moving in the respective experiments. It appears that each of the trajectories follows a relatively straight line. Based on the comparisons of the 2 rad/s trials it seems that trajectory shape and angle, relative to the horizontal, are

independent of the flapping amplitude. The location of the tip vortex at the end of plate movement and the net distance traveled by the vortex do appear to be proportional to the flapping amplitude.

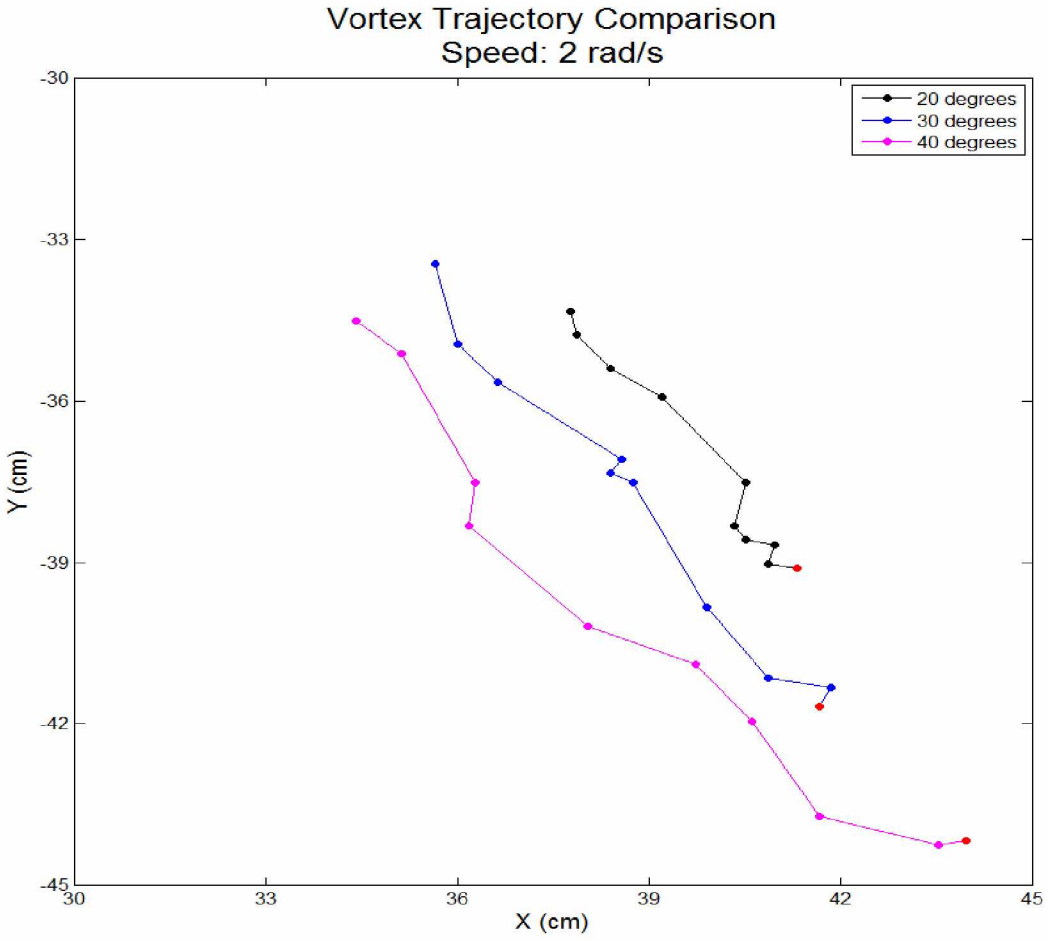

Figure 4.39 Vortex trajectory comparison, speed: 2 rad/s, red marker indicates starting point

4.11 Conclusion

The experiments investigating the vortices produced by a rigid cantilevered plate flapping at different speeds and amplitudes reveal several fluid dynamic correlations and behaviors. The evolution of the vorticity in each experiment was examined in a step by step process to better

understand the factors influencing the development and shedding of vorticity in vortices around the plate. Comparisons of circulation, total kinetic energy, and vortex trajectory were made in two ways: comparison of data sets with fixed amplitude and comparison with fixed speed.

The examination of the evolution of vorticity showed that two vortices, whose vorticity is of opposite sign, form near the plate at the beginning of its movement. One of these vortices forms generally between the plate's center and its center of rotation and remains close to the plate for the duration of its movement. The second of these vortices forms near the tip and entrains fluid that is displaced by, and given some rotational motion by, the tip of the plate. The vortex may neck significantly toward the tip of the plate as it entrains this displaced fluid. However, unlike the hugging vortex, the inertia of the fluid comprising the tip vortex causes it to lag significantly behind the motion of the plate, primarily in the vertical direction. Despite this lag in vertical motion the tip vortex exhibits significant horizontal displacement in comparison with the hugging vortex. As the plate decelerates a stopping vortex of the same vorticity as the plate hugging vortex may form above the tip of the plate if the flow is sufficiently energetic. This stopping vortex is often seen merging with the plate hugging vortex and appears to be responsible for some of the diminishing of the plate hugging vortex's circulation. In some of the more energetic experiments, often when a stopping vortex was also found, the tip vortex would develop a second strong area of vorticity next to its original center. This would occur during times when necking or full shedding of some of the tip vortex's vorticity was seen.

The comparisons of circulation and total kinetic energy data sets showed similar correlations to test parameters. The comparisons made by fixed amplitude were less telling than those made by fixed speed. However, the fixed amplitude comparisons did confirm some expected correlations. Namely, the maximum magnitudes attained, the accumulation rate, and

the dissipation rate of both circulation and kinetic energy are speed dependent. The comparisons made by fixed speed revealed more intriguing results.

It should be noted that some of the conclusions made from the fixed speed comparisons, particularly those about the post peak values of circulation and total kinetic energy, were only suggested by the data in the 1 rad/s comparison but confirmed by the 2 rad/s comparison. This was due to limited post peak value data in the 1 rad/s trial. Nevertheless, some definitive conclusions were made. It was found that the general form of the circulation and kinetic energy trend is independent of flapping amplitude. That is to say that the rate of accumulation and dissipation of either quantity does not vary with total flapping amplitude. The maximum values of these quantities are however, proportional to both speed and amplitude.

The comparison of vortex trajectory by fixed amplitude revealed no definitive results. The scattering of the recorded vortex locations in the 1 rad/s trial was too great to show clear trends or correlations when paired with the trajectory plot of the 2 rad/s vortex at the same speed. The comparison of the 1 rad/s vortex trajectories by fixed speed was somewhat more useful, yet only hinted at likely trends. The fixed speed comparison of the 2 rad/s vortex trajectories showed clear trends and confirmed indications of trends from the previous comparison. It was concluded that flapping amplitude does not influence the shape of vortex trajectory or the trajectory angle relative to the horizontal. However, the vertical location of the tip vortex at the time the plate comes to rest, relative to the starting point, and total distance traveled along the vortex trajectory are dependent on flapping amplitude.

Chapter 5 Vortex Ring Results

5.1 Investigation

The investigation into the vortex ring interaction with an inclined plate focuses on the relationship between the evolution of the vortex ring and the kinematic parameters of the plate. This research explores the question of what relevence plate inclination has to the changes in the vortex ring's fluid dynamic properties and general behavior. Similar experimental setups have been used in other research but these experiments leave questions, as to how the vortex ring evolves, unanswered.

5.2 Vortex Ring Experiments

The following experiments use a PIV analysis and susbsequent data processing to quantitatively and qualitatively describe the deformation of a vortex ring interacting with an inclined plate. The parameter of the plate varied in these experiments was its inclination relative to the normal axis of the undisturbed vortex ring. Three test were conducted, each with a different level of inclination. In these experiments inclination was considered to be the number of degrees that the lower tip of the plate rested below the normal axis of the vortex ring. Inclinations used in these experiments were 30, 60, and 90 degrees. The selection of these degrees of inclination was based on the desire to observe significantly different vortex ring behavior at different inclinations, as well as to observe both asymmetric (30 and 60 degree trials) and symmetric (90 degree trial) vortex ring behavior. The parameters of the vortex ring remained unchanged between experiments. The analysis performed on these experiments includes calculation and plotting of vorticity and circulation, as well as tracking and plotting the location of individual vortices. The time period considered for observation was from just before

the vortex ring's first sign of interaction with the plate to the degradation of the center of vorticity in either part of the vortex ring.

5.3 Inclination: 30 degrees

5.3.1 Vorticity Evolution

The figure below shows the evolution of vorticity in the flow field for the experiment at 30 degrees inclination. The vorticity in the upper and lower portions of the vortex ring undergoes different changes due to the asymmetrical orientation of the plate with the ring. Both parts of the vortex ring begin with high levels of vorticity at their center. At t = 0.47 s the first sign of interaction with the plate is clear; the lower part of the vortex ring has caused some rotation of the shear layer near the plate. By the next time period the area of opposite vorticity is gone and the lower part of the vortex ring has begun to neck between the plate and the upper part of the ring. At t = 1.40 s the lower portion of the vortex ring has slightly increased in vorticity at its center but is being pinched between the plate and upper part of the ring, which has remained relatively unchanged save for increased vorticity at its center. At t = 1.87 s the lower part of the vortex has shed an area of vorticity that is now concentrated above and to the left of the upper part of the ring. This is due to the action of the two areas of vorticity, opposite in sign, acting together to force fluid between them, as the plate is limiting their advance. The fluid forced between the areas of vorticity is rotated as it is forced between the plate and upper area of vorticity and results in the small vortex seen up and to the left of the upper part of the ring. In the remaining images the upper part of the ring gradually decreases in maximum vorticity while the lower part decreases fairly quickly. The pinched off vortex increases somewhat in vorticity and finally the center of vorticity of the upper part of the ring breaks up.

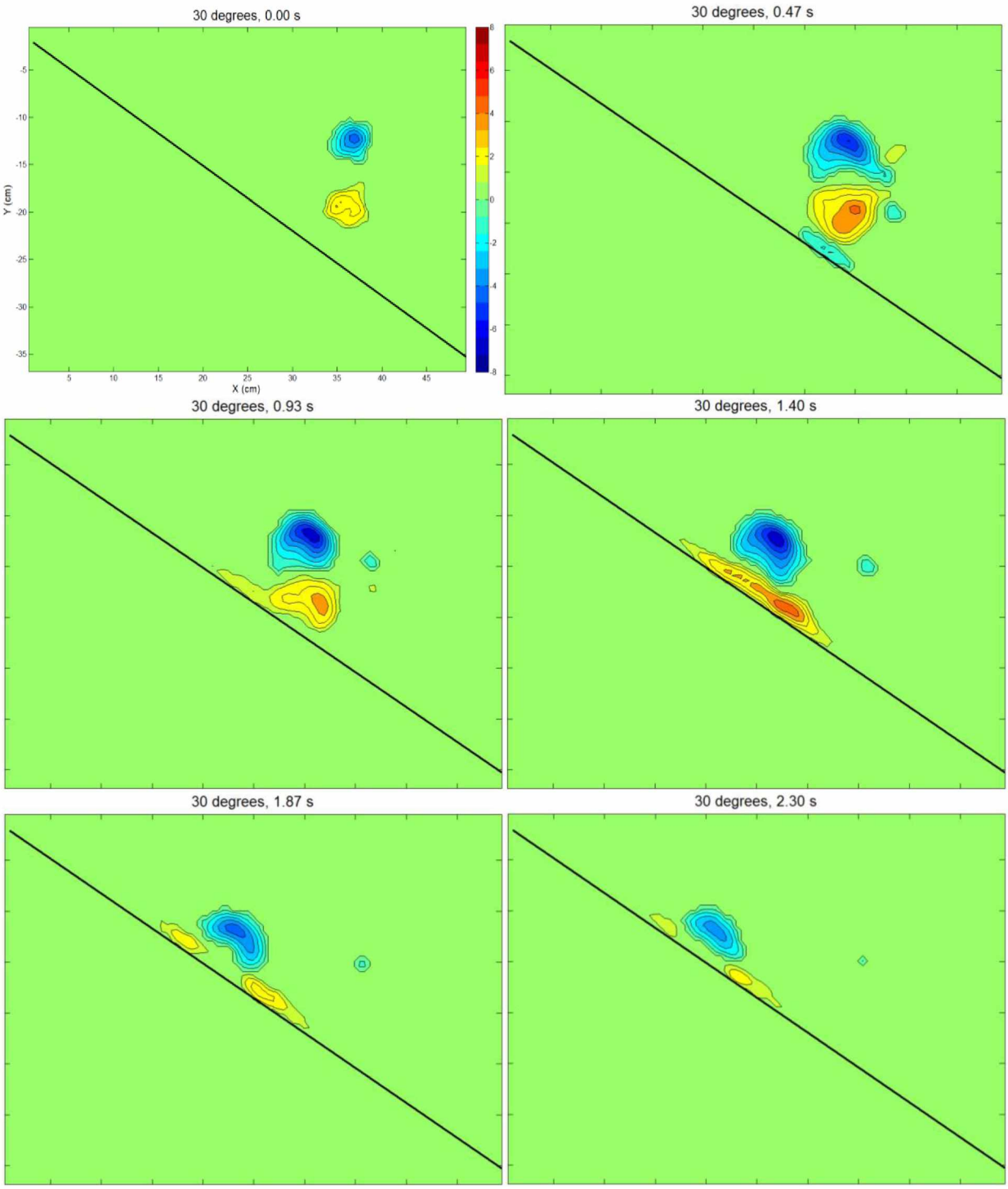

Figure 5.1 Vorticity plots: 30 degrees

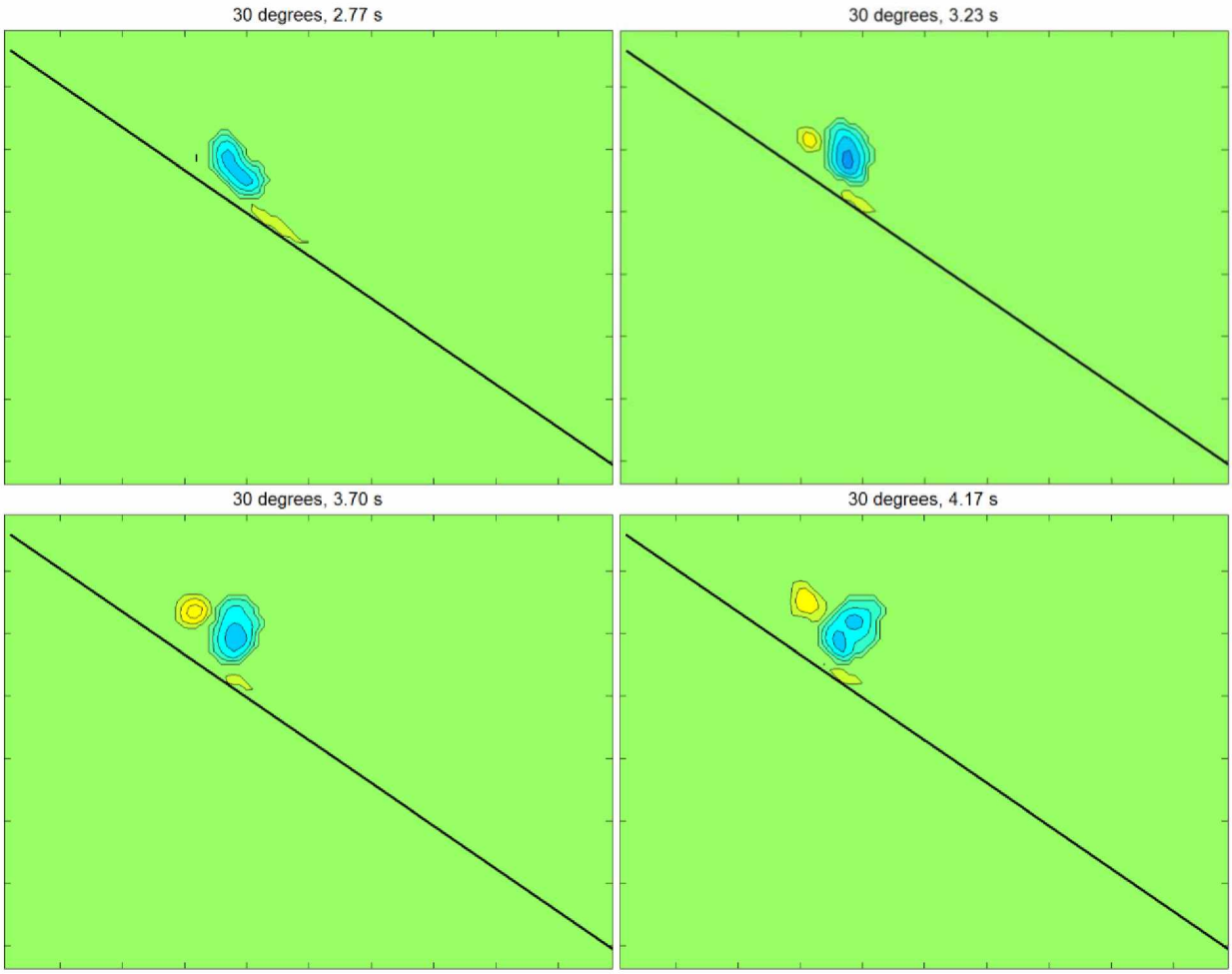

Figure 5.1 continued Vorticity plots: 30 degrees

5.3.2 Circulation

Below is a plot of circulation for each time period in the experiment at 30 degrees of inclination. Despite the obvious differences in the qualitative nature of the vortex ring halves seen in the vorticity evolution, the circulation levels for the two areas of vorticity are quite similar throughout the interaction. It should be noted that the lower portion of the vortex ring is an area of positive vorticity and its circulation values are also positive. The most interesting feature of the circulation plot is near the end of the experiment where the circulation of the lower part of the vortex ring is nearly constant but there is a slight rise in the circulation of the upper portion of the ring. This is due to some entrainment of the flow from the pinched off vortex into

the upper portion of the ring and explains the decrease in vorticity of the pinched off vortex while the upper portion of the ring maintains relatively high levels of vorticity.

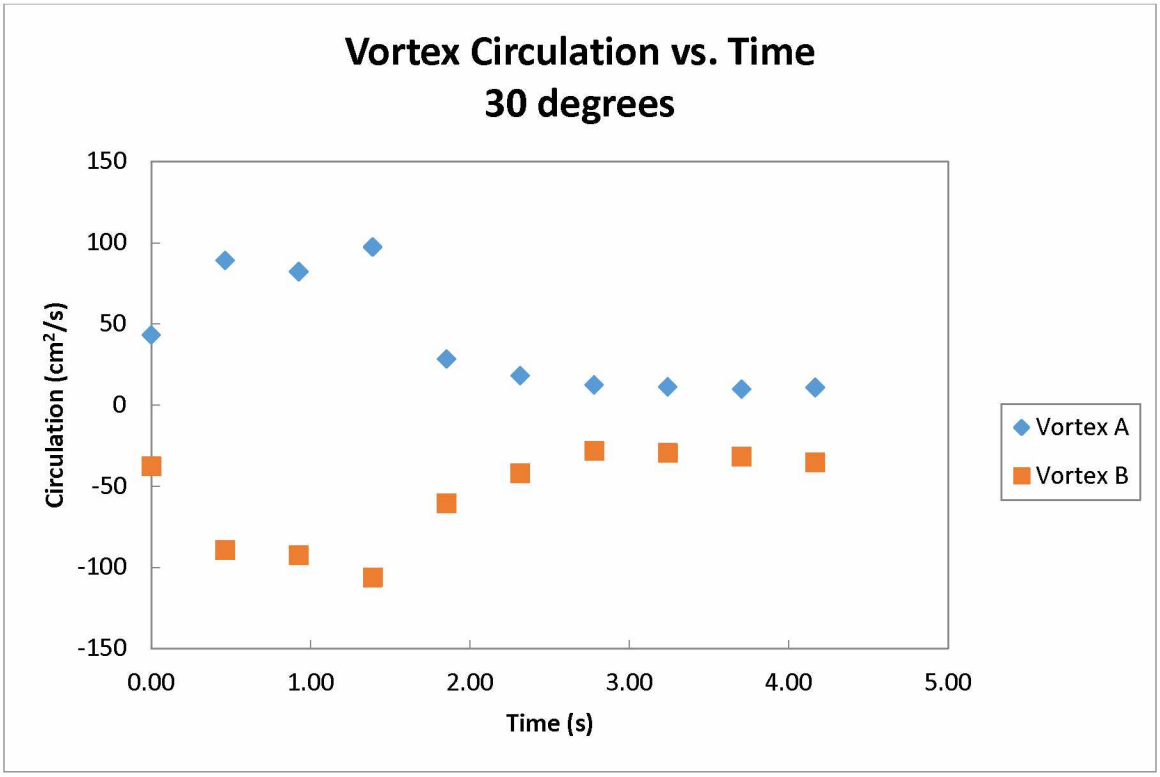

Figure 5.2 Vortex circulation vs. time: 30 degrees

5.5.3 Vortex Trajectories

The following figure is a plot of the trajectories of the upper and lower parts of the vortex ring. As indicated in the vorticity plots, the lower part of the ring is the first to interact with the plate. The lower ring is deflected upward along the surface of the plate while the upper portion of the ring continues along a straight path. In the last few data points the travel of the upper part of the ring has been significantly interrupted and both parts of the ring have become nearly stationary.

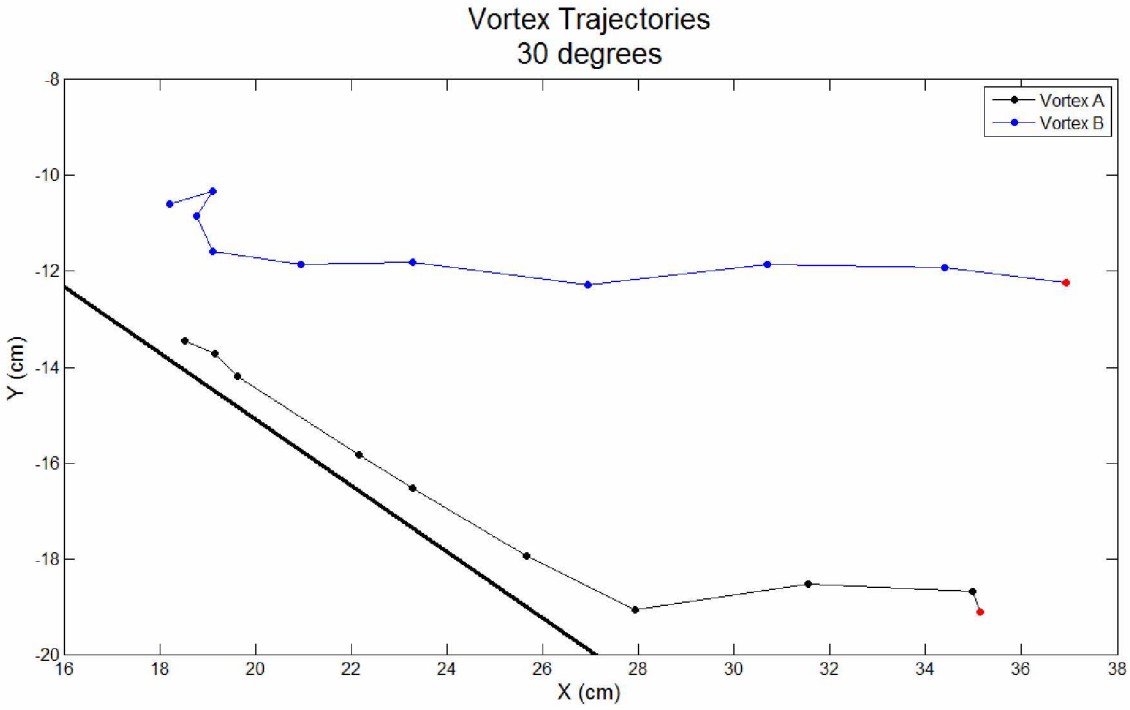

Figure 5.3 Vortex trajectories: 30 degrees, red marker indicates starting point

5.4 Inclination: 60 degrees

5.4.1 Vorticity Evolution

The evolution of vorticity shown below corresponds to the vortex ring interaction with the plate at an inclination of 30 degrees. The behavior of the rings exhibits the same key elements seen in the experiment at 30 degrees. These include an area of negative vorticity between the lower portion of the ring and the plate as the first sign of interaction, the necking of the lower part of the ring, the formation of a pinched off vortex, and the near complete degradation of the lower area of vorticity. At t = 0.23 s the area of opposite vorticity is seen between the lower area of vorticity and the plate, but a counterpart to this sign of interaction has formed between the upper area of vorticity and the plate as well. At t = 0.90 s a pinched off vortex has formed next to the upper area of vorticity and the lower area has experienced a

significant decrease in its maximum vorticity. The image from t = 1.37 s shows the lower portion on the ring greatly diminished in vorticity and necking back toward an area of vorticity near the vortex ring tube. Also in this image is a vortex just below the upper part of the ring that split off from the lower part but was not forced between the upper portion of the ring and the plate. In the remaining images all areas of vorticity simply decrease in maximum vorticity.

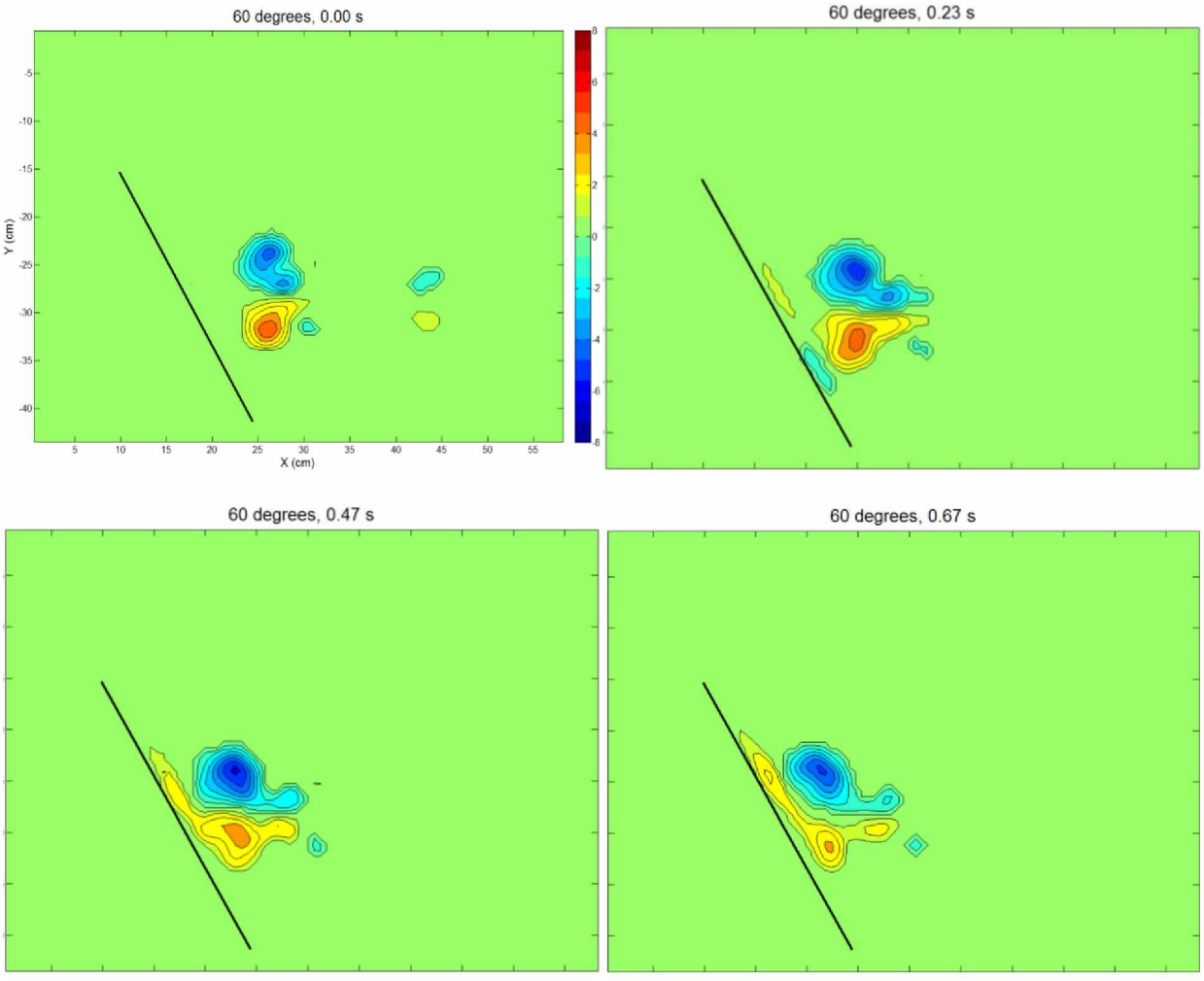

Figure 5.4 Vorticity plots: 60 degrees

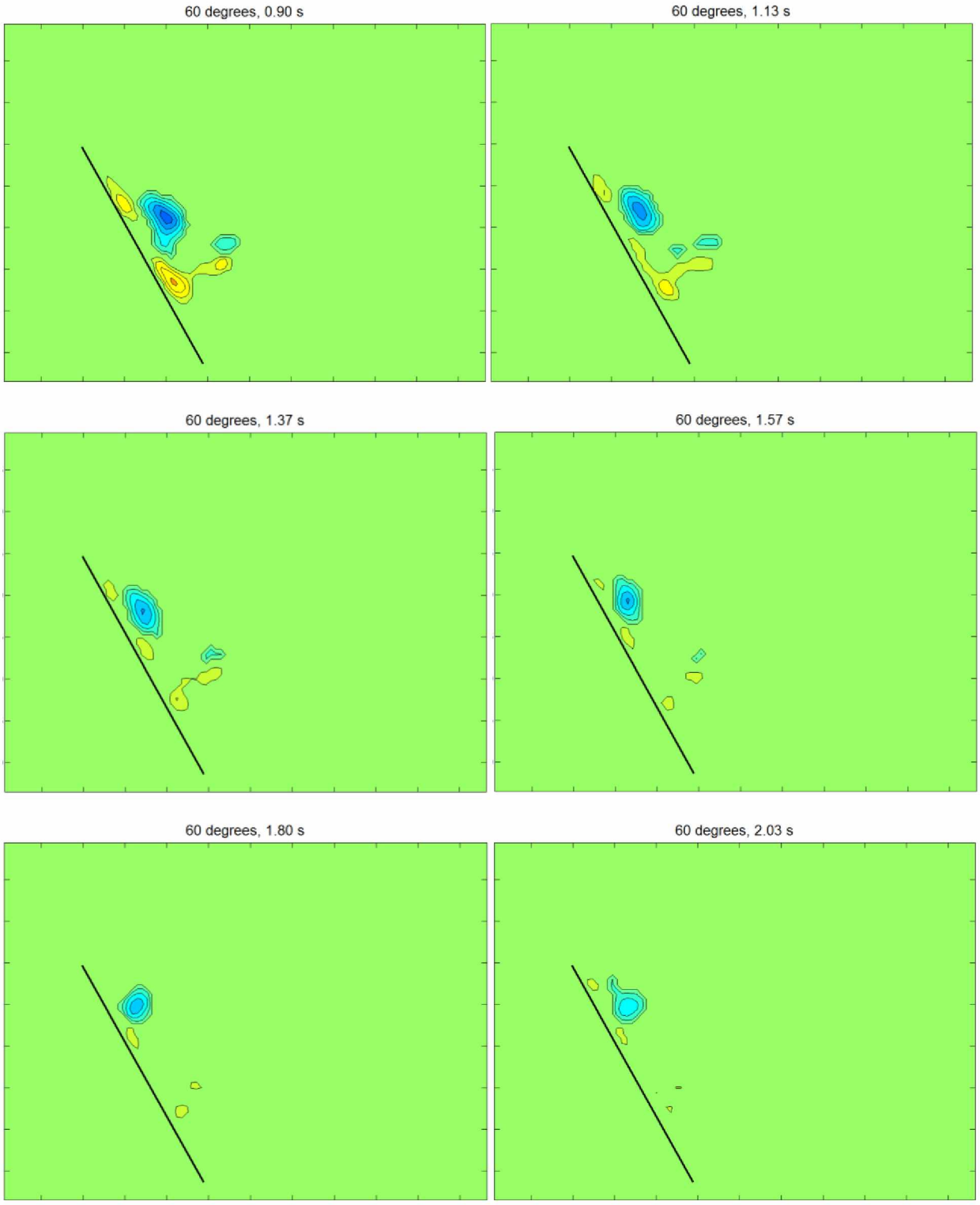

Figure 5.4 continued Vorticity plots: 60 degrees

5.4.2 Circulation

The circulation plot below depicts the value of circulation at each time period for the upper and lower parts of the vortex ring for the experiment at 60 degrees of inclination. It is clear that the circulation values for the upper part of the vortex ring were more stable than those of the lower part, after peak circulation was reached. This is attributed to the earlier and more intense interaction of the lower area of vorticity with the plate, slowing its rotation and causing it to shed some vorticity to help create the pinched off vortex. In addition to the fluctuating nature of the circulation the lower part of the ring, the circulation levels off at nearly zero and remains there while the circulation of the upper area of vorticity decreases very slowly and does not reach as low a magnitude as that of the lower area.

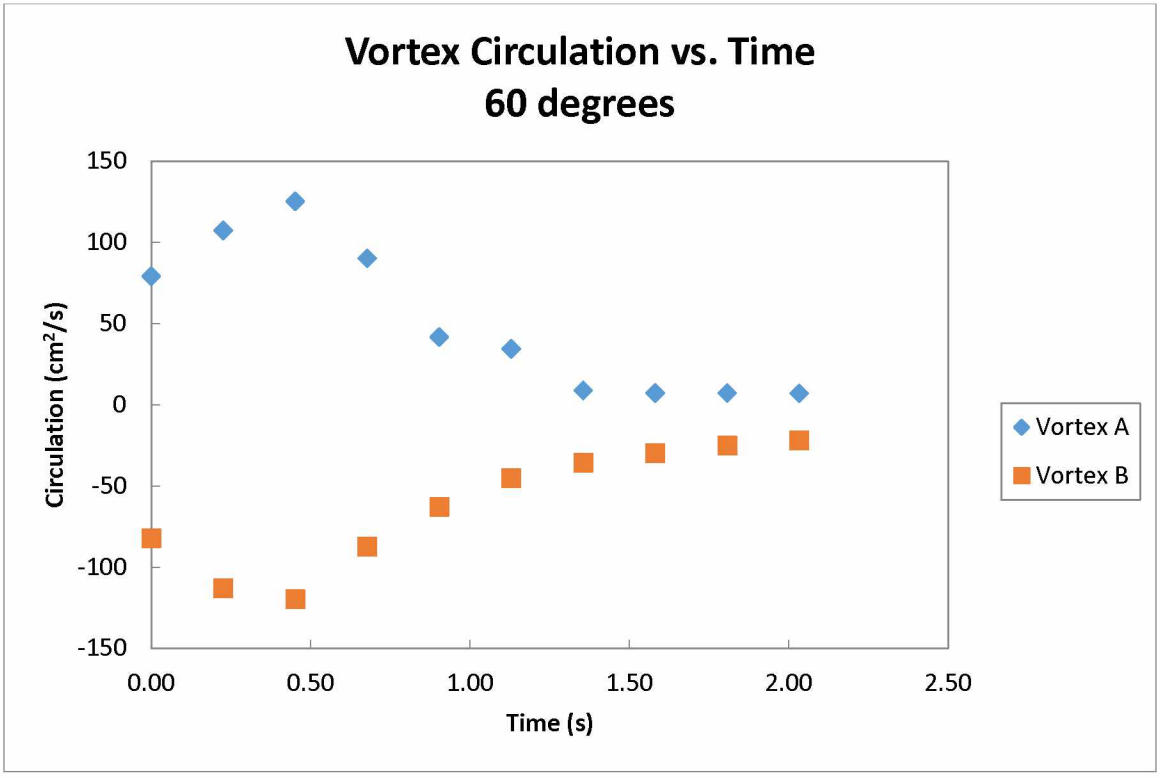

Figure 5.5 Vortex circulation vs. time: 60 degrees

5.4.3 Vortex Trajectories

In the trajectory plot below the paths of the upper and lower portions of the vortex ring in the experiment at 60 degrees of inclination are shown. In this case both vortices approach the plate and are deflected along its surface, but in opposite directions. The upper region of vorticity moves steadily up the side of the plate while the lower region hits the plate and moves downward slightly. The vertical deflection of the lower part of the vortex is significantly less than that of the upper part.

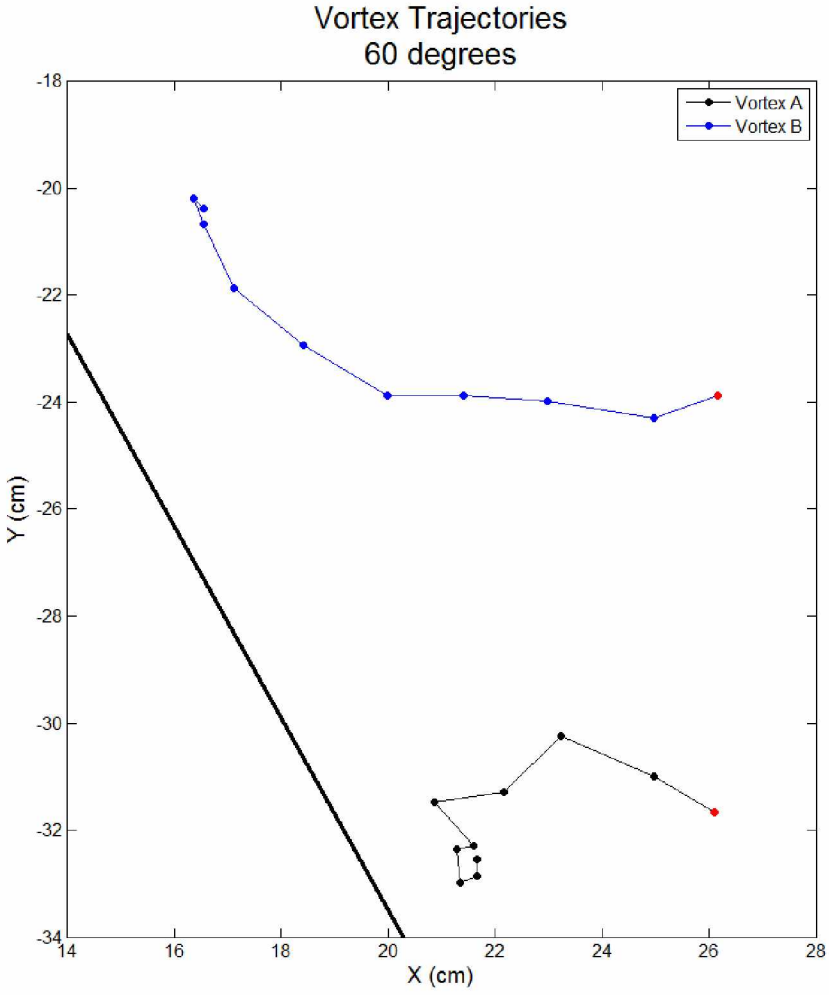

Figure 5.6 Vortex trajectories: 60 degrees, red marker indicates starting point

5.5 Inclination: 90 degrees

5.5.1 Vorticity Evolution

The figure blow shows the evolution of vorticity for the vortex ring interaction with the plate at 90 degrees of inclination. At t = 0.27 s the first sign of interaction with the plate is seen as each part of the vortex develops a buffering area of opposite vorticity between it and the plate. In the next image the buffering vortices have decreased slightly in size and have begun to move away from the center of the ring. At t = 0.80 s the buffering vortices are almost completely diminished and the maximum value of vorticity in each part of the vortex ring has diminished significantly. At t = 1.07 s a small vortex has begun to form just above the lower part of the ring and at t = 1.63 s this vortex has developed along with a second on the lower part of the lower section of the ring. The upper part of the ring has two of the small vortices as well. For the rest of the experiment the vortex ring halves diminish in vorticity strength, as do the respective pairs of hovering vortices.

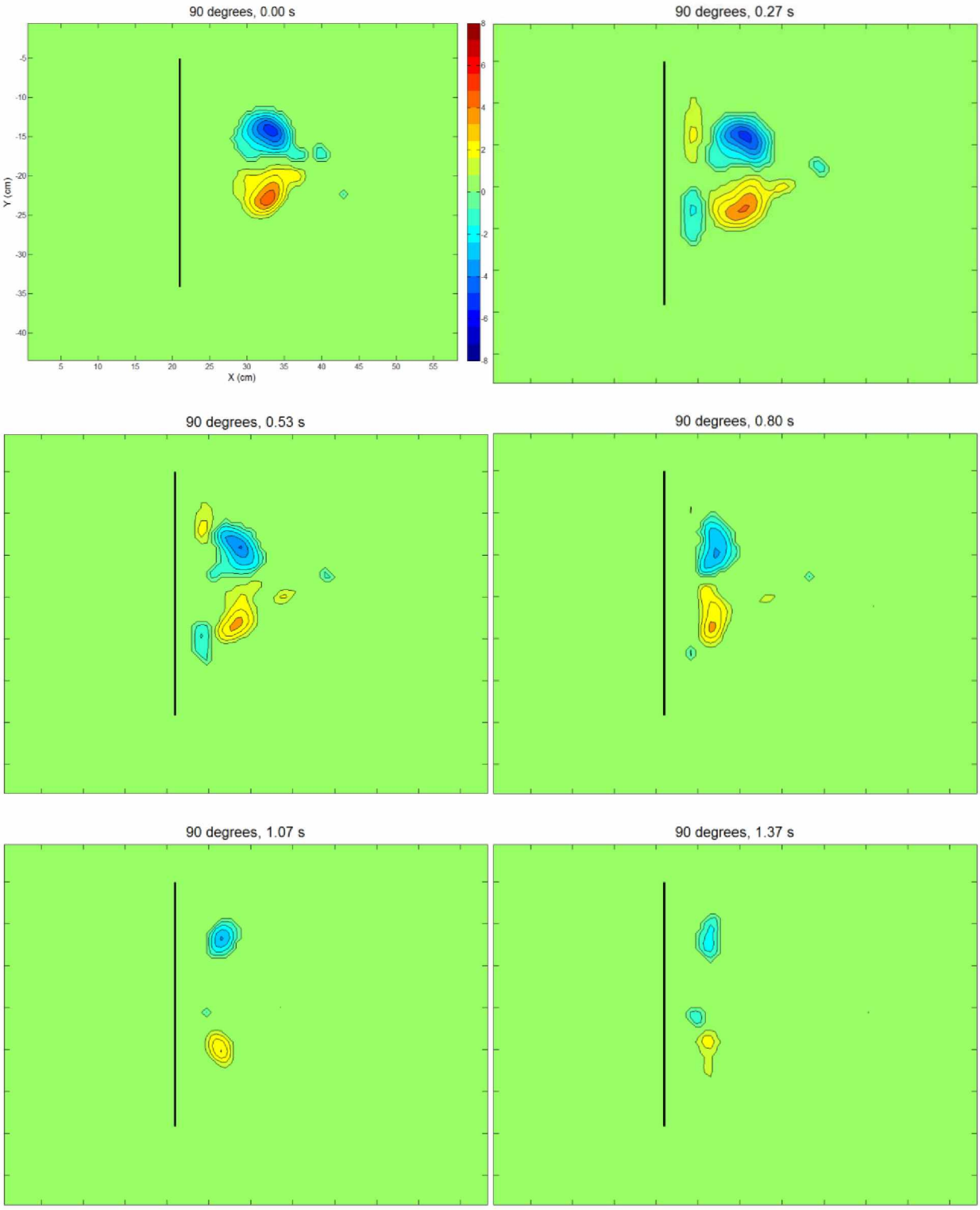

Figure 5.7 Vorticity plots: 90 degrees

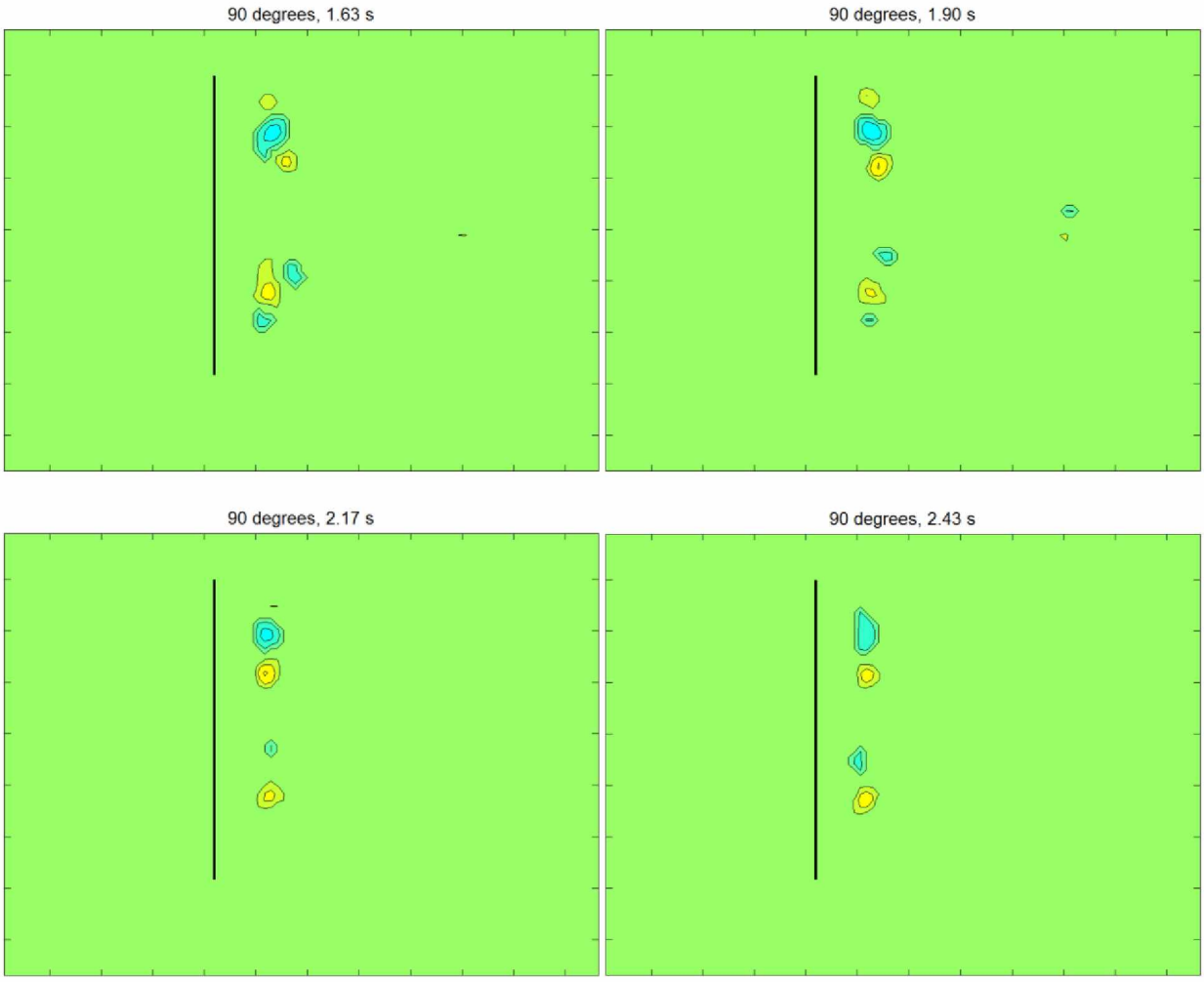

Figure 5.7 continued Vorticity plots: 90 degrees

5.5.2 Circulation

The figure below is a plot of the circulation for each part of the vortex ring throughout the experiment at 90 degrees of inclination. The two data sets display nearly identical trends, as is expected for a symmetrical vortex interaction. The small fluctuations during the large decrease in circulation for each data set are the result of instability of the ring and some shedding of vorticity to the flow field.

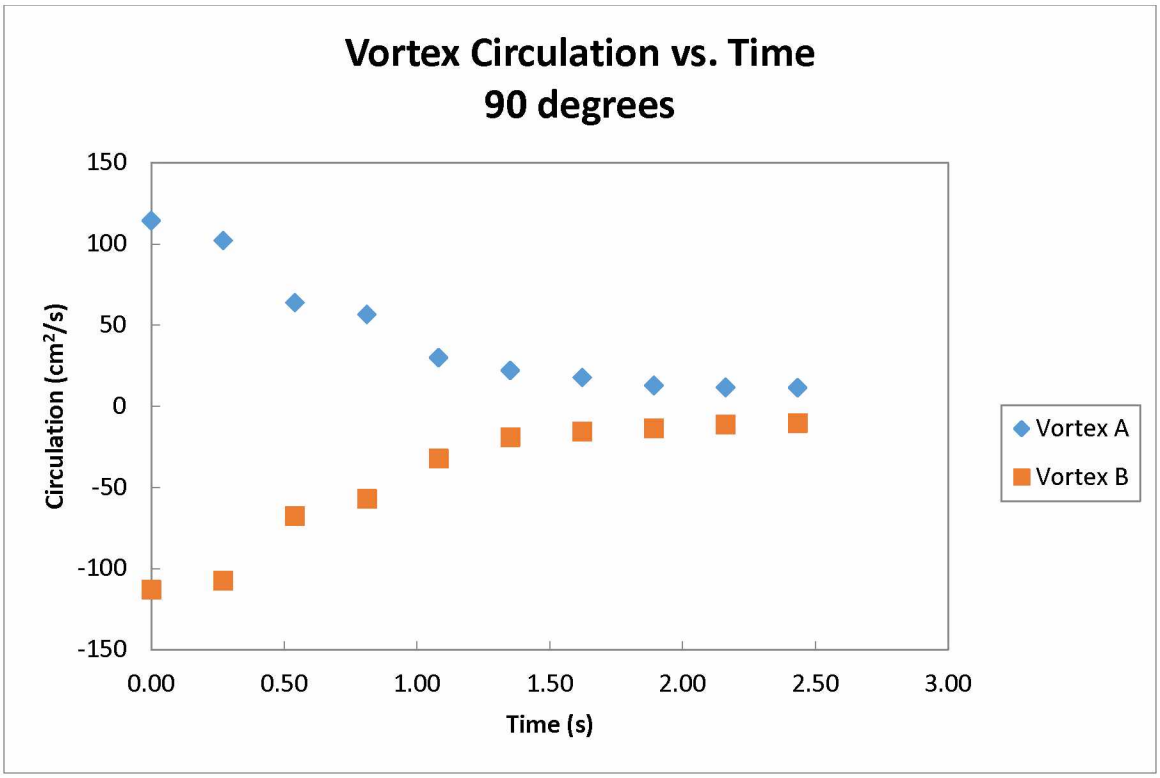

Figure 5.8 Vortex circulation vs. time: 90 degrees

5.5.3 Vortex Trajectories

In the figure below the trajectories of the two parts of the vortex ring are shown. The trajectories are nearly symmetrical which is to be expected for a symmetrical body interacting at with a uniform body. The two parts of the vortex ring travel directly toward the plate but are stopped short by the buffering vortices, at which point the vortex ring widens and the two parts of the cross section move apart vertically.

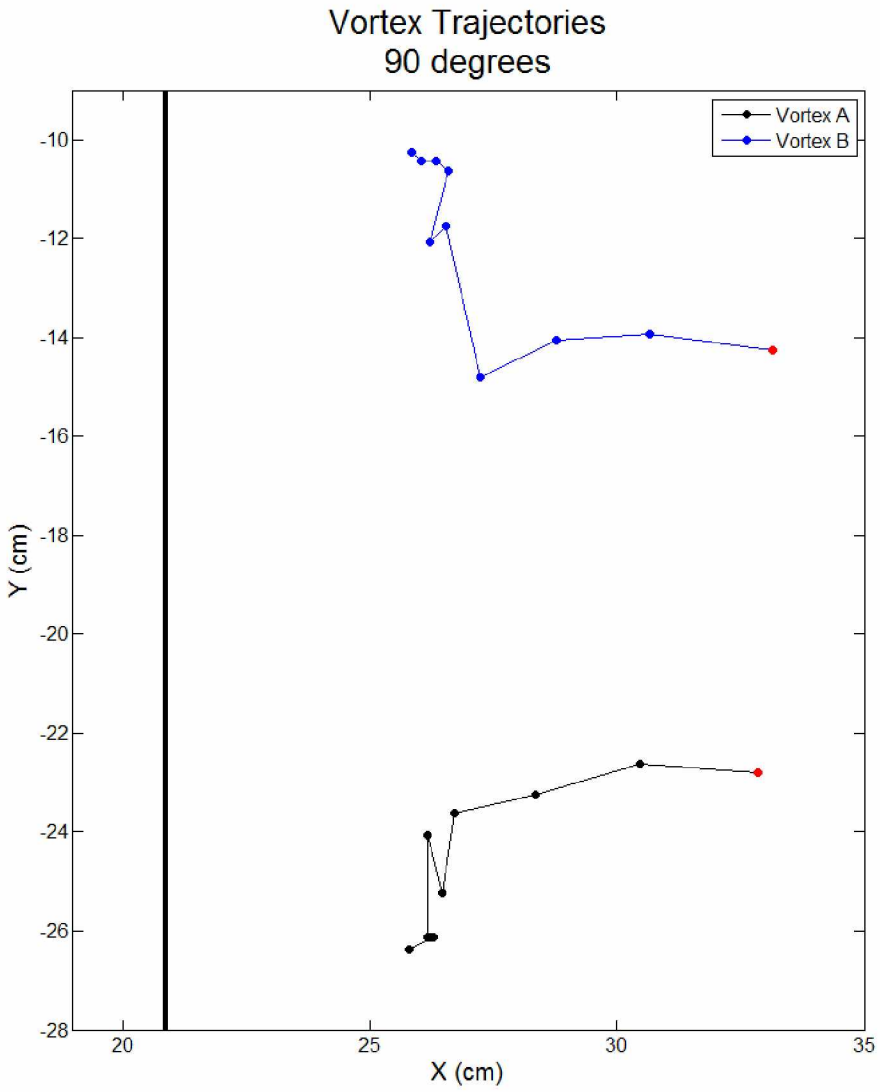

Figure 5.9 Vortex trajectories: 90 degrees, red marker indicates starting point

5.6 Data Comparisons

5.6.1 Comparison of Circulation

The figure below is a comparison of circulation levels of the two parts of the vortex ring for each of the three experiments. The general trends appear similar but there are some important differences to note. First, the data sets for the 30 and 60 degree trials show a peak after the first data point. This is an error in the execution of the experiment, attributed to having

the vortex generating tube to close to the plate and starting the image recording process when the vortex ring first interacted with the plate, but obviously had not yet fully formed. However, the vorticity images show that the vortex tube was a minor interference and the trend in each data set after peak circulation can be compared.

In all trials the circulation decreased with some slight fluctuation during the major decrease in magnitude to some vorticity shedding and exchange of circulation. The minimum levels of circulation in this figure are of particular interest, because they show an important distinction between symmetric and asymmetric vortex ring interactions. Particularly in the circulation for the upper part of the vortex, negative circulation, it is evident that an asymmetric interaction with a solid body allows one part of the vortex to maintain higher levels of circulation during the die out phase than would be present in a symmetrical interaction. This is illustrated by the data set for the upper part of the ring in the 90 degree interaction having lower magnitude circulation in the die out phase than either the 30 or 60 degree interactions. This is attributed to the upper part of the ring in the asymmetric interactions being further from the surface of the plate and entraining some of the fluid from the pinched off vortex. While the three data sets for the upper part of the ring show a linear correlation between plate inclination and circulation, there is not a clear trend for the lower part of the ring. However, it is intuitive that as the plate angle increases the lower vortex should experience less decrease in circulation due to the action of the buffer vortex, which appears to grow in strength with plate inclination.

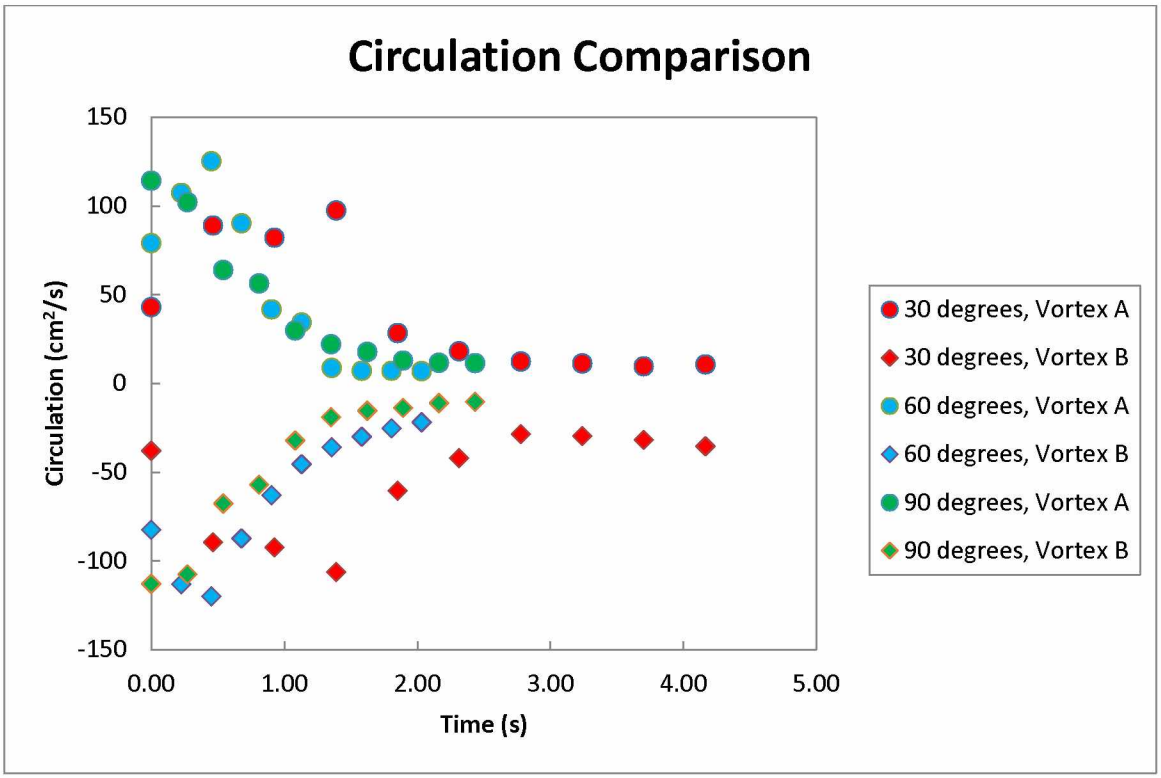

Figure 5.10 Circulation comparison

5.6.2 Comparison of Trajectories

The following plot is a comparison of the trajectories of the upper and lower parts of the vortex ring for each experiment. It should be noted that, for ease of illustration, unlike the other trajectory plots in this study the trajectories were manipulated so that they overlay one another at the starting points. Thus, the coordinates on the axis are to be used as a reference for displacement from the starting point and not as an indication of the location of the vortex ring in the tank.

The trajectory comparison plot shows two key results for the three experiments. First, the difference in the shape of the trajectories differs between the 30 and 60 degree, asymmetrical, trials and the 90 degree, symmetrical, trial. In the former trials the trajectories for the upper and lower parts of the vortex ring differ in either horizontal or vertical net displacement. In contrast,

the 90 degree trial exhibits trajectories that are very similar in both horizontal and vertical displacement. The second key result shown in this comparison is that while the trajectories ultimately converge for the 30 degree trial, they diverge for both the 60 and 90 degree trials. This indicates that there is some dependence of vortex ring diameter on plate inclination during the interaction. This dependence cannot simply be linear proportionality, as the angle for which divergence rather than convergence of the trajectories occurs lies between 30 and 60 degrees.

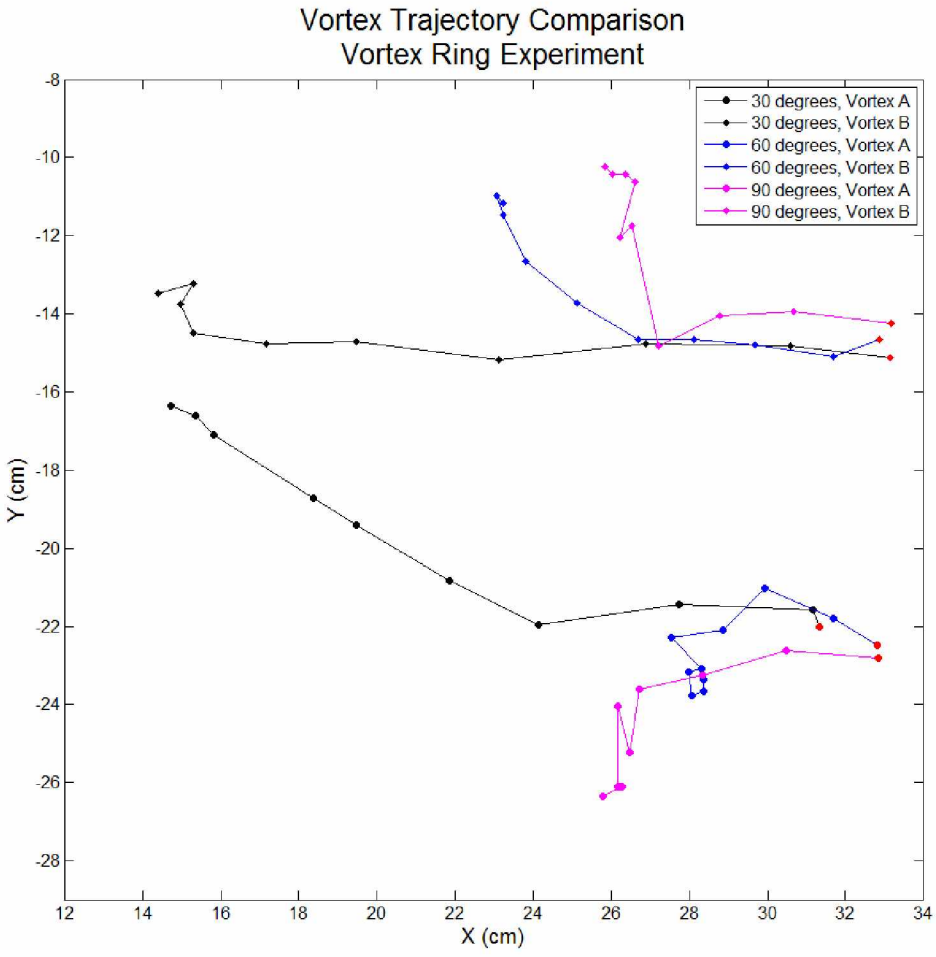

Figure 5.11 Vortex trajectory comparison, vortex ring experiment, red marker indicates starting point

5.7 Conclusion

The experiments investigating the interaction of a vortex ring with a plate at several levels of inclination reveal several fluid dynamic correlations and behaviors. The evolution of the vorticity in each experiment was examined in a step by step process to better understand the degradation of the vortex ring and formation of other notable areas of vorticity. Comparisons of circulation and vortex ring cross section trajectory in each of the three experiments were made by overlaying the results of the same data types. In general it was concluded that due to the difference between symmetrical and asymmetrical interactions there is dependence on plate inclination, of all data types examined and that this dependence is not linear proportionality.

The examination of the evolution of vorticity showed that significant events in the interactions differ between the 30 and 60 degree, asymmetrical trials, and the 90 degree, symmetrical trial. In the asymmetrical trials the vorticity in the lower portion of the ring decreases to much lower levels than for the 90 degree trial due the increased interaction of the lower part of the vortex with the plate and upper part of the vortex in the asymmetrical experiments. In addition it was found that for the 30 and 60 degree trials a single pinch off vortex forms in the gap between the plate and upper part of the ring. This differs from the symmetrical interaction in which each part of the ring ultimately develops two small hovering vortices that are not the result of pinching between the ring and plate. Thus it is concluded that the levels of vorticity, particularly in the lower part of the vortex ring, and the formation of additional vortices in the flow field are dependent on plate inclination and thus, the degree of asymmetry of the interaction.

The comparisons of circulation levels for the two parts of the vortex rings show correlation between plate inclination and circulation values. Particularly in the upper portion of

the ring, the magnitude of circulation in the die off phase was significantly greater for shallower plate inclinations. Again this is an attribute of separation of the vortex ring from the plate, a condition which varies with plate angle. The circulation levels for the lower part of the vortex ring during the die off phase did not show a clear correlation. It was concluded by data analysis that during the die off phase the circulation of the upper part of the vortex ring is inversely proportional to plate angle, by inference that circulation of the lower part of the vortex ring is proportional to plate inclination.

The comparison of the trajectories of the two parts of the vortex ring for the three experiments showed that trajectory is dependent on plate inclination. The relationship between plate inclination and vertical displacement of the two parts of the ring was found to be based on degree of symmetry. It was concluded that there is not linear proportionality between plate angle and vertical displacement of the upper and lower portions of the ring. Rather, at some inclination slightly less than 60 degrees the trajectory begins to take on an increasingly symmetrical nature.

Chapter 6 References

Akhmetov, D. G. (2008). Model of vortex ring formation. *Journal Of Applied Mechanics & Technical Physics*, *49*(6), 909-918. doi:10.1007/s10808-008-0113-4

Anderson, J.D., Jr., (2001), *Fundamentals of Aerodynamics* (3rd ed.). New York, NY: McGraw-Hill.

Arévalo, G., Hernández, R. H., Nicot, C., & Plaza, F. (2010). Particle image velocimetry measurements of vortex rings head-on collision with a heated vertical plate. *Physics Of Fluids*, *22*(5), 053604. doi:10.1063/1.3410800

Bandyopadhyay, P. R., & Leinhos, H. A. (2013). Propulsion efficiency of bodies appended with multiple flapping fins: When more is less. *Physics Of Fluids*, *25*(4), 041902-041902-23. doi:10.1063/1.4802495

Bernal, L. P., Song, M., & Tryggvason, G. (1992). Head-on collision of a large vortex ring with a free surface. *Physics Of Fluids A*, *4*(7), 1457.

Chirgwin, B. H., & Plumpton, C. (1967). *Elementary Classical Hydrodynamics*. London, England: Pergamon Press Ltd.

Chopra, I., Parsons, E., & Sirohi, J. (2007). Hover performance of a cycloidal rotor for a micro air vehicle. *Journal of the American Helicopter Society, 52,* 263–279.

Couch, L., & Krueger, P. (2011). Experimental investigation of vortex rings impinging on inclined surfaces. *Experiments In Fluids*, *51*(4), 1123-1138. doi:10.1007/s00348-011-1135-x

Crowe, C.T., Elger, D. F., Robertson, J. A., & Williams, B. C., (2010). *Engineering Fluid Mechanics* (9th ed.). Hoboken, NJ: John Wiley & Sons, Inc.

Eloy, C., Paraz, F., & Schouveiler, L. (2014). Vortex patterns generated by a heaving flexible plate. *Journal Of Visualization*, *17*(4), 295-297. doi:10.1007/s12650-014-0208-3

Felli, M., & Falchi, M. (2011). Propeller tip and hub vortex dynamics in the interaction with a rudder. *Experiments In Fluids*, *51*(5), 1385-1402. doi:10.1007/s00348-011-1162-7

Felli, M., Guj, G., & Roberto, C. (2009). Experimental analysis of the flow field around a propeller–rudder configuration. *Experiments In Fluids*, *46*(1), 147-164.

Ishii, T., Obi, S., & Suryadi, A. (2010). Stereo PIV measurement of a finite, flapping rigid plate in hovering condition. *Experiments In Fluids*, *49*(2), 447-460. doi:10.1007/s00348-009-0814-3

Kompenhans, J., Raffel, M., Wereley, S. T., & Willer, C. E. (2007). *Particle Image Velocimetry: A Practical Guide*. (2nd ed.). New York, NY: Springer.

Kondepudi, D., & Prigogine, I. (2015). *Modern Thermodynamics* (2nd ed.). West Sussex, United Kingdom: John Wiley & Sons, Inc.

Kriegseis, J., Rival, D. E., & Wong, J. G. (2013). An investigation into vortex growth and stabilization for two-dimensional plunging and flapping plates with varying sweep. *Journal Of Fluids & Structures*, *43*231-243. doi:10.1016/j.jfluidstructs.2013.09.010

Lai, J. C., Tian, F., & Young, J. (2014). Improving power-extraction efficiency of a flapping plate: From passive deformation to active control. *Journal Of Fluids & Structures*, *51*384-392. doi:10.1016/j.jfluidstructs.2014.07.013

Linden, P. F., & Turner, J. S. (2004). 'Optimal' vortex rings and aquatic propulsion mechanisms. *Proceedings Of The Royal Society B: Biological Sciences*, *271*(1539), 647-653.

Miloh, T., & Tyvand, P. A. (1994). Axisymmetric interaction between a vortex ring and a free surface. *Physics Of Fluids*, *6*(1), 224.

Munson, B. R., Okiishi, T. H., & Young, D. F. (1998). *Fundamentals of Fluid Mechanics*. New York, NY: John Wiley & Sons, Inc.

Obi, S., & Suryadi, A. (2011). The estimation of pressure on the surface of a flapping rigid plate by stereo PIV. *Experiments In Fluids*, *51*(5), 1403-1416. doi:10.1007/s00348-011-1150-y

Reynolds, A. J. (1974). *Turbulent Flows in Engineering. London, England*: John Wiley & Sons.

Appendix

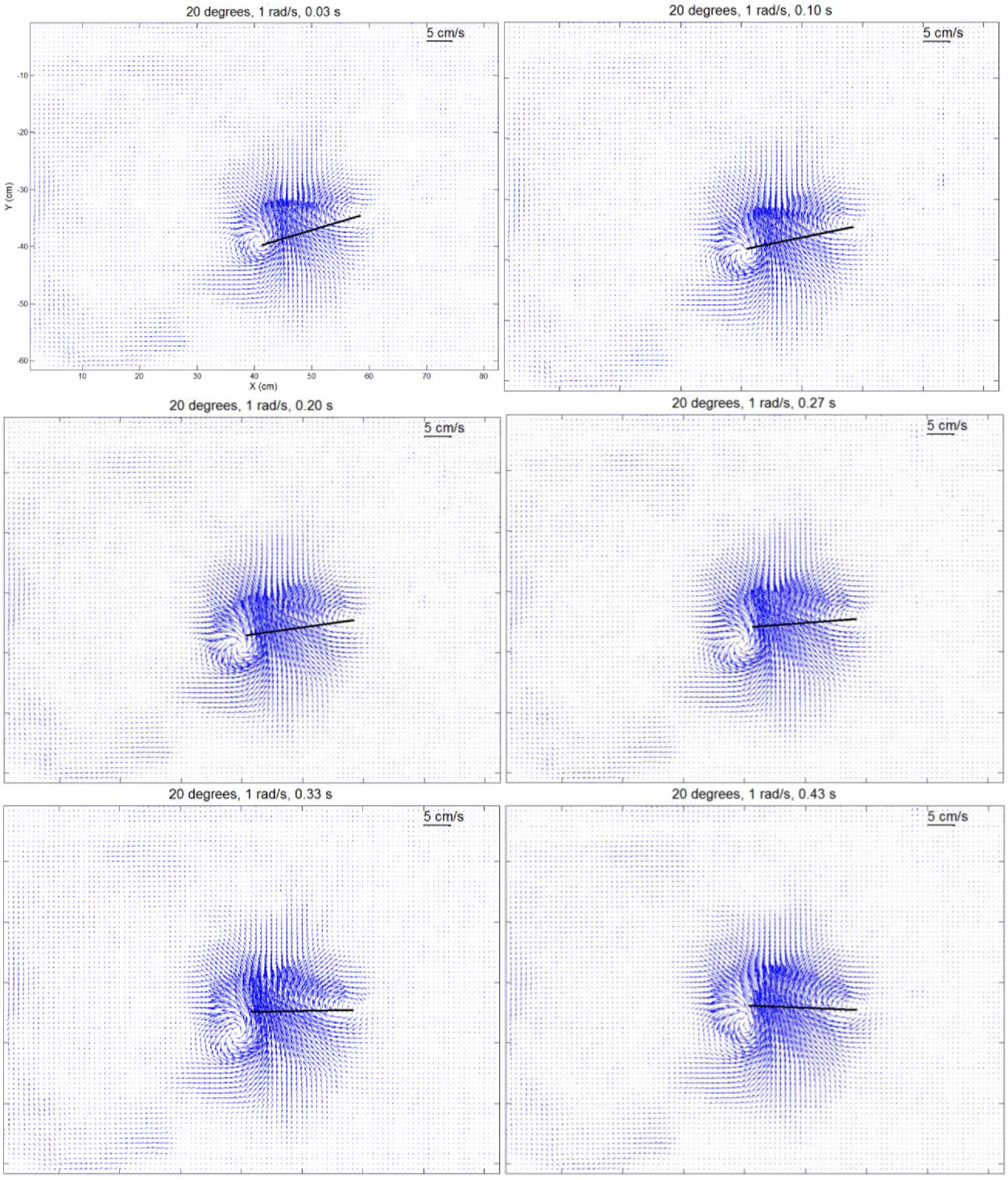

Figure A.1 Velocity plots: 20 degrees, 1 rad/s

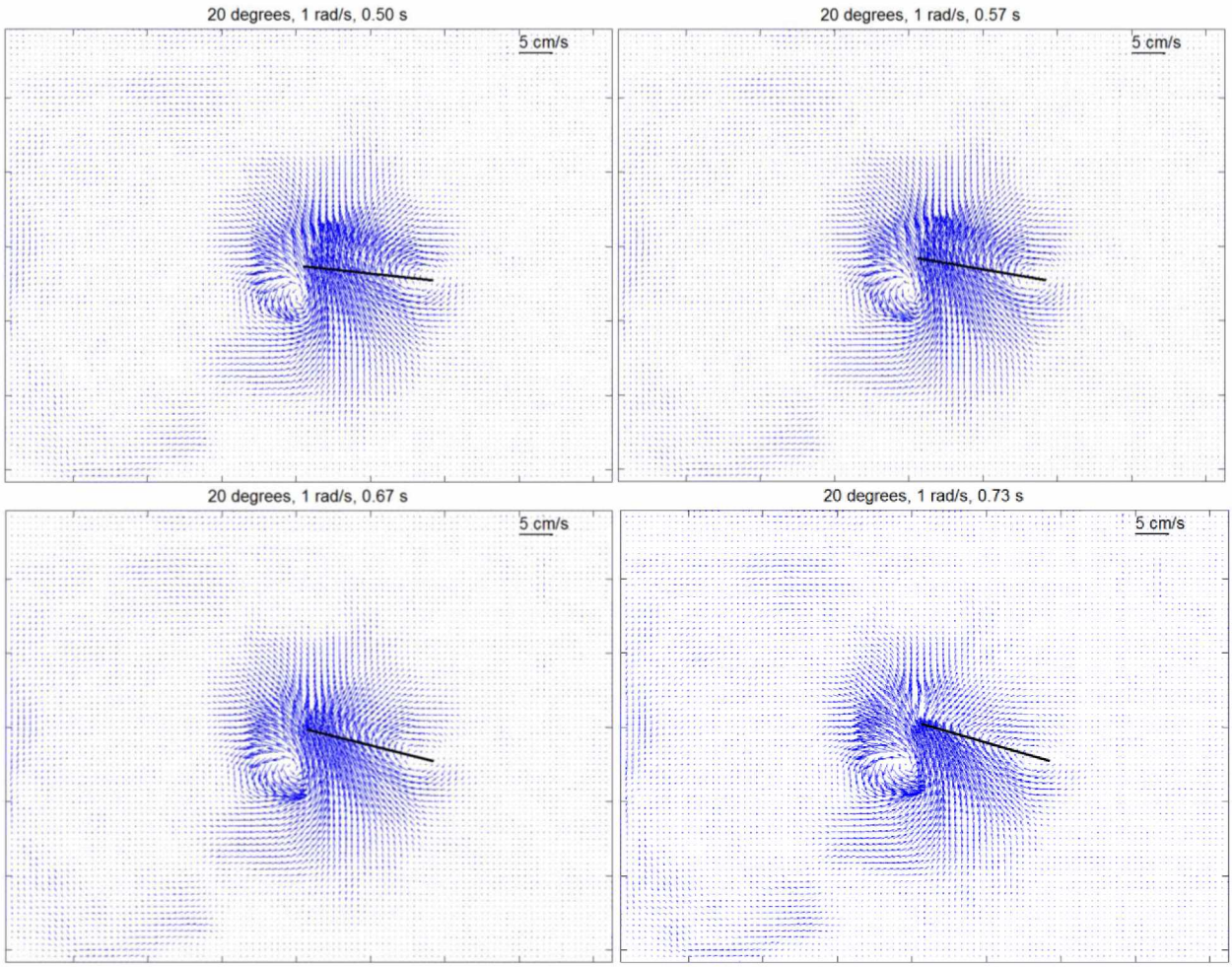

Figure A.1 continued Velocity plots: 20 degrees, 1 rad/s

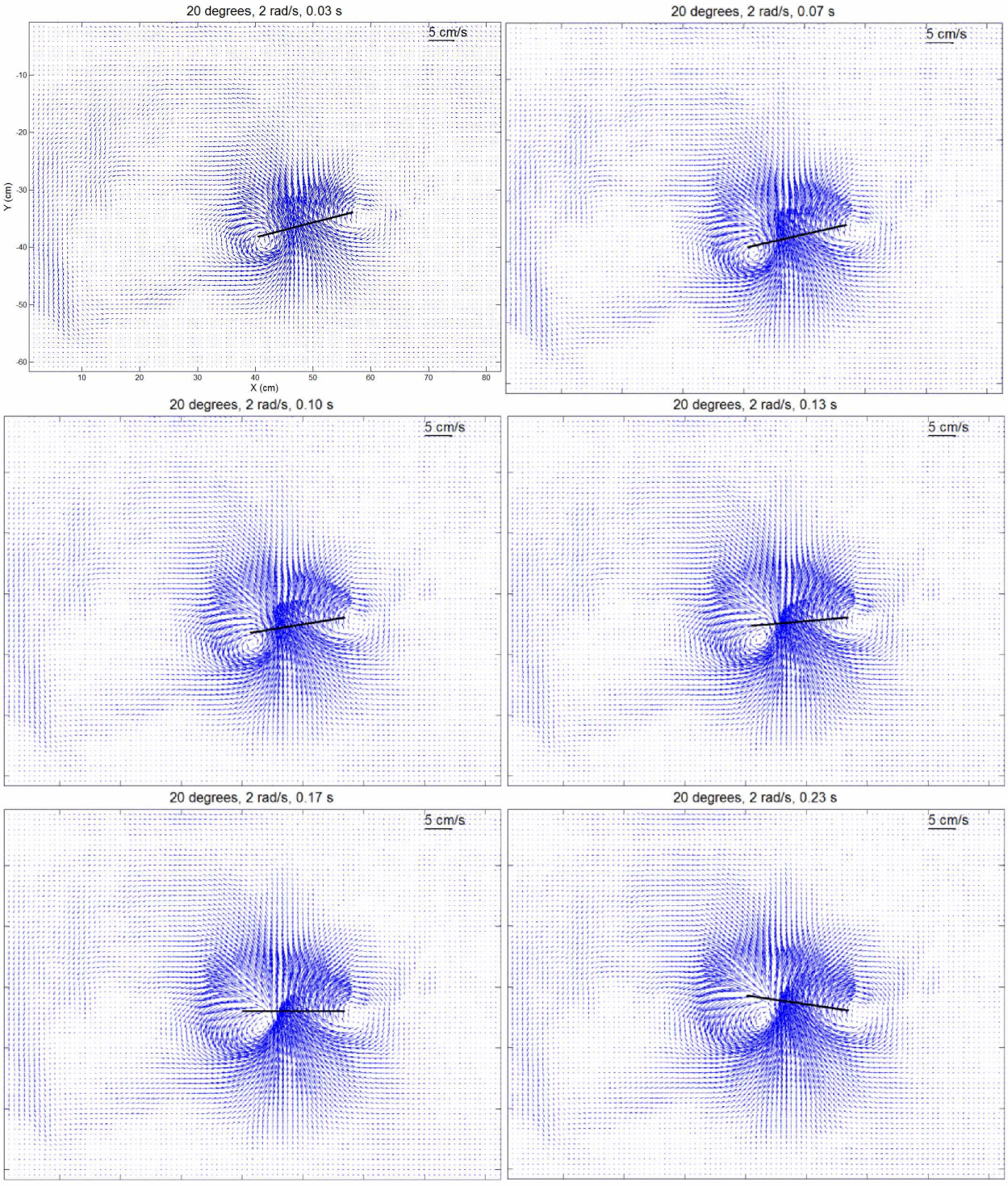

Figure A.2 Velocity plots: 20 degrees, 2 rad/s

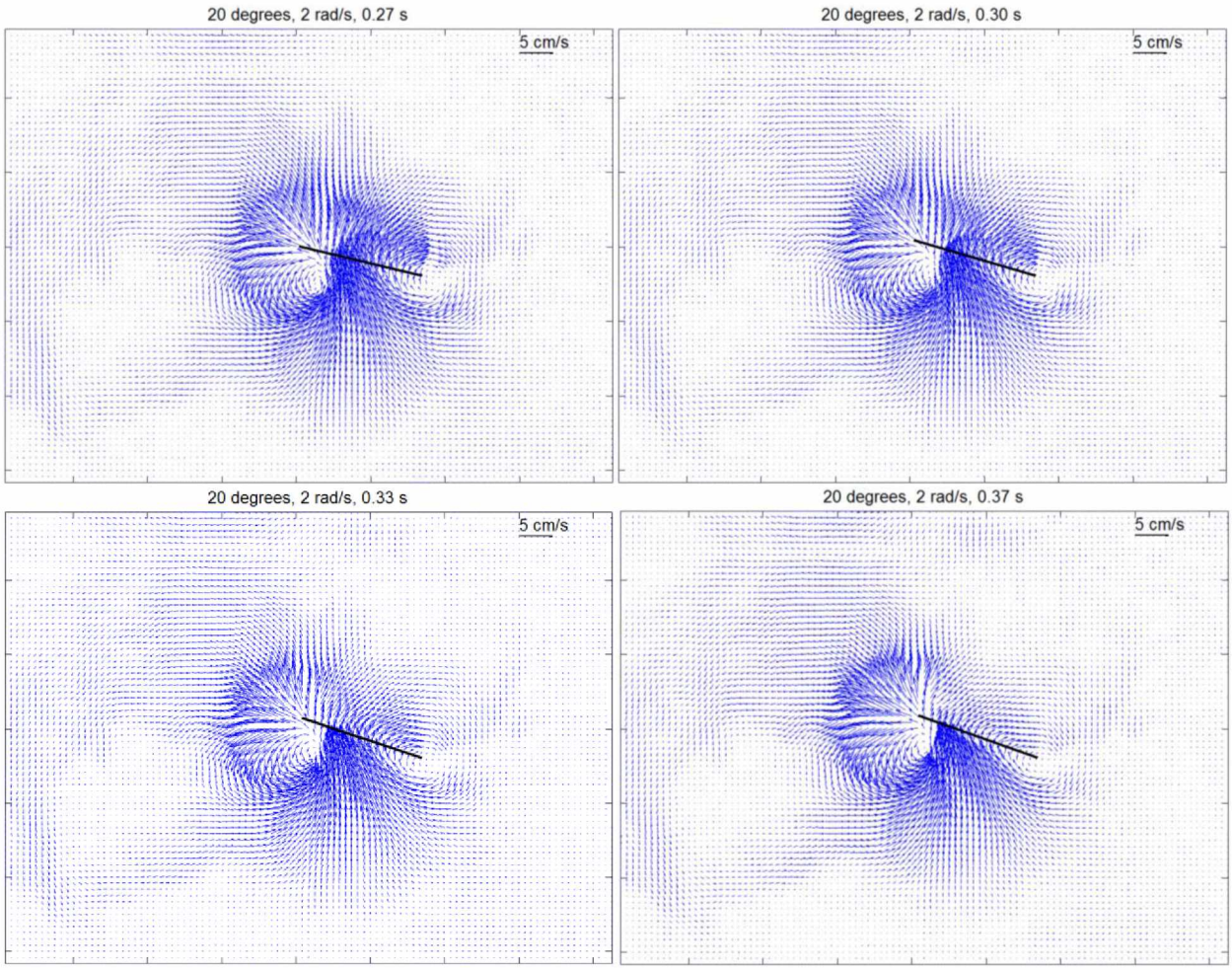

Figure A.2 continued Velocity plots: 20 degrees, 2 rad/s

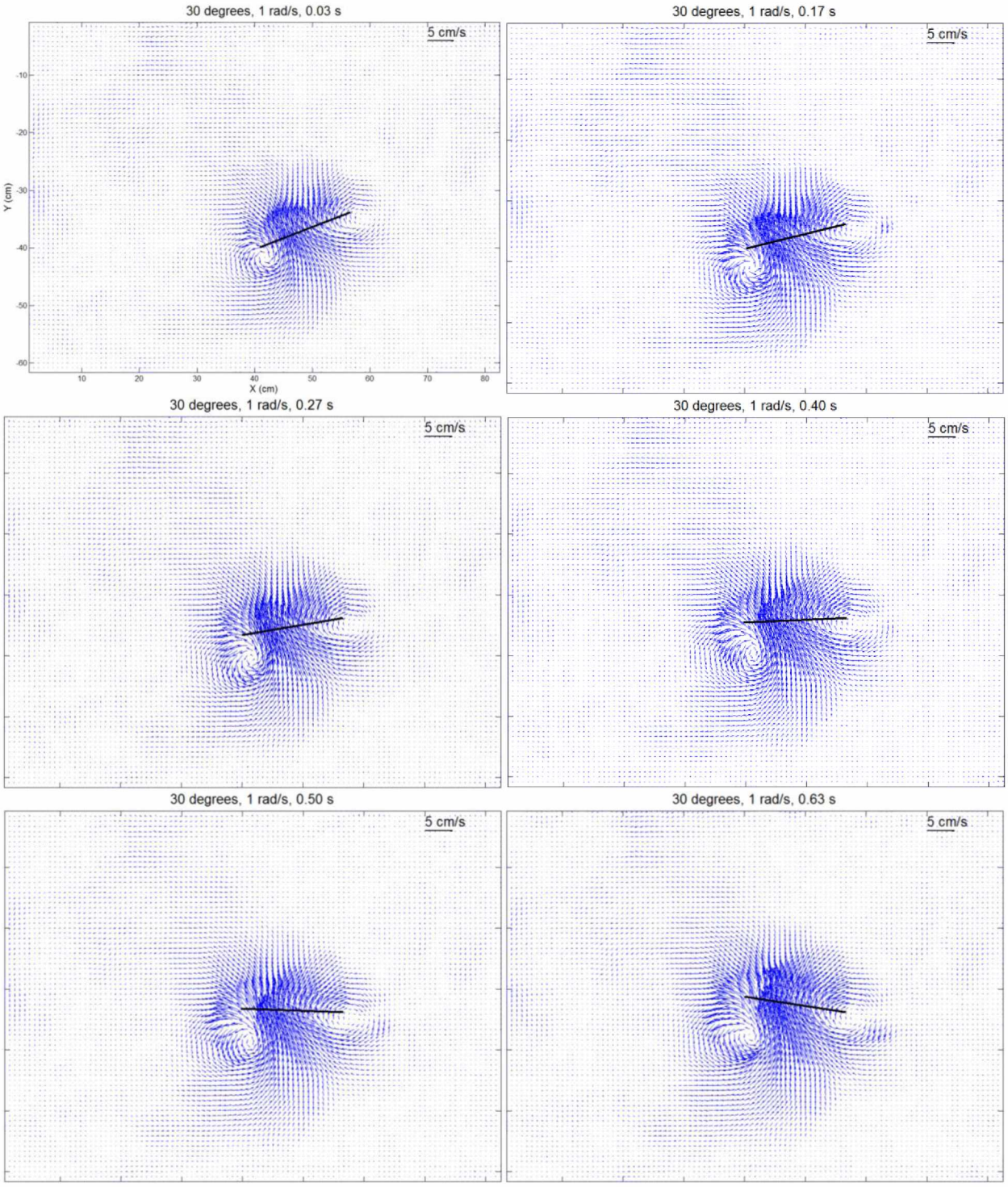

Figure A.3 Velocity plots: 30 degrees, 1 rad/s

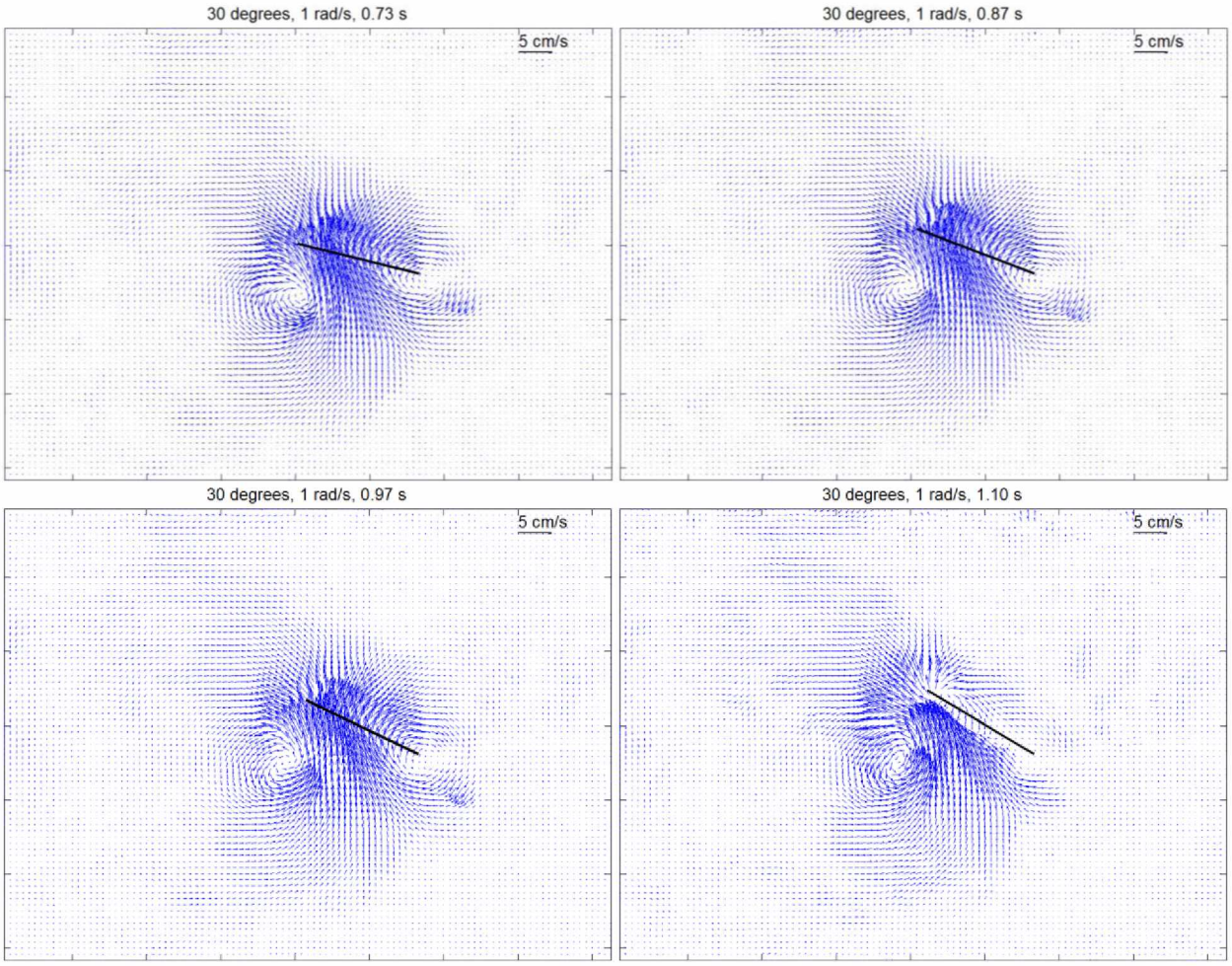

Figure A.3 continued Velocity plots: 30 degrees, 1 rad/s

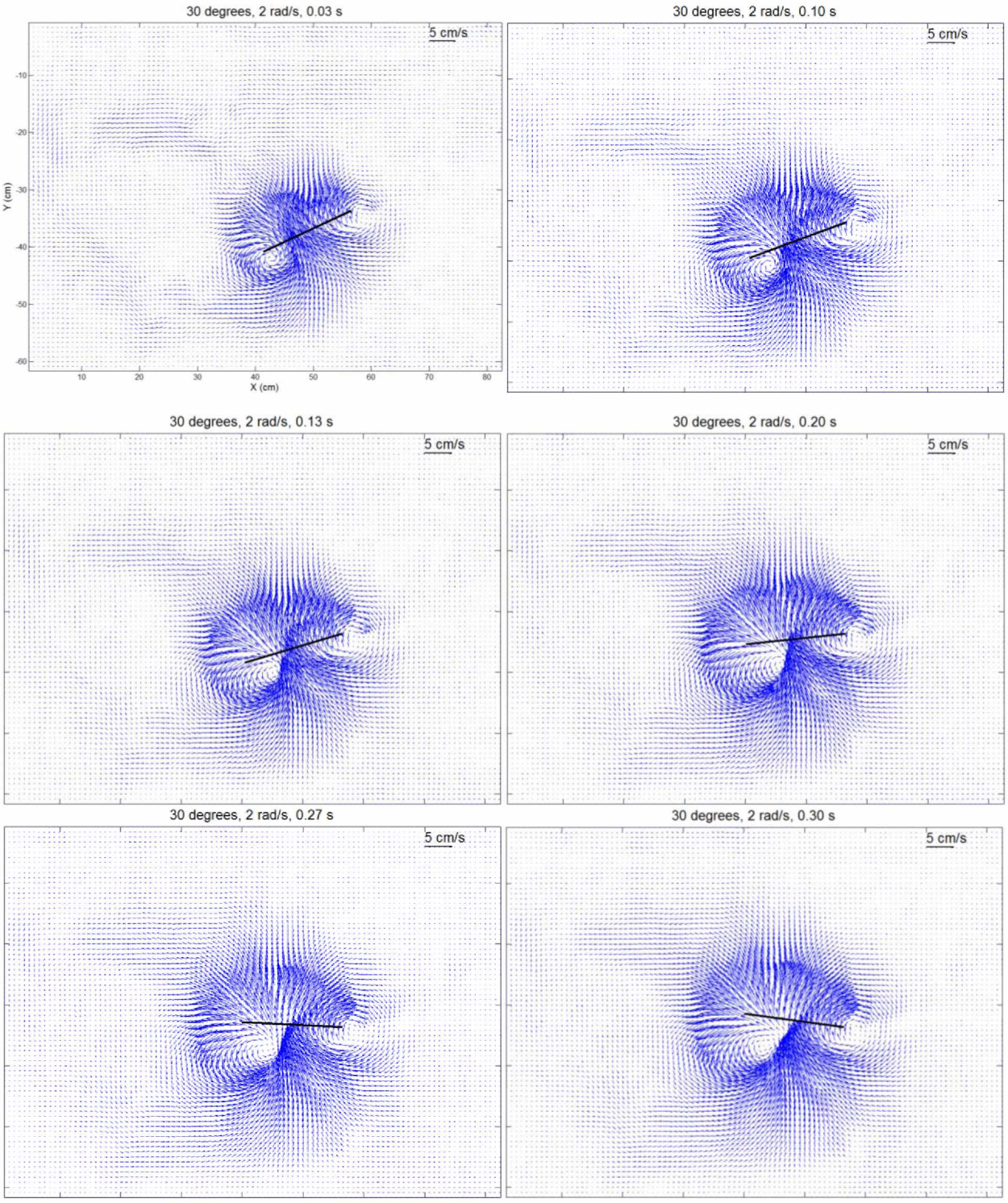

Figure A.4 Velocity plots: 30 degrees, 2 rad/s

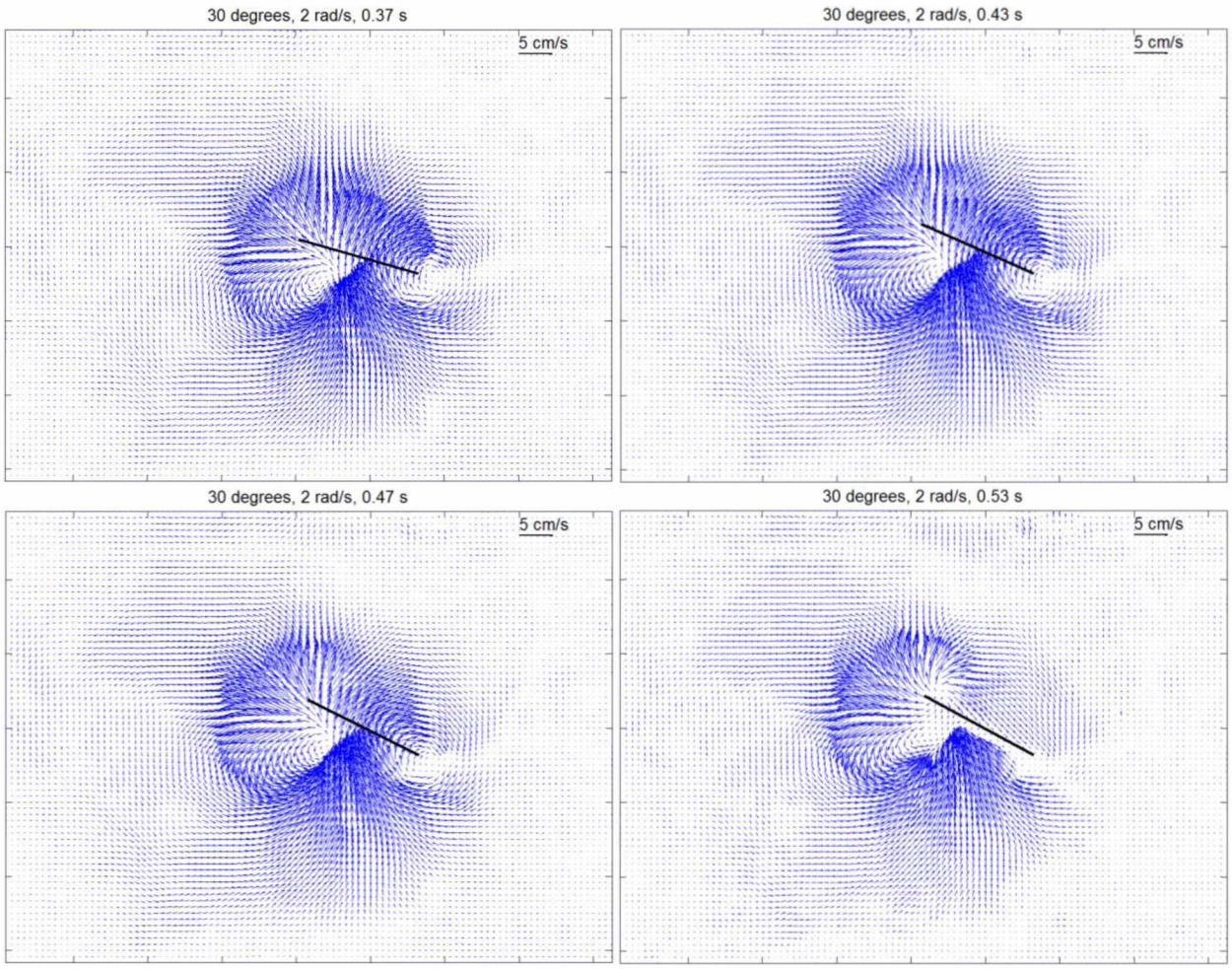

Figure A.4 continued Velocity plots: 30 degrees, 2 rad/s

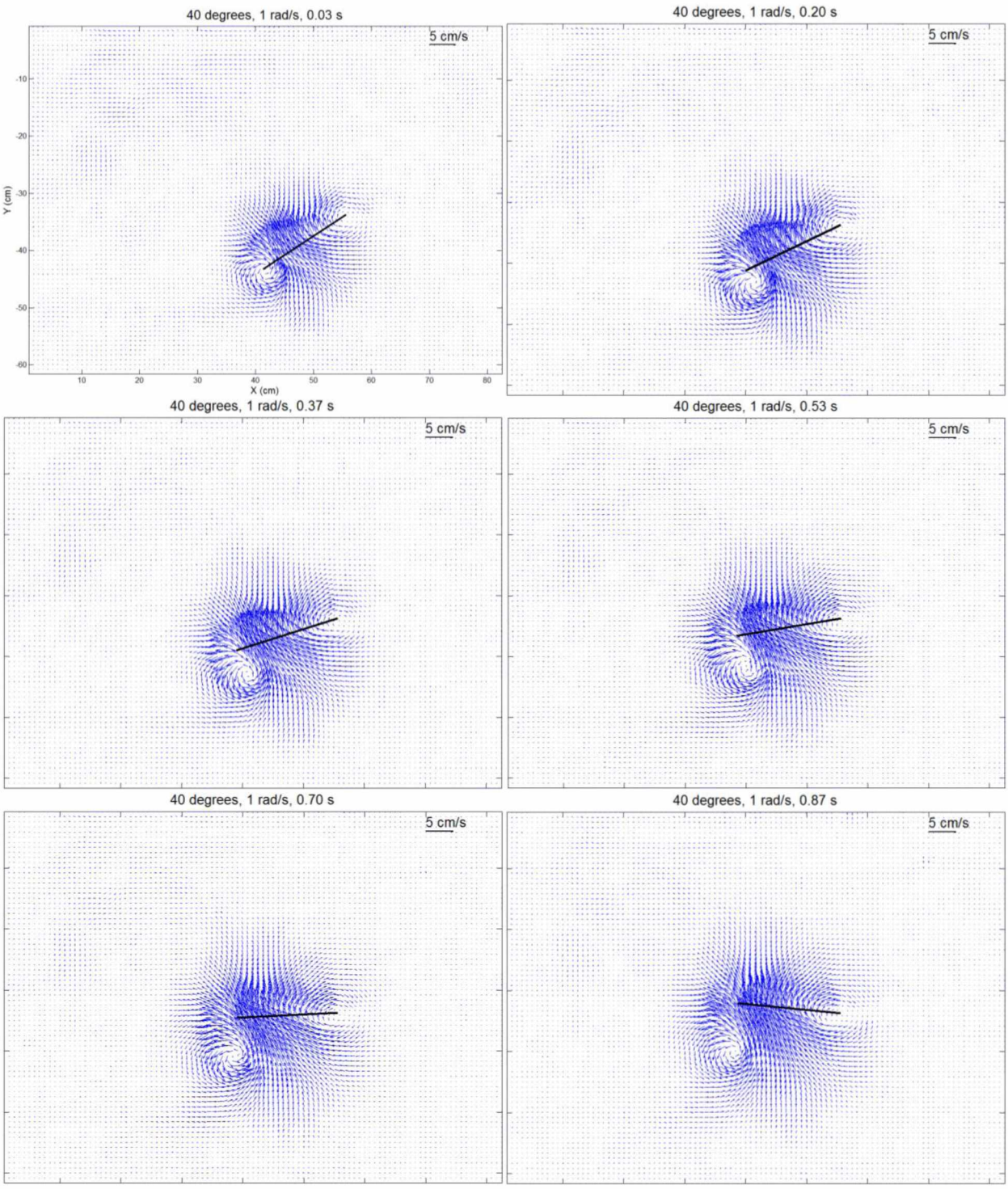

Figure A.5 Velocity plots: 40 degrees, 1 rad/s

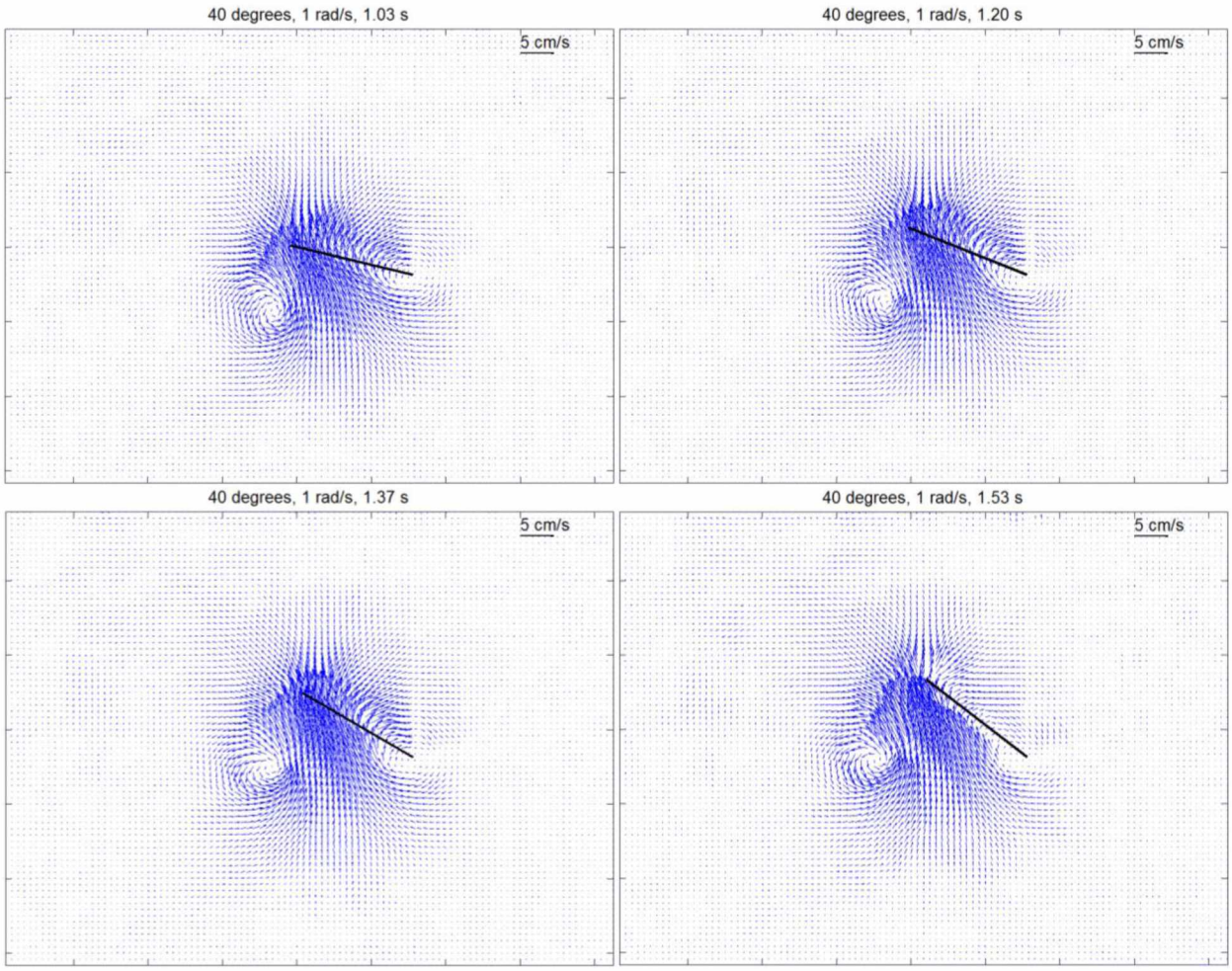

Figure A.5 continued Velocity plots: 40 degrees, 1 rad/s

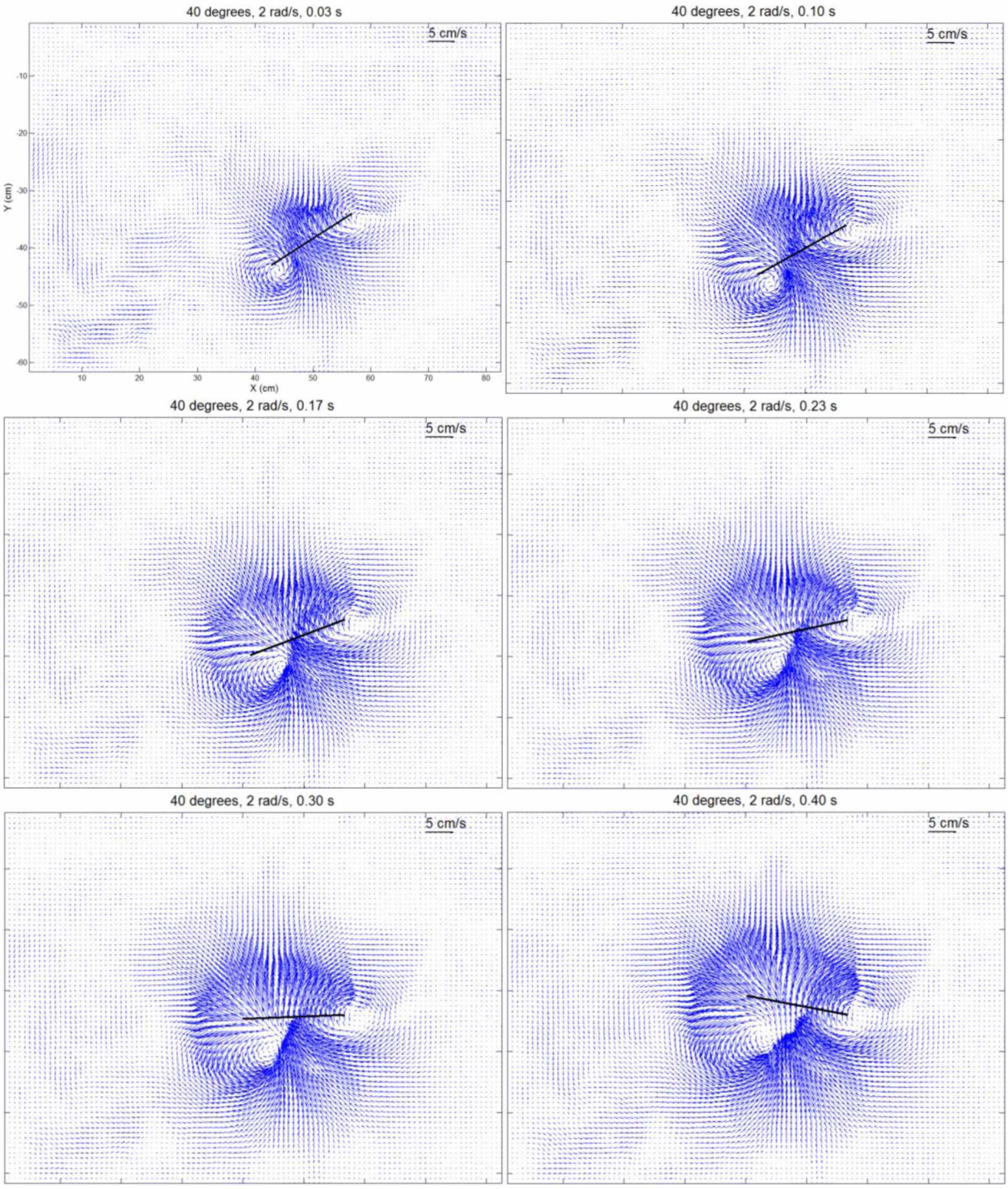

Figure A.6 Velocity plots: 40 degrees, 2 rad/s

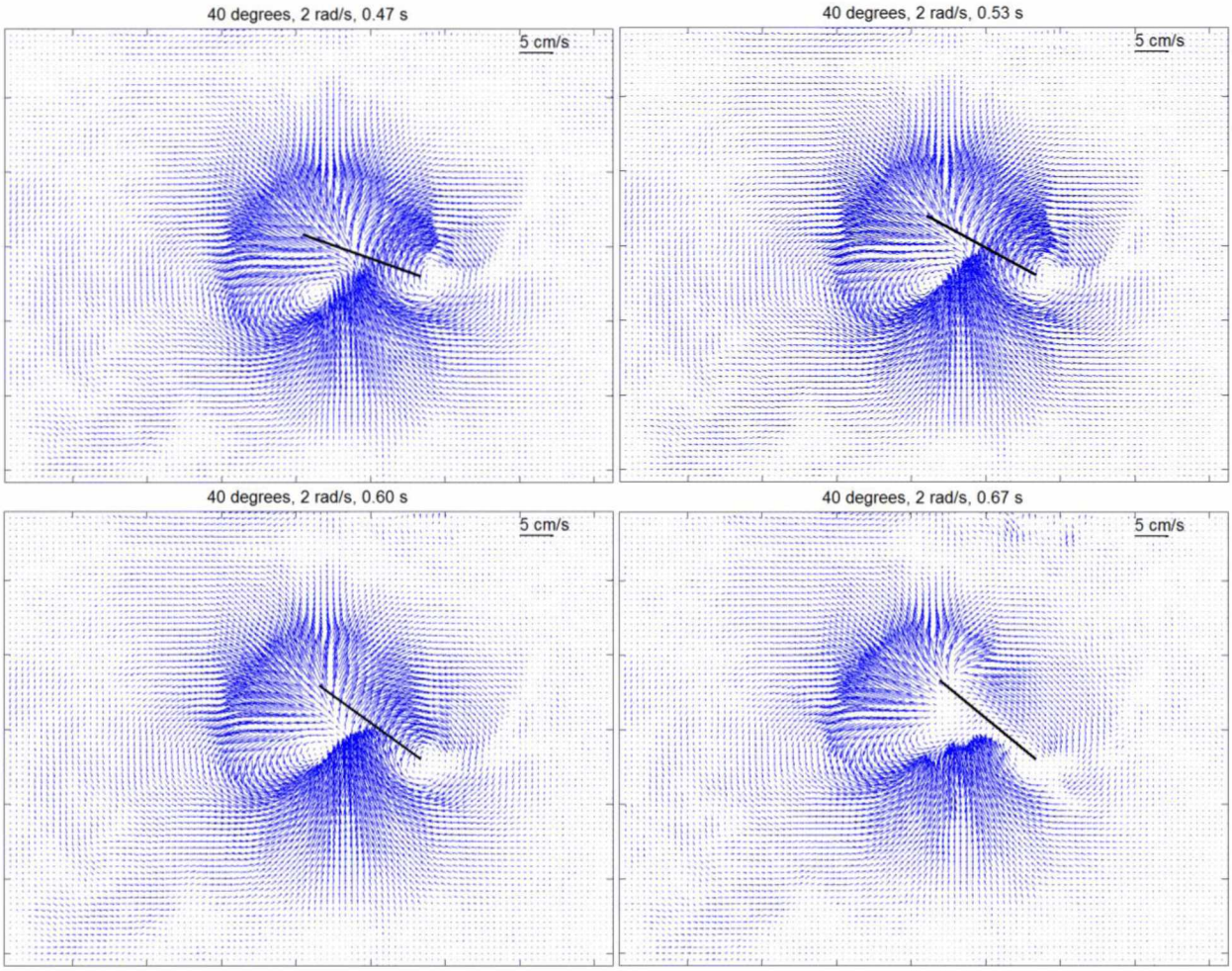

Figure A.6 continued Velocity plots: 40 degrees, 2 rad/s

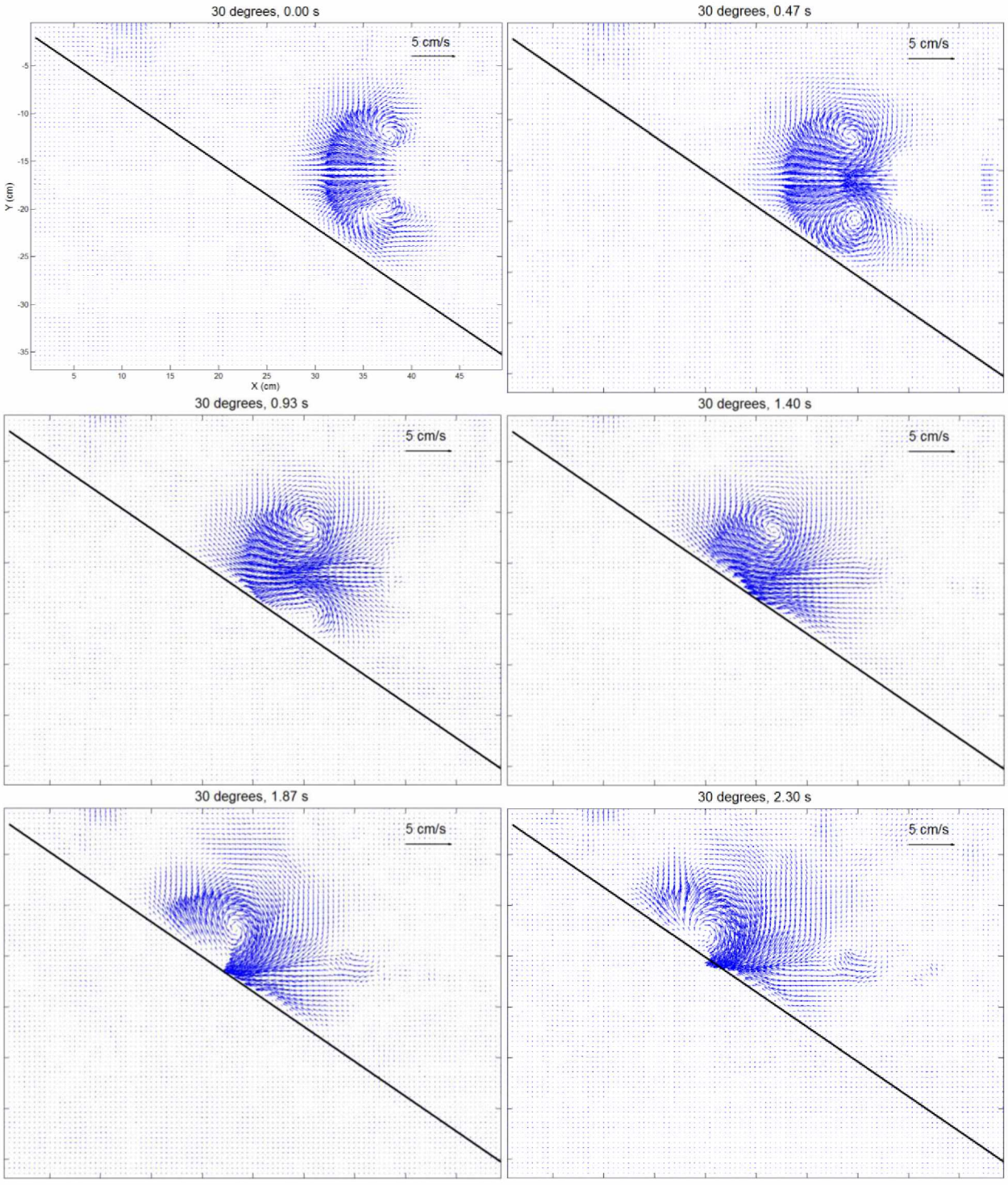

Figure A.7 Velocity plots: 30 degrees

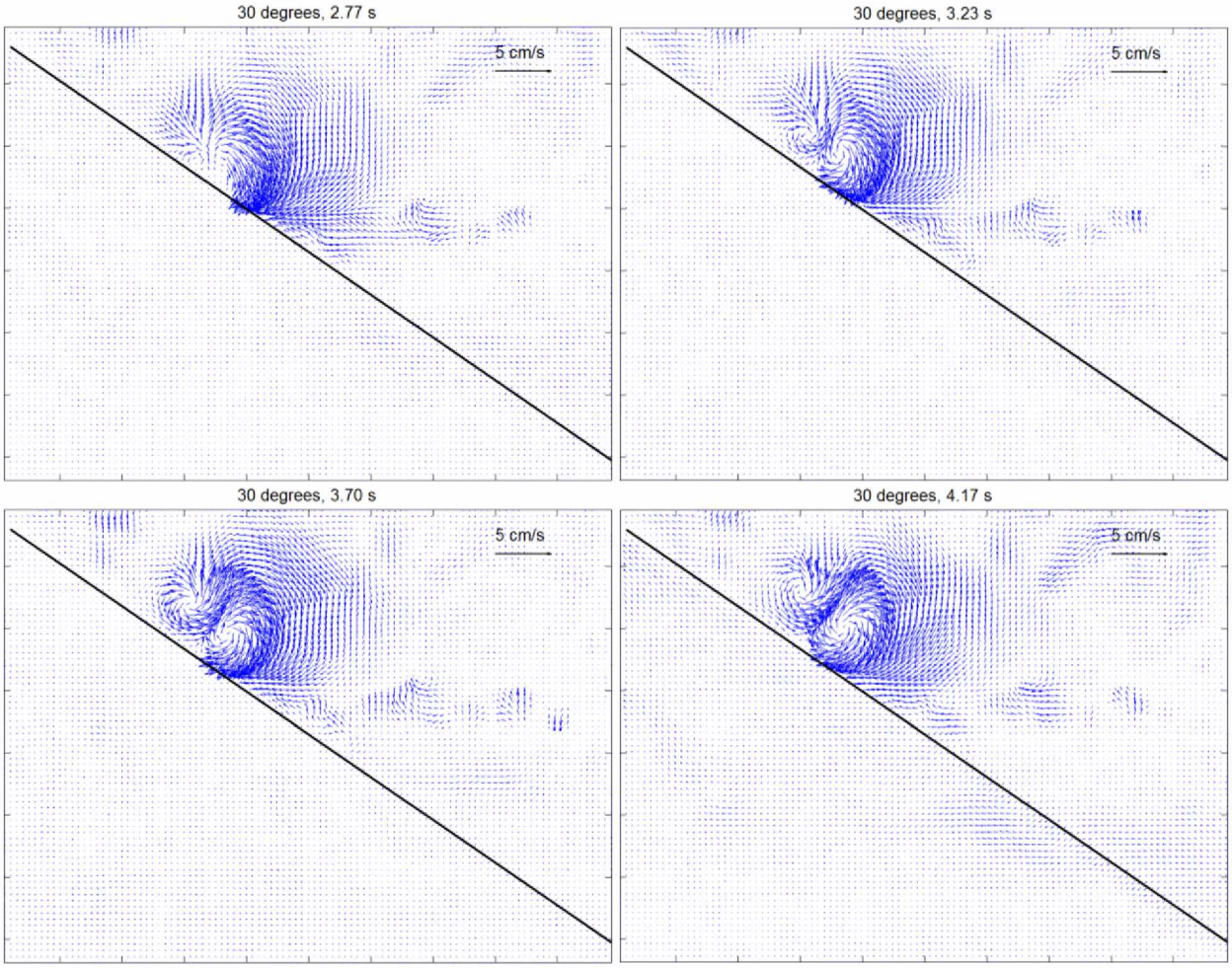

Figure A.7 continued Velocity plots: 30 degrees

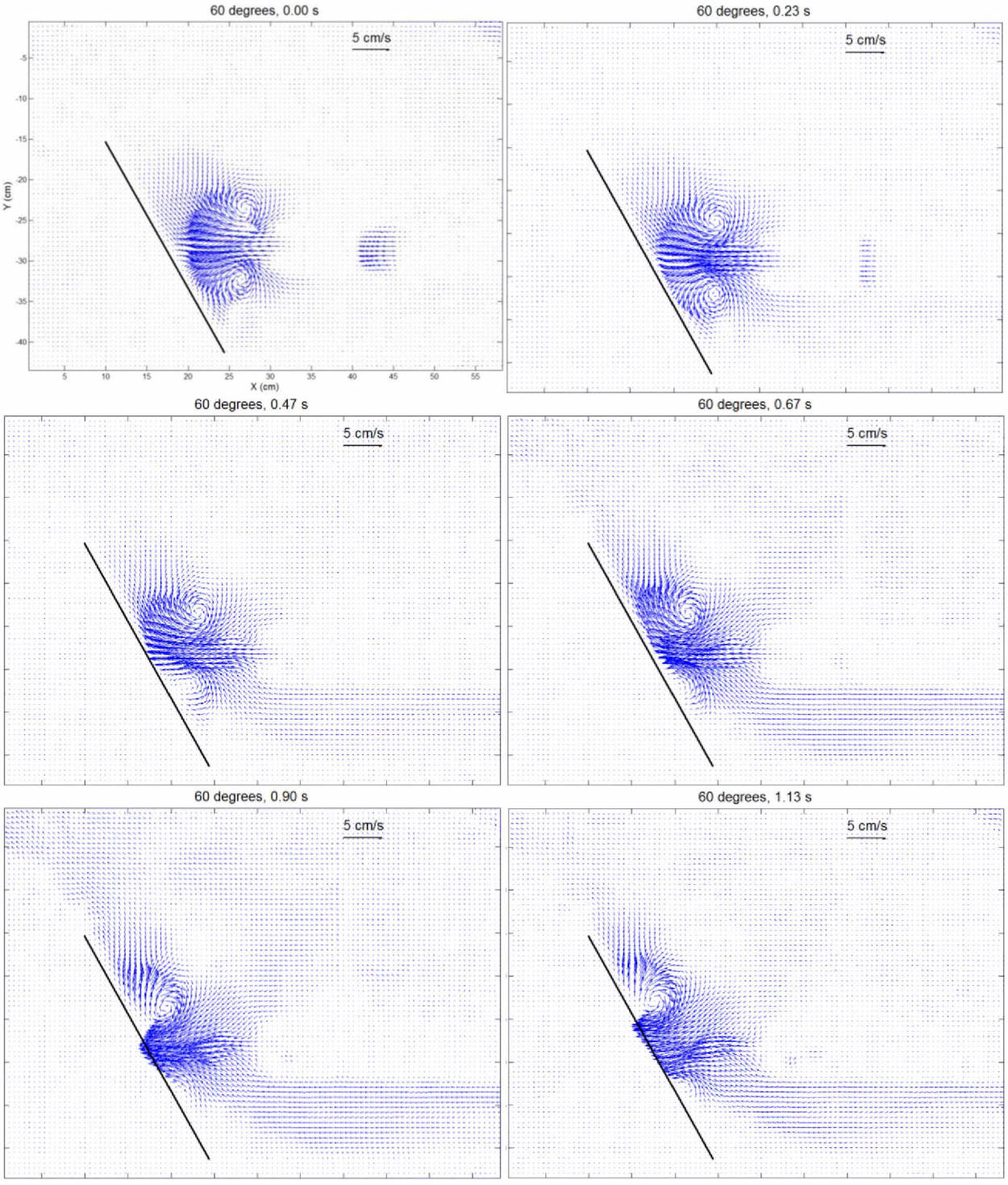

Figure A.8 Velocity plots: 60 degrees

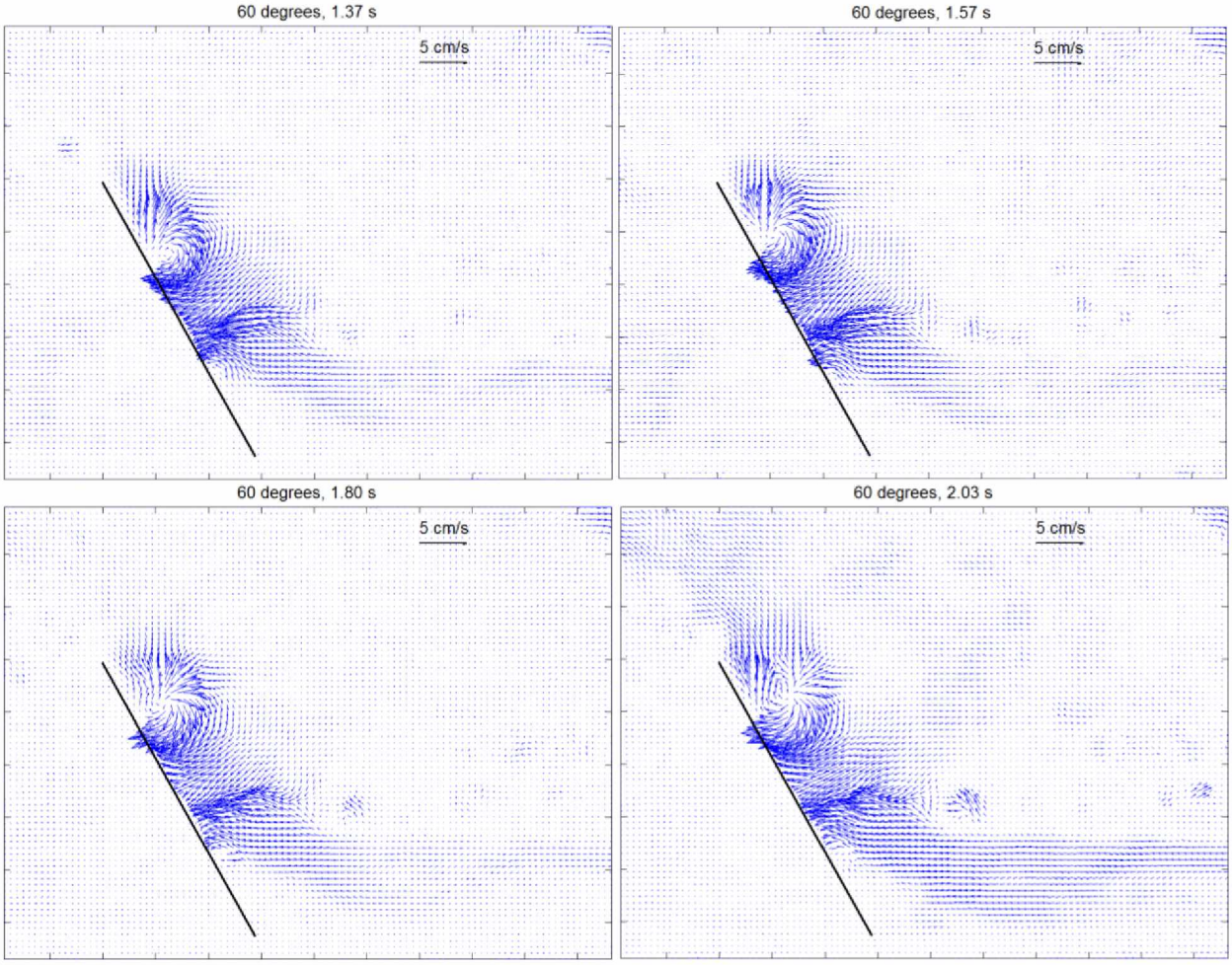

Figure A.8 continued Velocity plots: 60 degrees

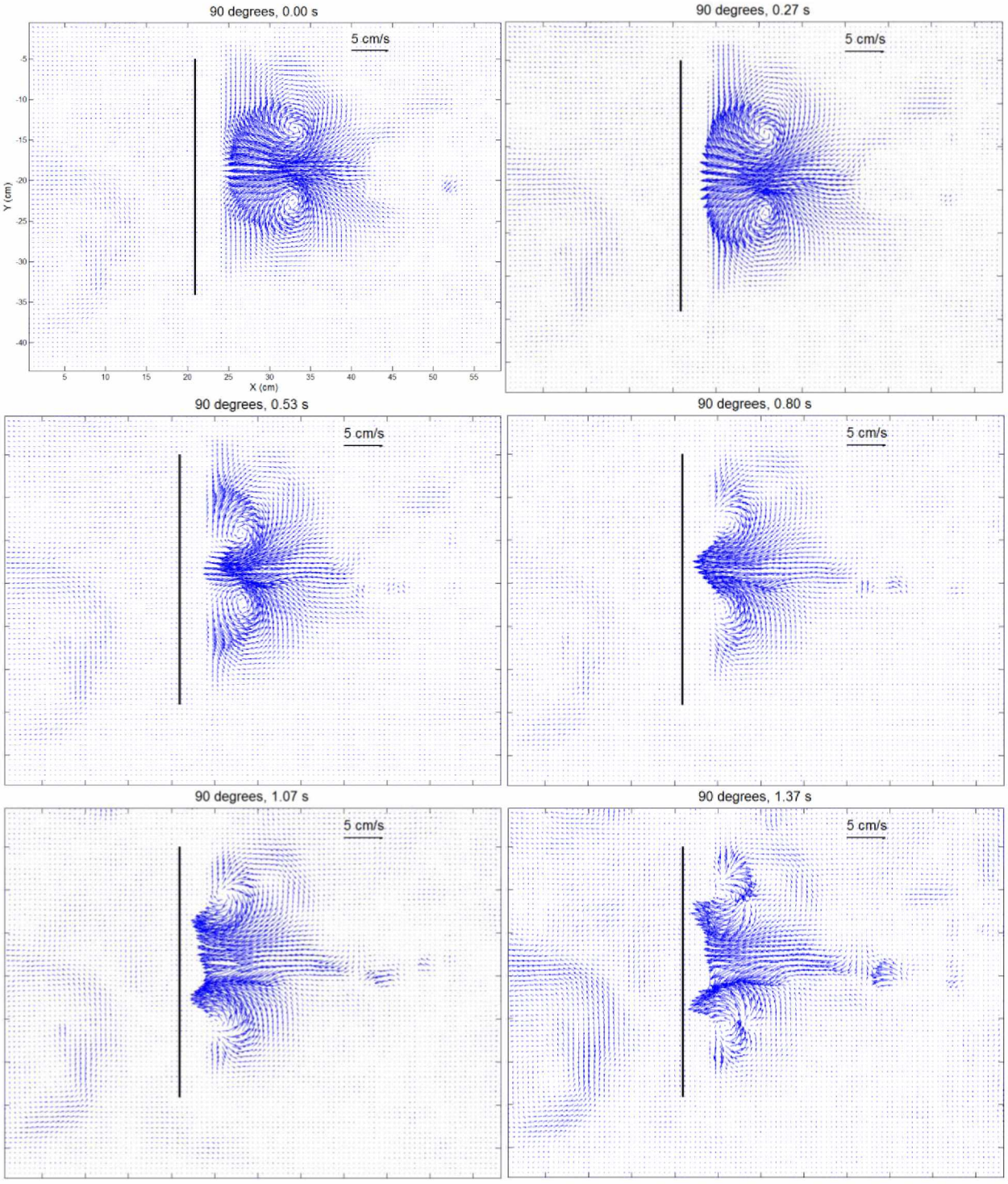

Figure A.9 Velocity plots: 90 degrees

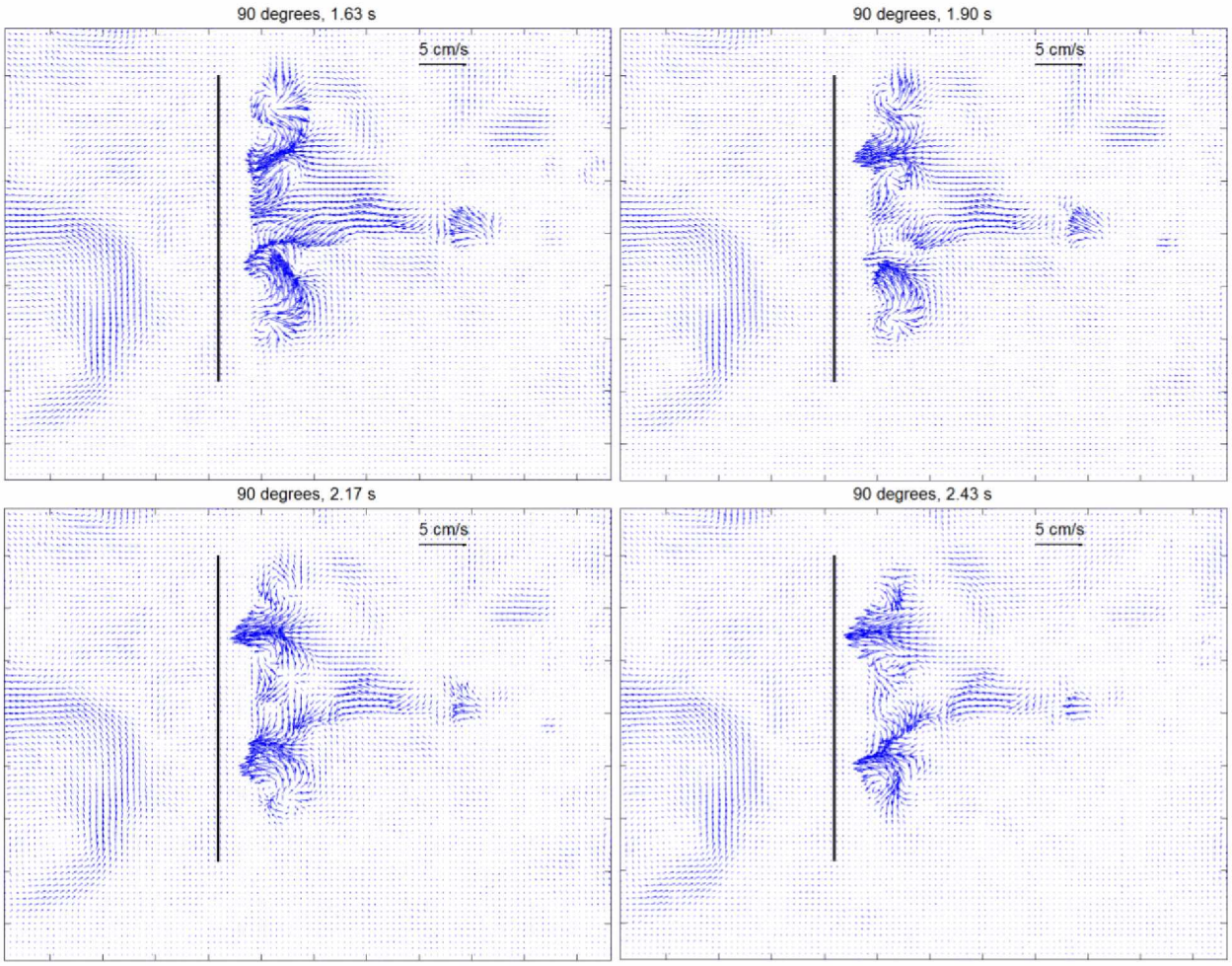

Figure A.9 continued Velocity plots: 90 degrees